1969

Correlation of particulate theory and behavior of real soils

Christopher Byron Groves

Department:

CORRELATION OF PARTICULATE THEORY AND BEHAVIOR OF REAL SOILS

BY

CHRISTOPHER BYRON GROVES

A

THESIS

submitted to the faculty of

THE UNIVERSITY OF MISSOURI - ROLLA

in partial fulfillment of the requirements for the

Degree of

MASTER OF SCIENCE IN CIVIL ENGINEERING

Rolla, Missouri

1969

Approved by

James C. Armstrong (advisor) Fernando A. Munoz

M. B. Neuenschwander

ABSTRACT

The behavior of granular soils subjected to triaxial stresses can be explained in terms of a combination of elastic deformation and sliding friction.

Three sands and a coarse silt at various initial void ratios were tested in drained triaxial compression. Cell pressures were varied between 50 and 1500 psi.

Prediction techniques for simulating laboratory data was based on various packings of equal radii spheres. Equilibrium and compatibility equations were used to calculate the principal strains under certain applied stresses. The assumed arrays predicted much smaller strains than those that the soils exhibited. If these strains were subtracted from those observed, residual strains could be analyzed in terms of sliding friction.

This method adequately described the actual behavior of the soils.

The sliding friction angle and the percentage of the volumetric and axial elastic strains increased with cell pressure.

ACKNOWLEDGMENT

The author wishes to express his thanks to his advisor Dr. J. C. Armstrong and to Dr. F. Tinoco for their help and guidance during the course of this work. Special thanks goes to Martin Hollingsworth for aid in setting up the equipment, and to Bill Green, Charles Miller, and Richard Franke for their moral support.

This project was funded by the National Science Foundation, under project No. NSF GK 3411, for studies of particulate theory and the behavior of real soils.

TABLE OF CONTENTS

LIST OF FIGURES

Page

Figure

Page

LIST OF TABLES

Page

Table

NOMENCLATURE

A - cross sectional area

a - outer radius of contact between speres

b - inner radius of contact between spheres

C - tangential compliance

E - Young's Modulus of Elasticity

F - force required to overcome friction

f - coefficient of friction

L - length of displacement

N - normal force

N_{xy} - normal force on the xy-plane

P_{xx} - force on the yz-plane

P_{xz} - force in the zx-plane

R - radius of sphere

S - tangential compliance; shear strength

T_{xy} - tangential force in the xy-plane

T_{zz} - tangential force on the xy-plane

α - vertical displacement between the centers of two spheres subjected to a normal force

δ - horizontal displacement between the centers of two spheres subjected to a tangential force

ϵ - axial strain

ϵ_{ii} - axial strain along the i-axes

γ_{ij} - shearing strain in the ij-plane

ν - Poisson's ratio

μ - shear modulus; coefficient of friction

Φ - total angle of internal friction

Φ_r - residual angle of friction

Φ_s - angle of solid friction

Φ_f - angle of friction at failure

Φ_μ - sliding friction

σ_1 - major principle stress

σ_3 - minor principle stress

σ_r - radial stress

I INTRODUCTION

In most foundation problems in which granular materials are involved the design is based on settlement considerations with a resulting high factor of safety on bearing capacity. Only when the footing is narrow, the water table high, and the sand loose is there much chance of one third of the bearing capacity being greater than the pressure causing 1 in. of settlement (Peck, Hanson, and Thornburn 1953). In order to improve the design of foundations on granular materials the lower portion of the stress-strain curve should be more closely examined.

Previous studies of the mechanisms of shear of a granular soil have been based either on a sliding friction relationship or an elastic analysis of equal radii spheres in idealized packings. Each approach has its problems: the frictional approach, based on energy considerations, can not predict stress-strain relationships and the assumption is made that no energy is stored elastically; and, the approaches based on elastic spheres is used for only small strains and these approaches tend to over predict the initial tangent modulus and the stress ratio at which sliding should occur. The objective of this investigation is to integrate these two approaches by separating the strains recorded in an actual soil for predicted elastic strains, and thus see if a combination of the two approaches better describes actual behavior.

II REVIEW OF LITERATURE

The common discussion of friction which often appears in the basic physics text (Sears and Zemansky 1949) is that of a bonding at high spots on the surface of contact of the two materials. It is commonly assumed that the friction force required to produce motion along the contact surface is independent of the area of contact and linearly dependent only on the normal force on this plane. This concept is commonly referred to as Amonton' s Law (1699).

$$F = \mu N \qquad \text{(II - 1)}$$

where:

μ = the coefficient of friction

N = the normal force on the plane of contact.

Furthermore the coefficient of friction is not considered to be constant but varies as a function of velocity on the contact surface.

Coulomb (1781) makes only the distinction between static and kinetic friction. Coulomb' s failure criterion is:

$$s = c + \sigma_r \text{ TAN } \Phi \qquad \text{(II - 2)}$$

where:

c = the cohesion

σ_r = the normal stress on the failure plane

Φ = the angle of internal friction.

No mention is made in this equation of relative velocities on the plane of contact.

Reynolds (1885) was the first to recognize the dilatancy effects in dense sand. Dilatancy is the expansion of a granular material during shearing. This phenomenon is the result of the geometric configuration of the particles. He

recognized this phenomenon while studying the deformation of a closed sack full of steel balls.

When a granular material dilates it is usually accompanied by an increase in shear strength. That is to say part of the shearing force is required to supply work to over come dilatancy while the remainder of the work goes to friction. Taylor (1948) attempted to separate dilatancy from strength measurements. He noticed that the residual strength at high axial strains appeared to be independent of the initial void ratio. At high axial strains the rate of volume change approaches zero, thus eliminating the work going into expansion and leaving only the work due to friction.

Bishop (1954) presented the $(\frac{\delta v}{\delta \epsilon_1})$ term in the equation for triaxial compression:

$$\text{TAN}^2 (45 + \Phi_r/_2) = (\sigma_1'/\sigma_3') - \sigma_3' (\frac{\delta v}{\delta \epsilon_1}) \qquad \text{(II - 3)}$$

where:

Φ_r = the residual angle of friction

σ_1' = major principal stress

σ_3' = minor principal stress

δv = rate of volumetric strain

$\delta \epsilon_1$ = rate of axial strain.

This term in conjunction with σ_3' serves to modify the stress ratio for work going into dilatancy.

Roscoe, Schofield and Thurzirajah (1963) introduced the equation for total energy change:

$$\delta E' = \delta W + \delta U \qquad \text{(II - 4)}$$

where:

$\delta E'$ = total energy change per unit volume

δW = energy dissipated in shear of frictional heat loss

δU = internal stored and recoverable elastic energy

Evaluating this equation for data from tests:

$$\delta E = \sigma'_1 \delta\epsilon_1 + 2\sigma'_3 \delta\epsilon_3 \qquad \text{(II - 5)}$$

where:

$\delta\epsilon_3$ = rate of lateral strain.

This equation represents an energy balance with the first term equal to the rate of energy into the sample and the second term is equal to minus the rate of energy out.

Rowe, Barden, and Lee (1964) recognized four components of energy: 1) friction with no volume change, 2) friction resulting from mass dilatancy, 3) external work due to volume change and, 4) elastic energy. These components were the result of their work on triaxial compression, triaxial extension, and direct shear tests.

The principal strains were divided into two components, one due to sliding and one due to the elastic properties of the material. The elastic component was assumed to be negligible and the following relationship derived (Rowe 1964):

$$\text{TAN}^2 (45 + \Phi/2) = \frac{\sigma'_1}{\sigma'_3 \left[1 - \left(\delta v / \delta\epsilon_1\right)\right]} \qquad \text{(II - 6)}$$

In order to evaluate the effects of frictional interaction and the effects of geometric constraints Tinoco and Handy (1967) used plots of $\frac{\sigma_1}{\sigma_3} - (1 + \frac{\delta v}{\delta\epsilon_1})$ versus $\frac{\sigma_1}{\sigma_3} + (1 + \frac{\delta v}{\delta\epsilon_1})$. The slope of this line is equal to the $\sin\Phi_s$ where Φ_s is the angle of solid friction.

Intercepts or shifts in this line signify the interference parameter Δ_{TC} (see Fig. 1).

Another approach to the study of shearing of granular material is that of particulate mechanics. For this type of analysis a packing of spheres is used with some assumed geometric configuration and forces are applied to the packing. The intergranular forces are then calculated by using equilibrium and compatibility equations based on the elastic behavior of the spheres. Hertz (1881) is responsible for the derivation of the equations for area of contact, normal force distribution and relative displacement. Cataneo (1938) and Mindlin(1949) extended the theory to include tangential forces. A set of compatibility equations can be developed for the packings studied.

Deresewicz (1957) used the compatibility equations to express the stress-strain relationship for a triaxial state of stress. There was a constant lateral stress and cyclic axial stress, on a simple cubic array (see Fig. 2). Duffy and Mindlin (1957) used a face-centered array (Fig. 3) and measured frequencies of vibration as a function of confinning pressure to check elastic modulus calculated from theory. Hendron, Fulton and Mohraz (1963) later used the equilibrium and compatibility equations derived by Duffy and Mindlin as a model for one dimensional strain. The equilibrium and compatibility equations are a system of simultaneous and non-linear differential equations, and Hendron solved them for hydrostatic state of stress and for the one-dimensional strain case.

Armstrong and Dunlap (1966) used a loose planar array, dense planar array, and a loose three dimensional array for prediction curves.. The prediction curves were used for comparisons with the tests on granular limestone gravel. The

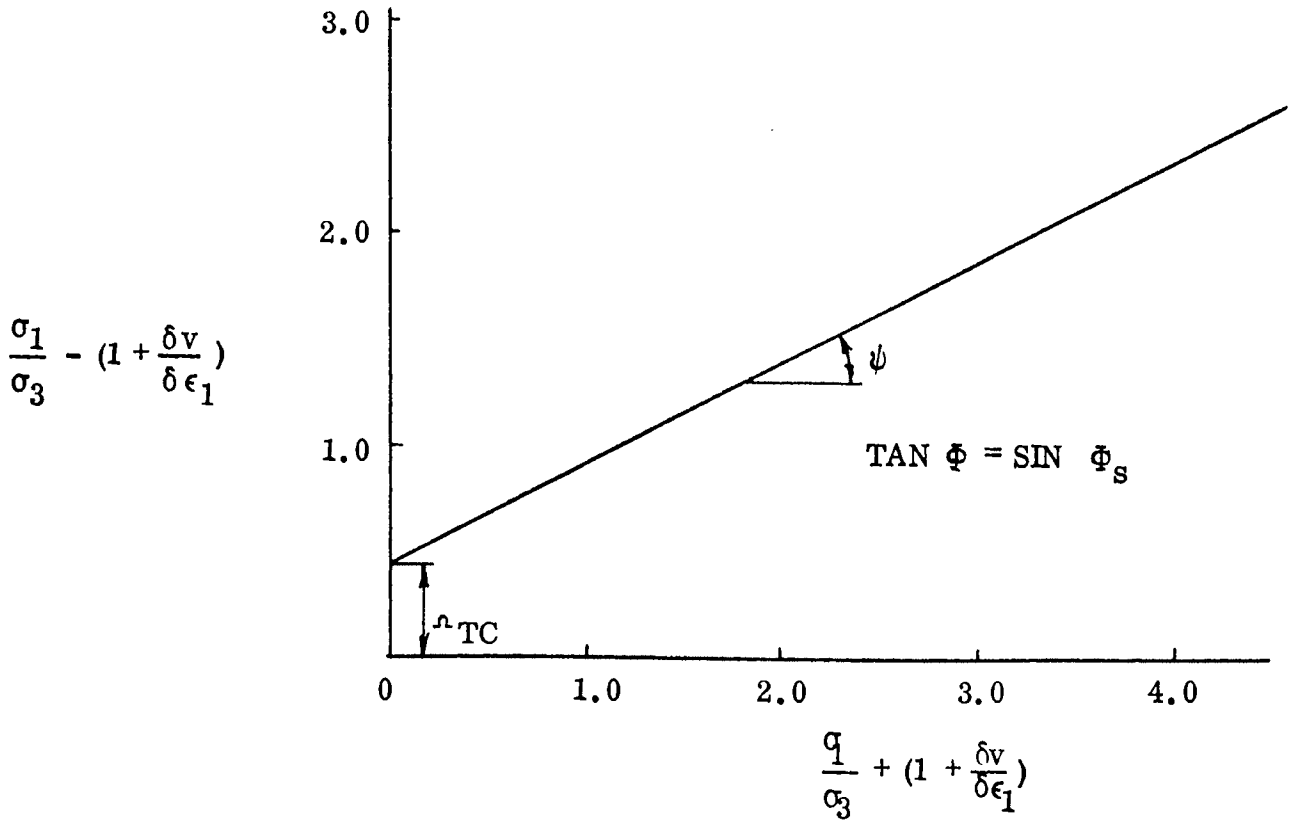

Fig. 1 $\frac{\sigma_1}{\sigma_3} - (1 + \frac{\delta v}{\delta \epsilon_1})$ versus $\frac{\sigma_1}{\sigma_3} + (1 + \frac{\delta v}{\delta \epsilon_1})$

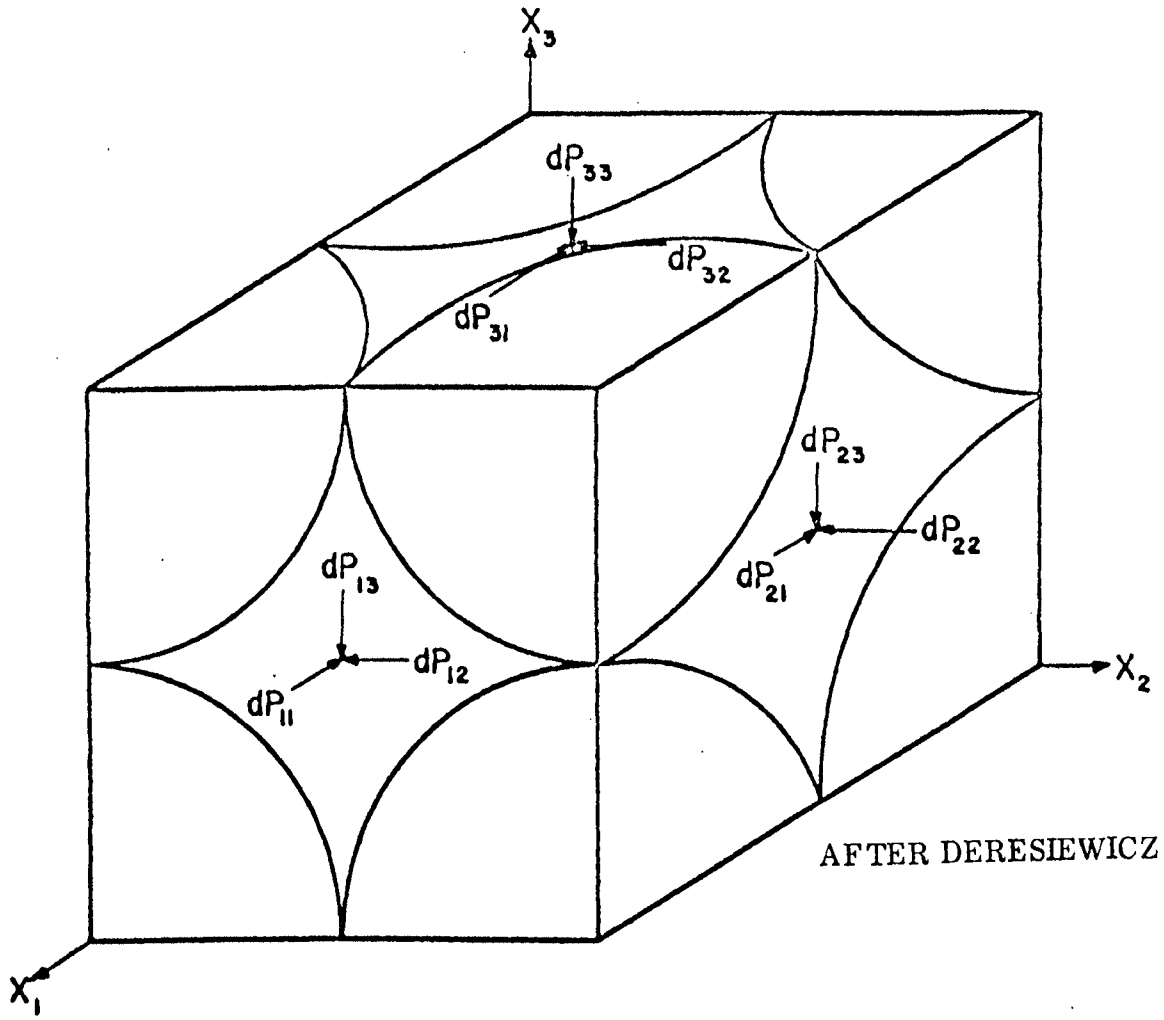

Fig. 2 Simple Cubic Array

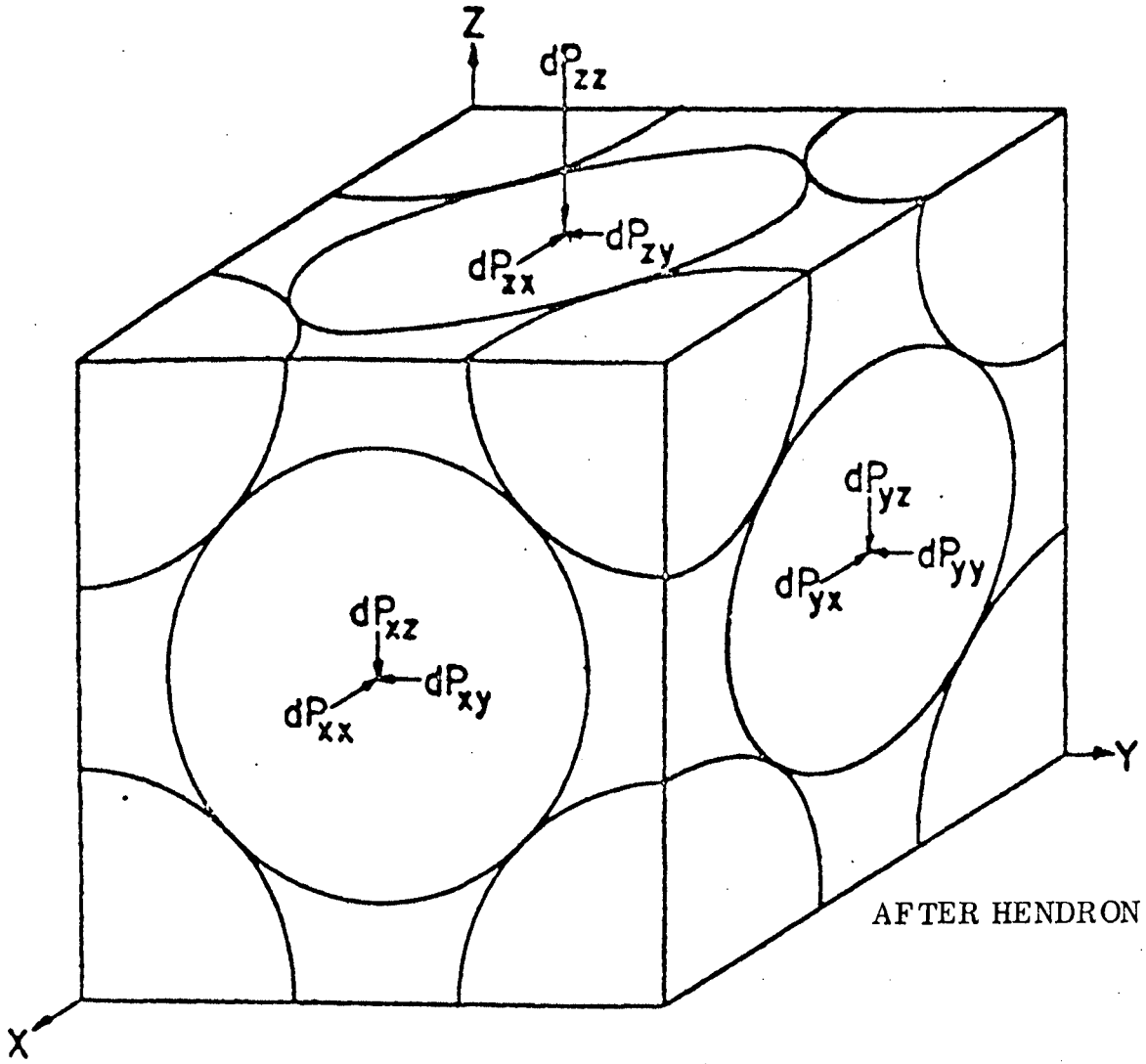

Fig. 3 Face Centered Cubic Array

loose planar array gave the best comparison but on the whole the initial tangent modulus of the stress strain curves was too high for all models considered.

In high pressure triaxial tests Hirschfeld and Poulos (1963) made several observations: 1) failure strain increased with increased cell pressure, 2) at strains above failure the deviator stress decreased pronouncedly, 3) no dilation (increase in volume) was observed at high pressures, 4) and the initial tangent modulus, E_i, increased with confining pressure but not linearly. Hirschfeld also noticed a curved shear envelope, but if the deviator stress was modified by $\frac{\sigma'_1}{1 + \frac{\delta v}{\delta \epsilon_1}} - \sigma'_3$, Rowe's modification for dilatancy, the envelope straightened out.

Bishop (1966) recognized that this reduction in the friction angle with increased cell pressure was most pronounced for materials which were dense and or of uniform grain size. Thus Bishop corroborated the hypothesis that this reduction in friction angle was a result of reduced dilation at higher pressures.

Vesic and Clough (1968) noticed a breakdown stress at high pressures where a soil exhibited a constant ϕ_s and an initial tangent modulus which was proportional to the mean normal stress. Vesic reasoned that these properties were solely dependent on crushing of grains and not on the initial void ratio. In this range of high stress the total area of interparticle contacts remains proportional to applied stress, and are not dependent on the void ratio.

Seed and Lee (1967) observed that drained shear strength is a function of: 1) sliding friction, 2) dilatancy, 3) particle crushing and rearranging. The latter was believed to require additional energy and crushing should increase the friction angle to a value larger than the corrections for dilatancy indicates. This was evident in their tests on Ottawa sand. Figure 4 illustrates the findings

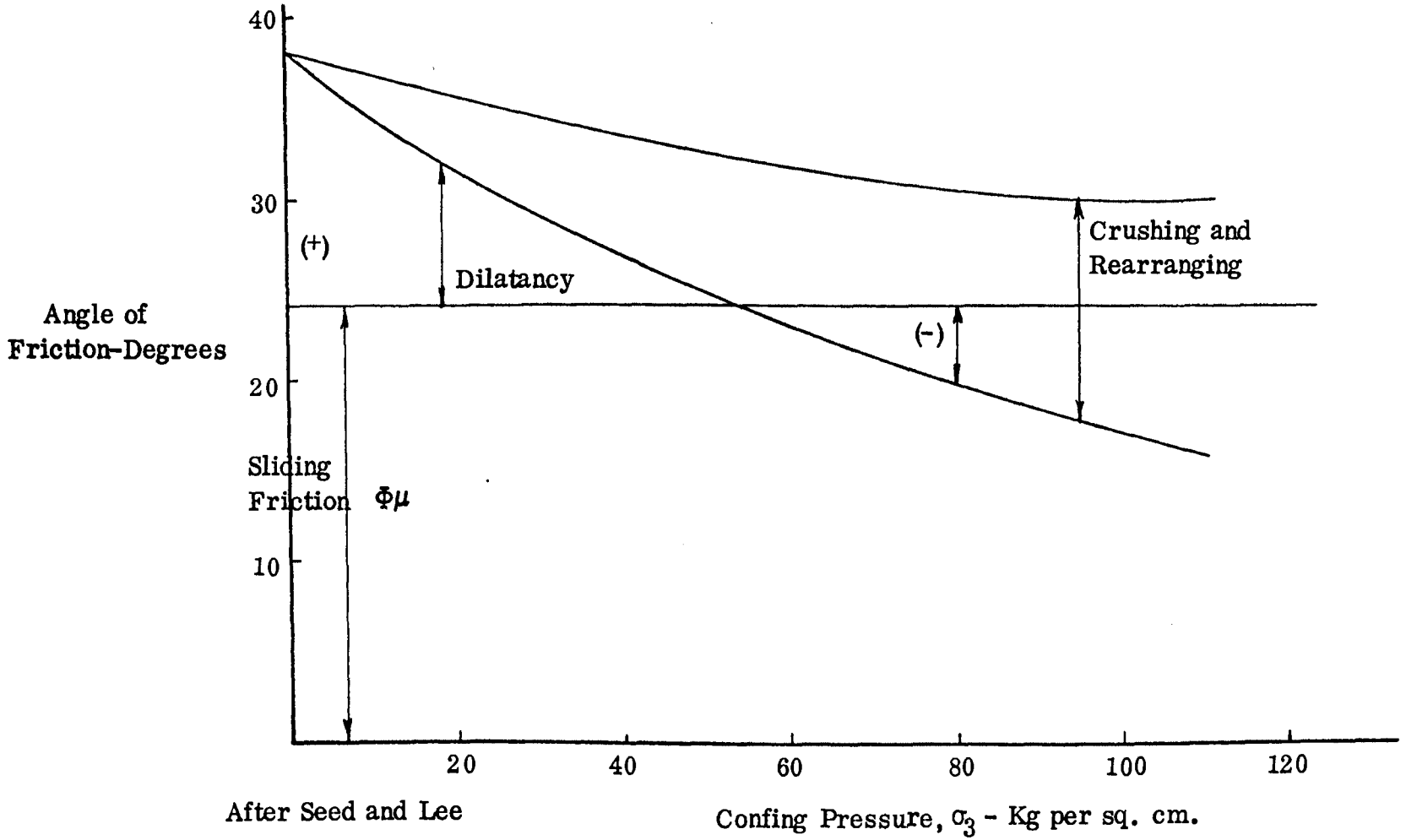

Fig. 4 Effect of Dilatancy and Crushing on the Measured Angle of Internal Friction

of Seed and Lee. For low cell pressures the measured Φ angle is made up of friction and dilatancy. As the confining pressure increases the effect of negative dilatancy reduces the angle to a lower value than that due to friction alone. The effect of crushing and rearranging increases as confining pressure increases and causes the Φ angle to increase. The net affect is a reduction in the total angle of internal friction with increasing confining pressure.

III RESEARCH PROGRAM

A. Soils

In order to examine the previously mentioned theories four materials were selected to compare theory with experimental results. The materials were all granular with a rounded or subrounded grain, and they were selected to obtain variations in void ratio, grain size, and gradation. The materials selected had a range of void ratios from 0.5 to 1.6, with particle sizes ranging from a coarse sand to a coarse silt. See Table 1 for PHYSICAL PROPERTIES.

The first material tested was 20-30 Ottawa sand. This is a quartz sand with uniform rounded grains with all grains passing the number 20 sieve and being retained on the number 30 sieve.

Subsequently a Meramec River sand was used. This sand was sieved on a No. 10 sieve to remove the coarser material which punched holes in the sample membranes. The remainder was largely a rounded and well graded fine silica sand with the coarser fraction being more angular in nature.

The third material tested was a laboratory prepared coarse grained uniform quartz silt. This material was prepared by a grain size separation through sedimentation.

The final material was a residual tailing from a vanadium mine in Arkansas. This material was unique in its characteristically high void ratios (1.0 to 1.6). This peculiarity is probably a result of the chemical treatment which was part of the refining process. The ore was first treated with salt, then fired, and finally leached with sulfuric acid. The result is possibly a grain with high surface activity, and an absorbed water layer indicative of the free drained moisture contents close to 20%.

PHYSICAL PROPERTIES

TABLE I

	Ottawa Sand	Meramec River Sand	Silt	Tailings
G_s	2.67	2.65	2.64	2.77
% Passing				
No. 10 Sieve	100	100		
N0. 20 Sieve	98	86		99
No. 40 Sieve	1	53		83
No. 60 Sieve	1/2	16		53
No. 140 Sieve		1		22
No. 200 Sieve			100	13
10 Microns			16	4
2 Microns				
Initial Void Ratio	0.52-0.74	0.50-0.77	0.81-1.03	1.10-1.55

B. The Testing Program

The testing program consisted of three series of 6 tests for each material. Each series was at either a dense, medium, or loose state and 6 different confining pressures. Table 2 indicates the triaxial test which were performed and the number system which will be used in referring to test results. In addition a grain size analysis was performed on each sample after the test to determine the amount of degradation during testing.

C. Research Equipment and Instrumentation.

The triaxial tests were conducted with Wykeham Farrance equipment. The cell and constant pressure device were both capable of 1500 psi. lateral pressures. A proving ring was used, due to its greater sensitivity, to measure deviator stresses for those tests performed at 50 and 100 psi. cell pressures while a load cell was used on the remainder of the tests. For the high pressure tests a 10 kip load cell was used with load read out on a strain indicator.

An adjustable mercury "U" tube was connected, one end to the base of the sample and the other end to a dash pot (Fig. 5). A constant pressure of 25 psi. was maintained in the dash pot and the mercury was maintained level in the U-tube. The U-tube was adjusted by hand so that the mercury level was held at the same position on both sides. Recordings were made of the adjustments in the U-tube and these values were converted to volume change by the following equation:

$$\Delta V = A \times L \qquad \text{(III - I)}$$

where:

A = cross sectional area of tubing

L = length of tube displacement

NUMBERING SYSTEM FOR TESTS PERFORMED
TABLE II

Material	Cell Press.	Dense	Medium	Loose
Ottawa Sand	50	1 - 1 - 1	1 - 1 - 2	1 - 1 - 3
	100	1 - 2 - 1	1 - 2 - 2	1 - 2 - 3
	200	1 - 3 - 1	1 - 3 - 2	1 - 3 - 3
	400	1 - 4 - 1	1 - 4 - 2	1 - 4 - 3
	800	1 - 5 - 1	1 - 5 - 2	1 - 5 - 3
	1000	1 - 6 - 1	1 - 6 - 2	1 - 6 - 3
Meramec River Sand	50	2 - 1 - 1	2 - 1 - 2	2 - 1 - 3
	100	2 - 2 - 1	2 - 2 - 2	2 - 2 - 3
	200	2 - 3 - 1	2 - 3 - 2	2 - 3 - 3
	400	2 - 4 - 1	2 - 4 - 2	2 - 4 - 3
	800	2 - 5 - 1	2 - 5 - 2	2 - 5 - 3
	1000	2 - 6 - 1	2 - 6 - 2	2 - 6 - 3
Silt	50	3 - 1 - 1	2 - 1 - 2	3 - 1 - 3
	100	3 - 2 - 1	3 - 2 - 2	3 - 2 - 3
	200	3 - 3 - 1	3 - 3 - 2	3 - 3 - 3
	400	3 - 4 - 1	3 - 4 - 2	3 - 4 - 3
	800	3 - 5 - 1	3 - 5 - 2	3 - 5 - 3
	1000	3 - 6 - 1	3 - 6 - 2	3 - 6 - 3
Tailings	50	4 - 1 - 1	4 - 1 - 2	4 - 1 - 3
	100	4 - 2 - 1	4 - 2 - 2	4 - 2 - 3
	200	4 - 3 - 1	4 - 3 - 2	4 - 3 - 3
	400	4 - 4 - 1	4 - 4 - 2	4 - 4 - 3
	800	4 - 5 - 1	4 - 5 - 2	4 - 5 - 3
	1000	4 - 6 - 1	4 - 6 - 2	4 - 6 - 3

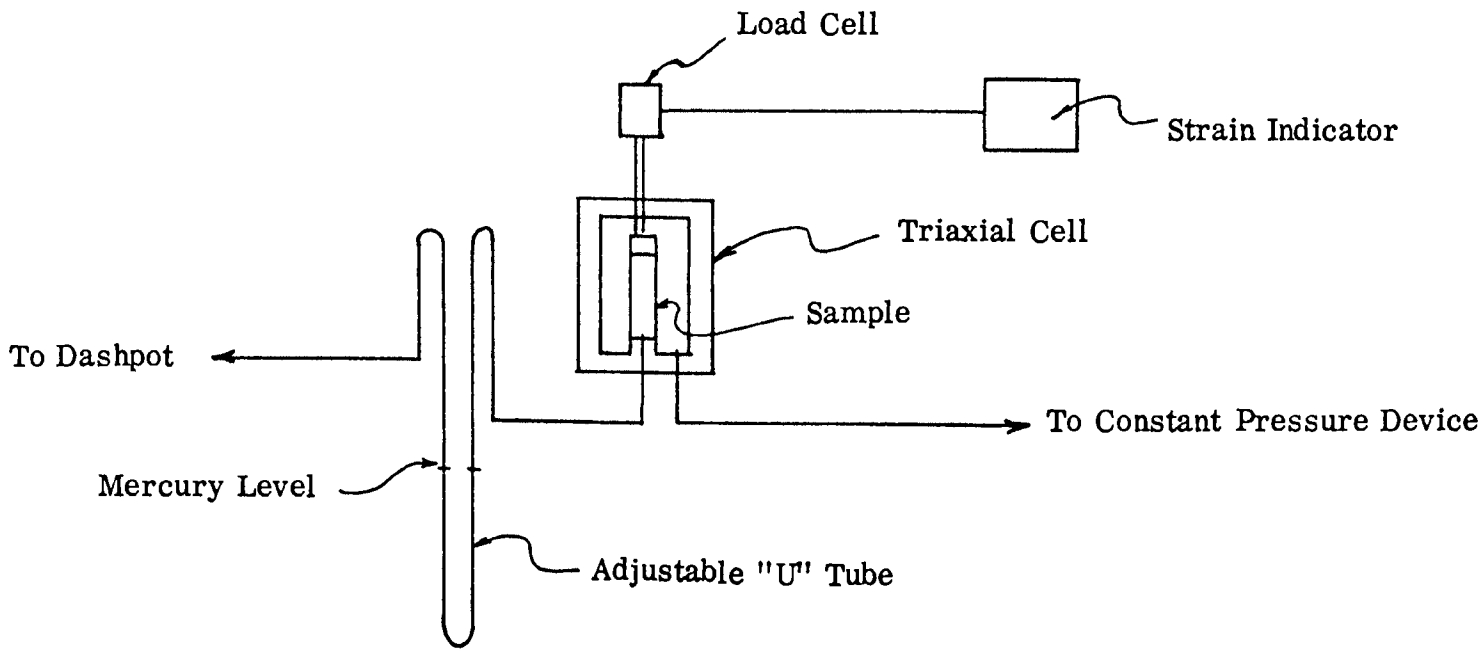

Fig. 5 Equipment Layout

This volume change device had a limiting sensitivity of 0.0001cc. which was compatible with the response of the dash pot.

D. Laboratory Test Procedure

Samples were prepared with a 1.5 in. diameter split sample former. The wet material was placed into the membrane full of water. With the coarse materials, rodding and or vibration was used to achieve the desired densities. With the silt, various negative pressures were applied at the base of the sample to control the rate at which the sample was sedimented and thus controlling the void ratios. After the sample was formed, the loading cap placed, and a small negative pore pressure was applied, the height and diameter of the sample were measured. The cell was then assembled and the sample was ready for testing.

The tests were conducted at deflection rates of 0.005 in/min. to 0.02 in/min. based largely on the convenience of recording data. For this relatively small range in strain rates no strain rate dependent variations were noticed, which is compatible with Whitman' s (1957) results.

IV THEORETICAL DEVELOPMENT

According to Hertz (1881) the radius of contact of two elastic equal radius spheres in compression is:

$$a = \left[\frac{3\,(1-v)\,RN}{8\,\mu}\right]^{1/3} \qquad \text{(IV - 1)}$$

where:

a = the radius of the contact area

v = Poisson's ratio

R = radius of the sphere

N = the normal force

μ = shear modulus

with the relative approach of their centers:

$$d\alpha = c\,dN \qquad \text{(IV - 2)}$$

where:

$$c = \frac{1-v}{2\,a\mu} \qquad \text{(IV - 3)}$$

and

dN = the change in the normal force.

If a tangential shear force is applied the relative displacement of their centers is $d\delta$:

$$d\delta = S\,dT \qquad \text{(IV - 4)}$$

where:

$$S = \frac{2-v}{4\mu a} \qquad \frac{dN}{dT} \geq \frac{1}{f} \qquad \text{(IV - 5)}$$

and

dT = the change in the shear force

to the point where sliding occurs. See Fig. 6 for normal and shearing force

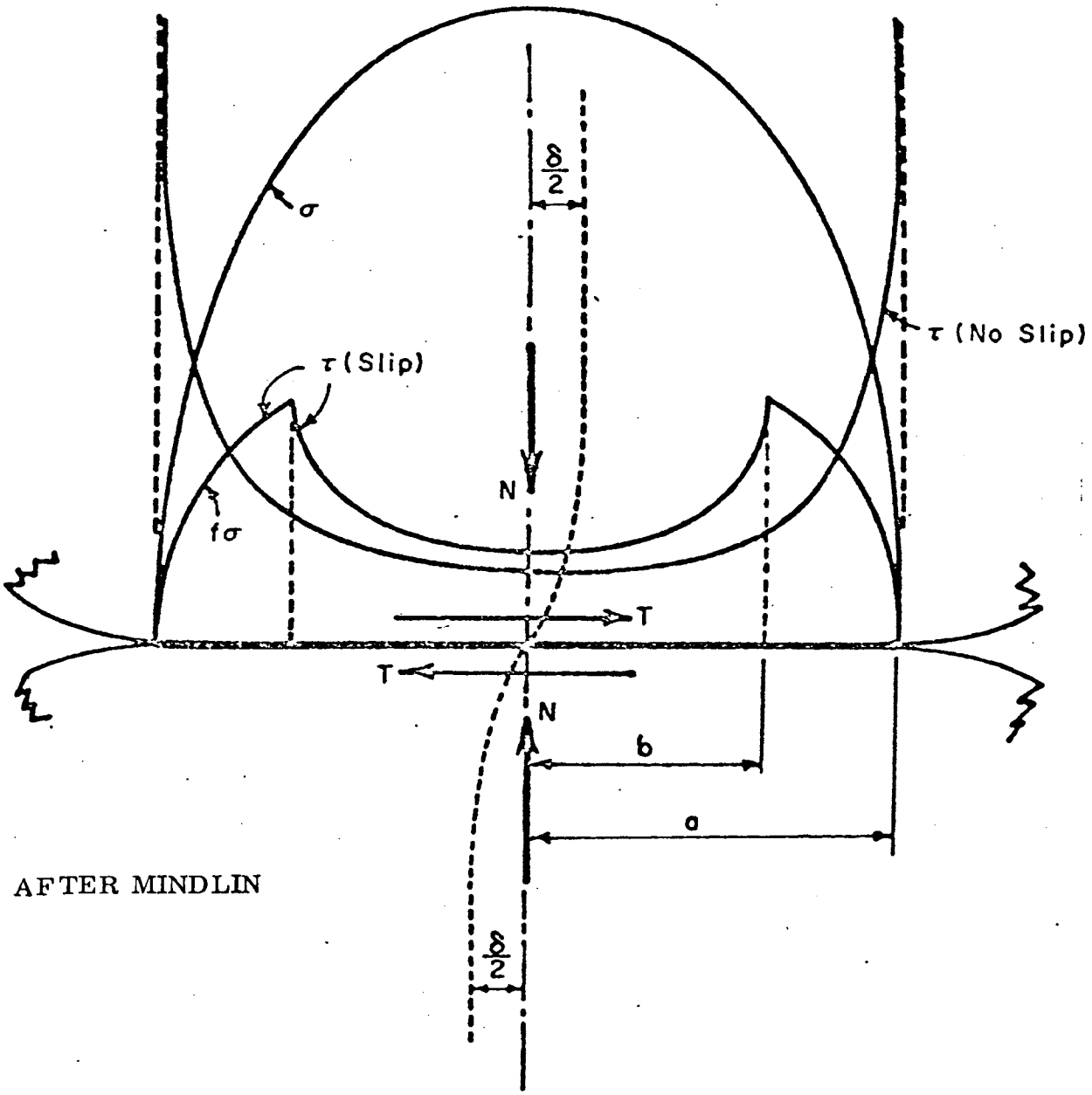

Fig. 6 Normal and Shearing Stress Distribution on Contact Areas

distributions along with the relative displacements. If however, $0 \leq \frac{dN}{dT} \leq \frac{1}{f}$ then

$$S = \frac{2 - v}{4\mu a} \left[f \frac{dN}{dT} + (1 - f \frac{dN}{dT}) (1 - \frac{T}{fN})^{-1/3} \right] \qquad \text{(IV - 6)}$$

The reason for the separate equations stems from the origin of the slip. Slip is movement between two contact surfaces but not over the entire surface of contact, while slide is displacement over the complete contact surface.

Referring to Fig. 6, in the region from the center of the area of contact to a distance, b, from the center there is no slip because $\tau < f\sigma$. From b out to a radius, a, slip occurs because $\tau = f\sigma$. When the normal force increases the radius, b, approaches the radius, a, and compatibility conditions in equation (IV - 5) apply. If the shear force increases, the radius, b, decreases and the compatibility conditions in equation (IV - 6) apply.

Spheres may be placed in a packing as shown in Fig. 3 with force increments applied as shown. In this particular packing each sphere has 12 points of contact with one normal force and two shear components at each point of contact. The notation N_{xy} means the normal force whose components lie in the xy coordinate plane. The tangential forces T_{xy} and T_{zz} lie in and normal to the xy coordinate planes, respectively (Fig. 7). If the direction cosines of the normal force has signs unlike those of the force components, primes are used. From symmetry the contact forces diametrically opposed on each sphere are equal, thus reducing to 18 the number of independent contact forces.

Each octant of the sphere must remain in equilibrium so the octants can be removed as shown in Fig. 8 and three independent equilibrium equations written. With three octants the following nine equations may be written.

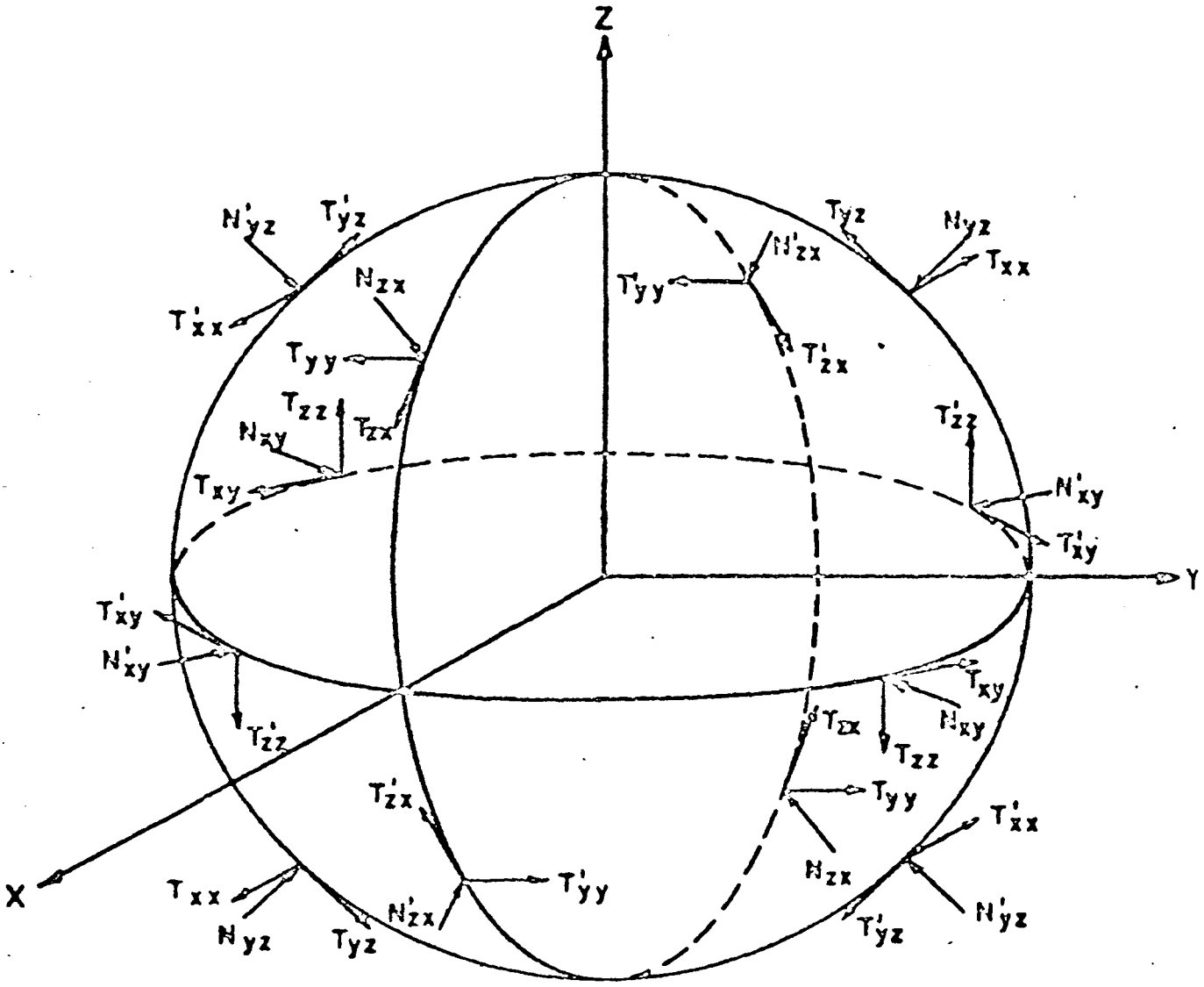

AFTER HENDRON

Fig. 7 Forces Acting on a Typical Sphere

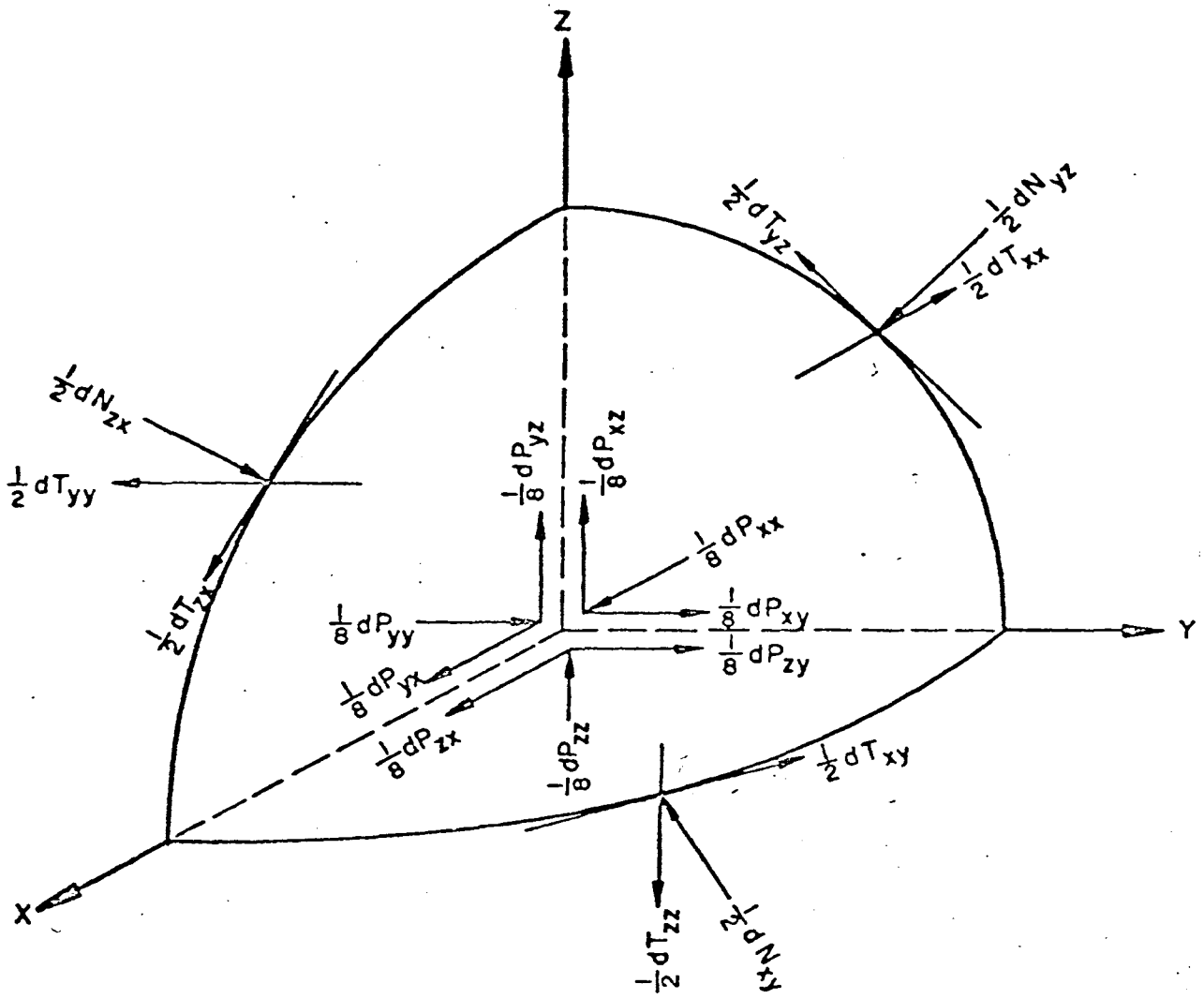

AFTER HENDRON

Fig. 8 Forces Acting on an Octant of a Sphere

$$dP_{xx} + dP_{xy} + dP_{zx} = 4dT_{xx} + 2 \quad (dN_{zx} + dN_{xy} - dT_{zx} + dT_{xy}) \qquad \text{(IV - 7)}$$

$$dP_{yy} + dP_{yz} + dP_{xy} = 4dT_{yy} + 2 \quad (dN_{xy} + dN_{yz} = dT_{xy} + dT_{yz}) \qquad \text{(IV - 8)}$$

$$dP_{zz} + dP_{zx} + dP_{yz} = 4dT_{zz} + 2 \quad (dN_{yz} + dN_{zx} = dT_{yz} + dT_{zx}) \qquad \text{(IV - 9)}$$

$$dP_{xx} + dP_{xy} - dP_{zx} = 4dT'_{xx} + 2 \quad (dN'_{zx} + dN_{xy} - dT'_{zx} + dT_{xy}) \qquad \text{(IV - 10)}$$

$$dP_{yy} + dP_{yz} - dP_{xy} = 4dT'_{yy} + 2 \quad (dN'_{xy} + dN_{yz} - dT'_{xy} + dT_{yz}) \qquad \text{(IV - 11)}$$

$$dP_{zz} + dP_{zx} - dP_{yz} = 4dT'_{zz} + 2 \quad (dN'_{yz} + dN_{zx} - dT'_{yz} + dT_{zx}) \qquad \text{(IV - 12)}$$

$$-dP_{xx} + dP_{xy} + dP_{zx} = 4dT_{xx} - 2 \quad (dN'_{zx} + dN'_{xy} - dT'_{zx} + dT'_{xy}) \qquad \text{(IV - 13)}$$

$$-dP_{yy} + dP_{yz} + dP_{xy} = 4dT_{yy} - 2 \quad (dN'_{xy} + dN'_{yz} - dT'_{xy} + dT'_{yz}) \qquad \text{(IV - 14)}$$

$$-dP_{zz} + dP_{zx} + dP_{yz} = 4dT_{zz} - 2 \quad (dN'_{yz} + dN'_{zx} - dT'_{yz} + dT'_{zx}) \qquad \text{(IV - 15)}$$

The problem is statically indeterminate and compatibility conditions must be written using displacements $d\alpha_{ij}$, $d\delta_{ij}$, and $d\delta_{kk}$ corresponding, respectively, to forces dN_{ij}, dT_{ij}, and dT_{kk}. Summing the relative displacements around a closed path the following nine equations may be written.

$$\sqrt{2}d\delta_{zz} = -d\alpha'_{yz} + d\alpha_{zx} + d\delta'_{yz} + d\delta_{zx} \qquad \text{(IV - 16)}$$

$$\sqrt{2}d\delta_{zz} = d\alpha_{yz} - d\alpha'_{zx} - d\delta_{yz} - d\delta'_{zx} \qquad \text{(IV - 17)}$$

$$\sqrt{2}d\delta'_{zz} = -d\alpha_{yz} + d\alpha_{zx} + d\delta_{yz} + d\delta_{zx} \qquad \text{(IV - 18)}$$

$$\sqrt{2}d\delta_{xx} = -d\alpha'_{zx} + d\alpha_{xy} + d\delta'_{zx} + d\delta_{xy} \qquad \text{(IV - 19)}$$

$$\sqrt{2}d\delta_{xx} = d\alpha_{zx} - d\alpha'_{xy} - d\delta_{zx} - d\delta'_{xy} \qquad \text{(IV - 20)}$$

$$\sqrt{2}d\delta'_{xx} = -d\alpha_{zx} + d\alpha_{xy} + d\delta_{zx} + d\delta_{xy} \qquad \text{(IV - 21)}$$

$$\sqrt{2}d\delta_{yy} = -d\alpha'_{xy} + d\alpha_{yz} + d\delta'_{xy} + d\delta_{yz} \qquad \text{(IV - 22)}$$

$$\sqrt{2}d\delta_{yy} = d\alpha_{xy} - d\alpha'_{yz} - d\delta_{xy} - d\delta'_{yz} \qquad \text{(IV - 23)}$$

$$\sqrt{2}d\delta'_{yy} = -d\alpha_{xy} + d\alpha_{yz} + d\delta_{xy} + d\delta_{yz} \qquad \text{(IV - 24)}$$

The compatibility conditions being a function of force increments as shown:

$$d\alpha_{ij} = C_{ij}dN_{ij} \qquad \text{(IV - 25)} \qquad d\alpha'_{ij} = C_{ij}\,dN'_{ij} \qquad \text{(IV - 28)}$$

$$d\delta_{ij} = S_{ij}dT_{ij} \qquad \text{(IV - 26)} \qquad d\delta'_{ij} = S'_{ij}dT'_{ij} \qquad \text{(IV - 29)}$$

$$d\delta_{ij} = S_{kk}dT_{kk} \qquad \text{(IV - 27)} \qquad d\delta'_{kk} = S'_{kk}dT'_{kk} \qquad \text{(IV - 30)}$$

The result is 18 non-linear simultaneous equations with compliances which are a function of the normal forces.

The normal and shearing strains for the element shown in Fig. 3 may be written as a function of the compliances.

$$d\epsilon_{ii} = \frac{1}{4R}\,(d\alpha_{ij} + d\delta_{ij} + d\alpha'_{ij} + d\delta'_{ij}) \qquad \text{(IV - 31)}$$

$$d\gamma_{ii} = \frac{1}{2R}\,(d\alpha_{ij} - d\alpha'_{ij}) \qquad \text{(IV - 32)}$$

where:

ϵ_{ij} = normal strain along the i axis

δ_{ij} = shear strain in the ij plane

Equations (IV - 7) to (IV - 32) were derived by Duffy and Mindlin (1957). Hendron (1963) solved the equations for only the hydrostatic state of stress and the case of one dimensional strain. With these states of stress several equations could be reduced through knowledge of certain shears, normals, and displacements to facilitate a direct solution.

Using the 18 equations and Hendron' s solution for the hydrostatic state of stress a solution for triaxial compression has been developed. The method first applies a hydrostatic state of stress and calculates the normal forces with Hendron' s solution. With these normals the compliances can be evaluated. An incremental deviator stress is then applied and the 18 simultaneous equations are solved for this stress increment using the compliances from the previous state of stress. This method involves the assumption that the compliances will not appreciably change under the load increment. To justify this assumption a series of 3 tests were performed using increments of stress varying from 4 to 16 psi., and there was a 4% change in the results.

The intergranular forces are then updated by adding the solutions for the differentials to the previous normals and shears. With the new values corrected, compliances may again be evaluated and the operation repeated with an additional increment of stress. The normal and shearing strain increments are also calculated and summed to integrate the total strains.

This operation is repeated with constant checks for sliding between points of contact ($T \geq fN$). At each point of contact the compliances for shear must be checked for $\frac{dN}{dT}$ greater than or less than 1/f so that the appropriate compliance equations may be used.

There is some accumulation of error because the compliance which is used is always the one for the previous load increment; however due to the fact that the compliance is a function of the normal raised to the 1/3 power the change in compliance becomes very small thus introducing little error.

A fortran IV computer solution to these equations for the case of triaxial compression is included in Appendix A.

Two other arrays, which could be computed directly, were used (Armstrong and Dunlap).

A loose three dimensional array shown in Fig. 9.

$$T = 0.940r^2(\sigma_1 - \sigma_3) \quad \text{(IV - 33)}$$

$$N = 0.665r^2\sigma_1 + 1.771r^2\sigma_3 \quad \text{(IV - 34)}$$

The equations for relative displacements are:

$$\delta = [3(2-v)fN / 8\mu a][1 - (1-{}^{T}/_{fN})^{2/3}] \quad \text{(IV - 35)}$$

$$\alpha = 2[3(1-v^2)N/4E]^{2/3} r^{-1/3}. \quad \text{(IV - 36)}$$

The principal strains are:

$$\epsilon_1 = (0.706\delta + 0.5\alpha)/r \quad \text{(IV - 37)}$$

$$\epsilon_3 = (0.66\alpha - 0.47\delta)/r \quad \text{(IV - 38)}$$

where:

ϵ_1 = strain in the σ_1 direction

ϵ_3 = strain in the σ_3 direction.

A dense planar array shown in Fig. 10 (Armstrong 1966).

$$T = R^2(\sigma_1 - 3\sigma_3) \quad \text{(IV - 39)}$$

$$N = \sqrt{3}\,R^2(\sigma_1 + \sigma_3) \quad \text{(IV - 40)}$$

The equations for the relative displacements are:

$$\delta = [3(2 - v)fN / 8\mu a][1 - (1 - {}^{T}/_{fN})^{2/3}] \quad \text{(IV - 41)}$$

$$\alpha = 2a^2/R \quad \text{(IV - 42)}$$

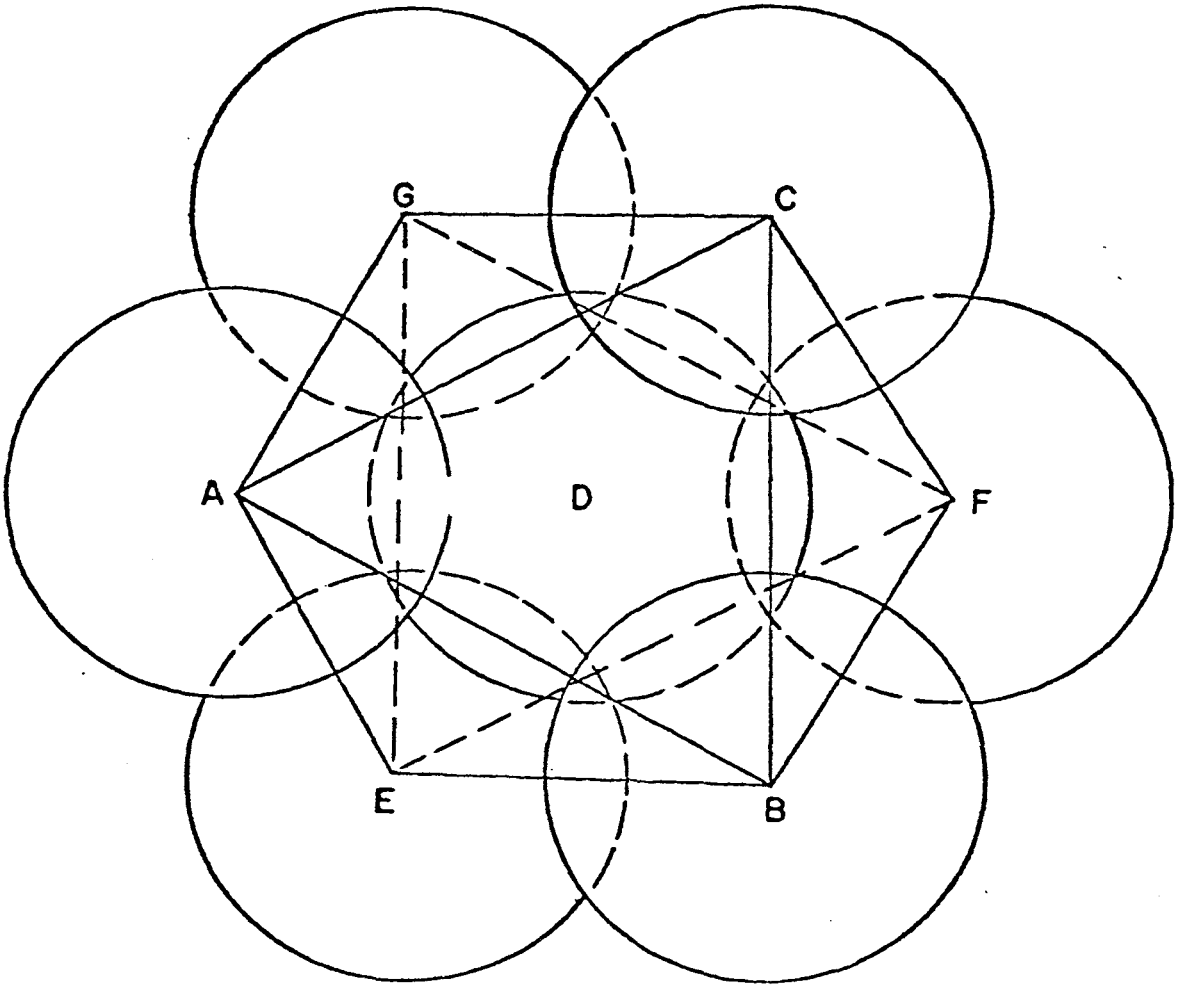

AFTER ARMSTRONG

Fig. 9 Loose Three Dimensional Array

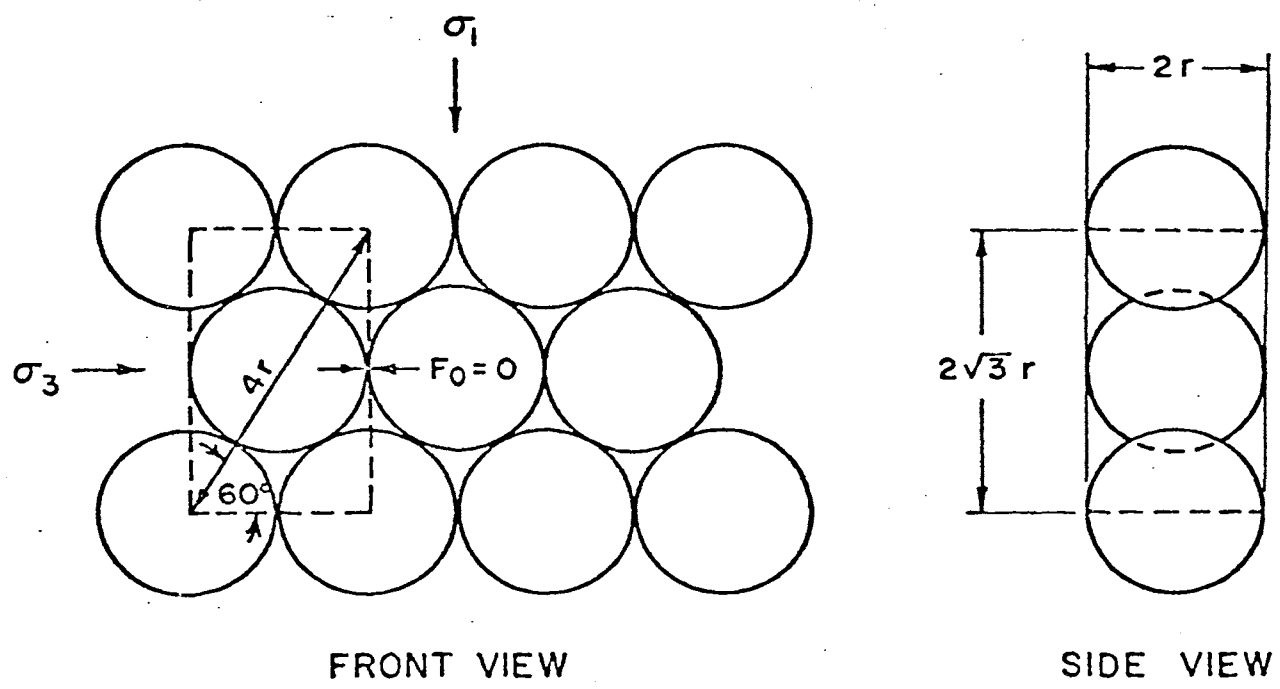

AFTER ARMSTRONG

Fig. 10 Dense Planar Array

The principal strains may be calculated from:

$$\epsilon_1 = \frac{2\delta + 2\sqrt{3}\,\alpha}{4\sqrt{3}\,R} \qquad \text{(IV - 43)}$$

$$\epsilon_3 = \frac{\alpha\sqrt{3}\,\delta}{2R} \,. \qquad \text{(IV - 44)}$$

These equations were also programmed for various physical properties and they produced stress-strain curves used for comparisons with test results.

V DISCUSSION OF TEST RESULTS

A. Parameters for deformation Equations

Several parameters appear in the deformation equations developed in Chapter IV. These paramenters are unique for the material studied, and since all the materials were essentially quartz, typical values from previous studies made by Armstrong and Dunlap (1966) were used. The coefficient of friction was assumed to be 0.4, Poisson's ratio 0.3, and Young's modulus of elasticity 7×10^6 psi. Variations of the coefficient of friction had little effect on the slopes of the stress ratio versus strain curve or the volumetric strain versus axial strain curve, but the magnitude of stress ratio at which sliding occurred was proportional to the coefficient of friction (Fig. 11).

Poisson's ratio had virtually no effect on the stress ratio versus strain curve, but it significantly affected the volumetric strain versus axial strain curve. Increases in Poisson's ratio resulted in greater lateral expansions during shearing, thus less decrease in volume with stresses below the point of sliding (Fig. 12).

Young's modulus of elasticity had the greatest effect on the stress ratio versus strain curve and the volumetric strain versus axial strain curve. Increases in Young's modulus produces proportional increases in the slope of the stress ratio versus strain curve and significant reductions in the magnitude of volume changes (Fig. 13).

B. The Three Dimensional Dense Array

Two dense packings were considered, the first a planar array, and second a three dimensional array. The prediction curves for these two packings

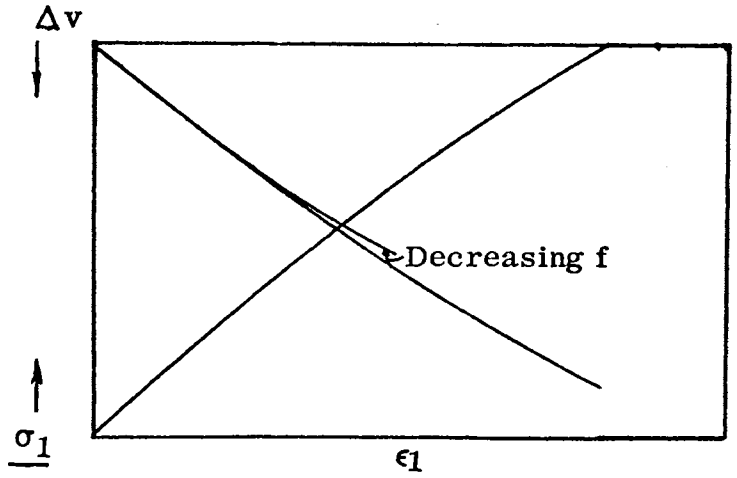

Fig. 11 Effect of Variation in Coefficient of Friction.

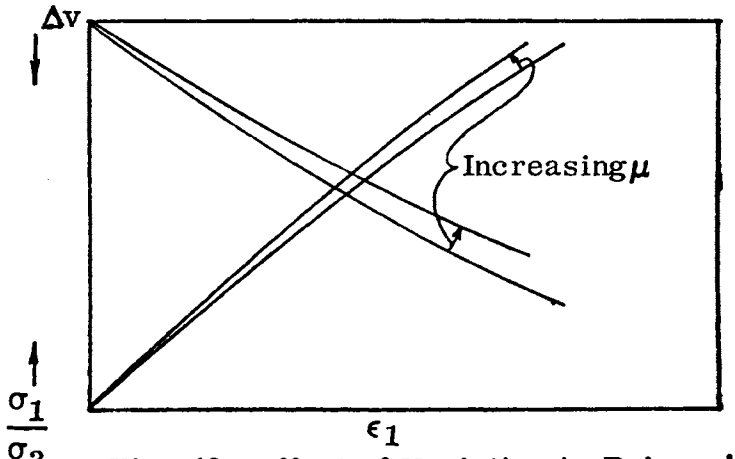

Fig. 12 Effect of Variation in Poisson's Ratio

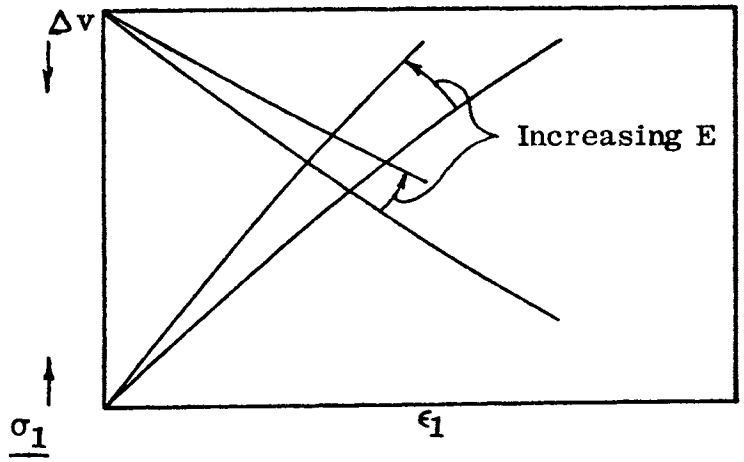

Fig. 13 Effect of Variation in Young's Modulus

were quite similar so only the three dimensional analysis was used. Fig. 14 shows the fan shaped family of stress strain curves resulting from varying the confining pressures. The shape of these curves and their positions relative to one another is about what would be expected for such a series of tests, but the the predicted initial tangent modulii, were 3 to 10 times higher than the values obtained from testing actual soils. The predicted stress ratio versus axial strain curves are slightly curved and exhibited the pronounced effect which confining pressure has on this curve, i.e., the higher the cell pressure the greater the predicted axial strain before sliding occurs.

The volumetric strain versus axial strain curves indicate that for a given axial strain the effect of different cell pressures on the volumetric strain would be small (Fig. 15). The volumetric strain is principally a function of the axial strain. It is also interesting to note that the volumetric strain versus axial strain curve becomes convex to the axial strain axis before sliding occurs. This could be associated with impending dilation.

C. The Three Dimensional Loose Array

The results of the three dimensional loose array prediction curves are shown in Fig. 16. Again a typical fan shaped family of stress-strain curves were calculated for increasing cell pressures. The initial tangent modulii for these curves varied from 3 to 20 times higher than values determined from experimental data.

The results of the loose array were quite similar to the dense array. The stress ratio versus axial strain curves had flatter slopes,and the indication of impending dilation on the volumetric strain versus axial strain curves were slightly more pronounced (Fig. 17).

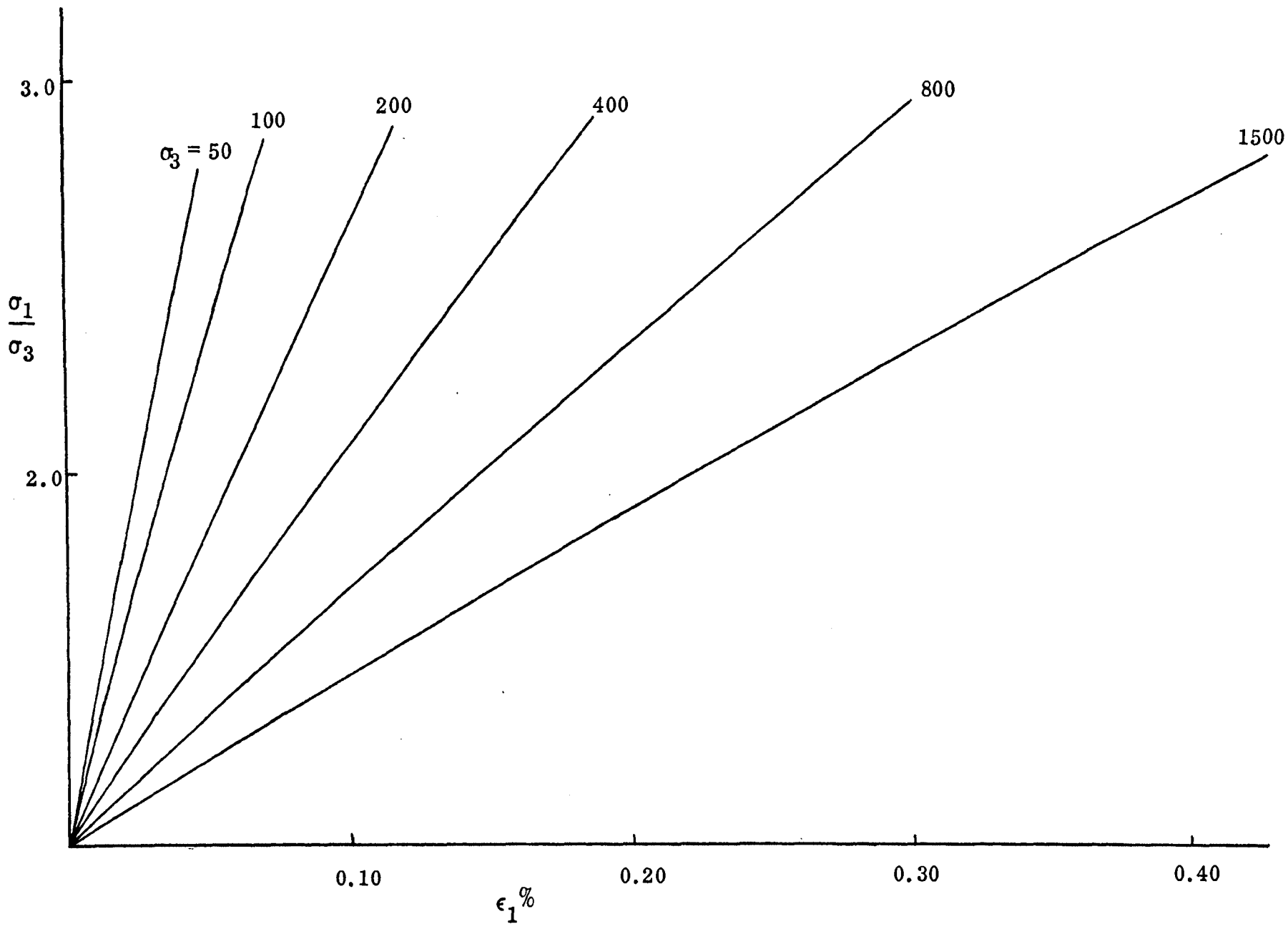

Fig. 14 Predicted $\frac{\sigma_1}{\sigma_3}$ Versus ϵ_1 For Dense Array

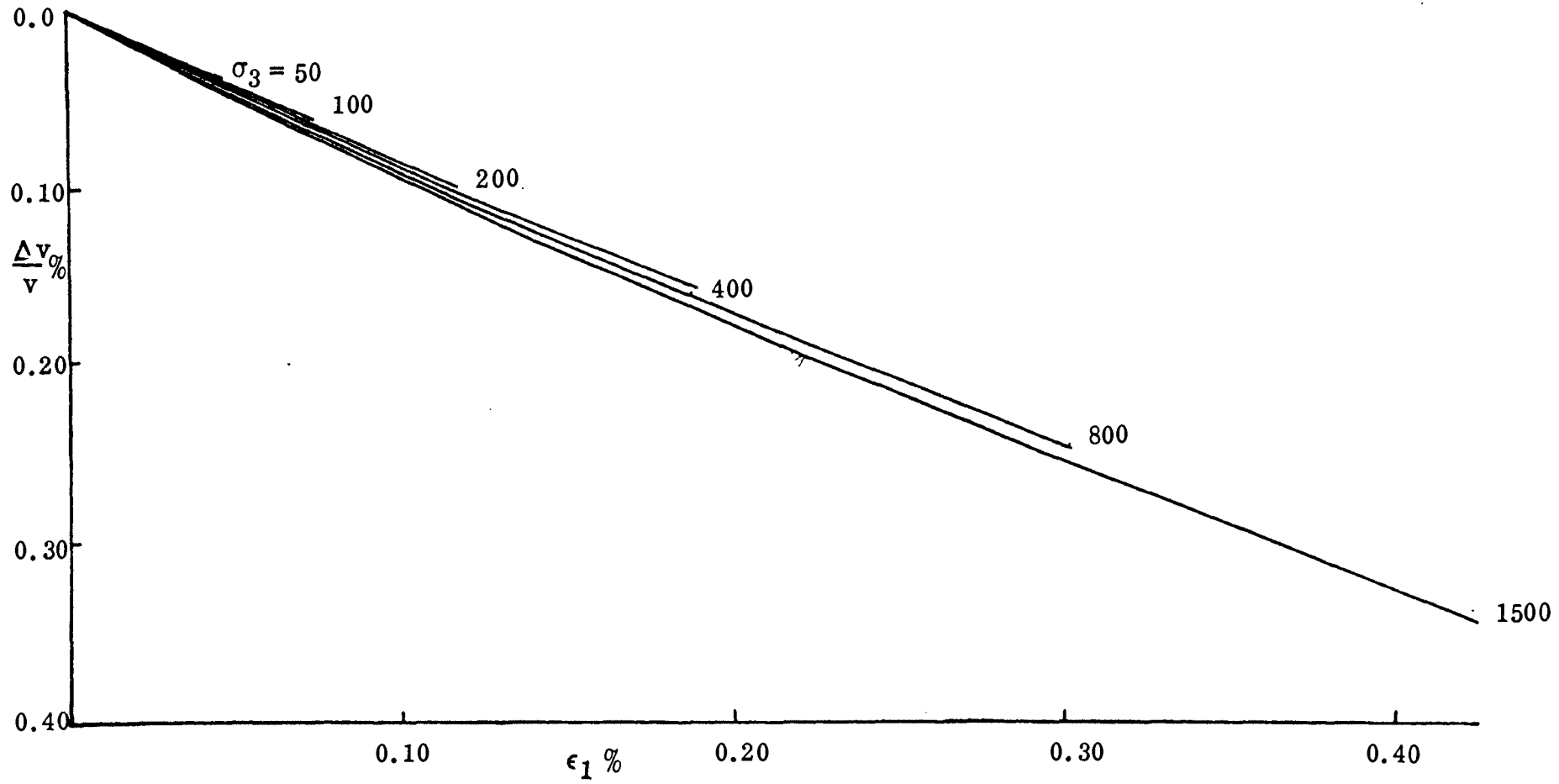

Fig. 15 Predicted $\frac{\Delta v}{v}$ Versus ϵ_1 For Dense Array

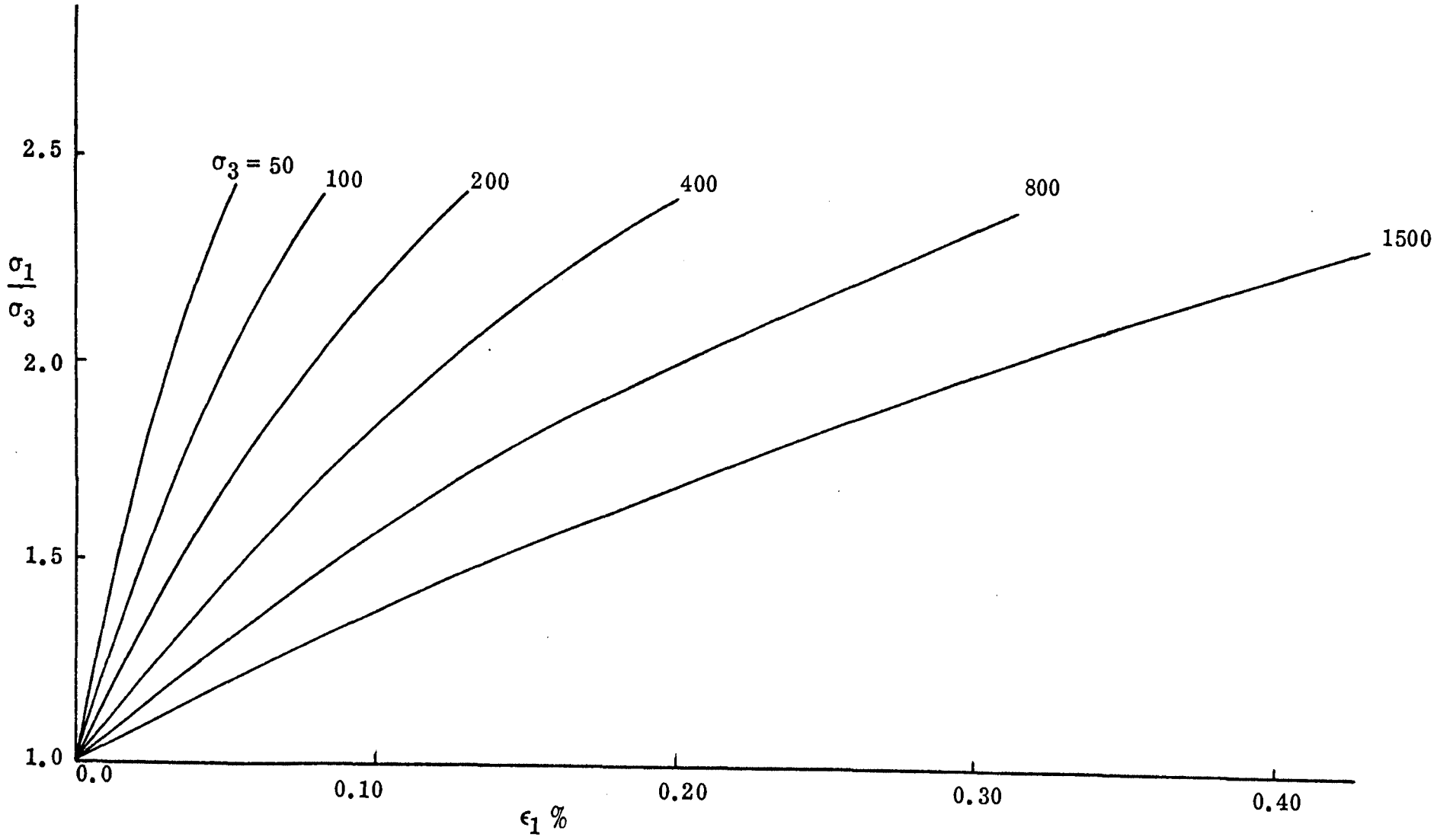

Fig. 16 Predicted $\frac{\sigma_1}{\sigma_3}$ Versus ϵ_1 For Loose Array

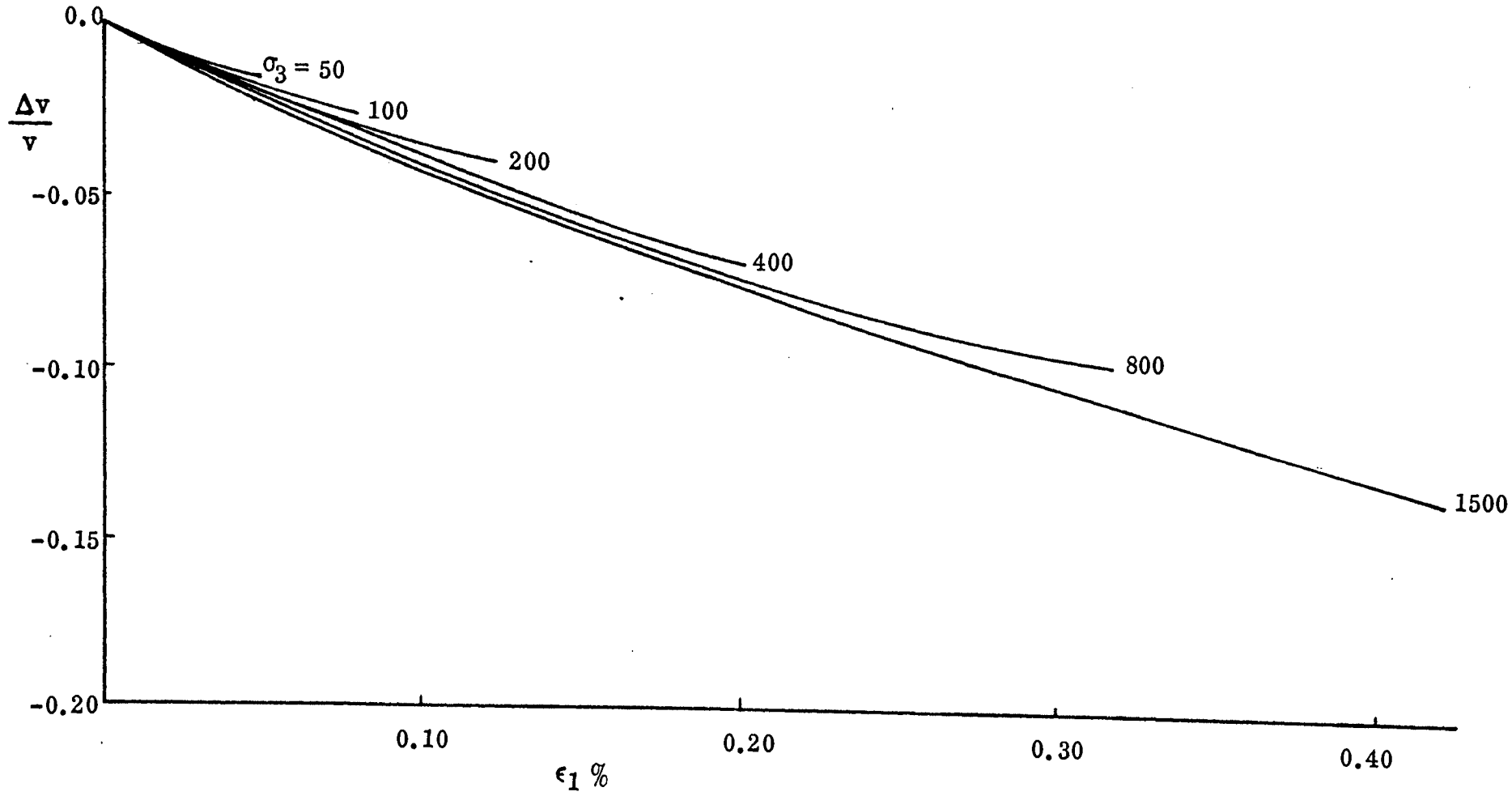

Fig. 17 Predicted $\frac{\Delta v}{v}$ Versus ϵ_1 Loose Array

D. Validity of Prediction Techniques

Examining the characteristic ratios of the predicted initial tangent modulus over the observed initial tangent modulus it appears that the major portion of the axial strain is not dependent on elastic behavior. However, there may be several mechanisms producing axial strain.

There may be particles or groups of particles sliding or rolling at the points of contact. There may also be particles or packings of particles absorbing elastic energy. Finally there may be particles rotating without sliding. All of these mechanisms are probably occurring simultaneously but the extent of their individual effects are difficult to evaluate.

In the problem of an unstable structure, strains would be largely made up of inelastic movements. In this case even though elastic strains are present other types of deformation predominate. If, however, the structure is such that the magnitude of strains is small, elastic strains may constitute a significant portion of the total.

Comparison of the predicted values obtained from analysis of ideally packed arrays to the experimental values reveals that the difference is quite large. This would indicate that the approximate magnitude of elastic strains that occur in the real soil must necessarily be independent of the packing of the real soil. Some other form of deformation may be occurring simultaneously and changing the geometry and the number of contact points, however these changes probably would not change the magnitude of elastic strains. Therefore a reasonable assumption is to consider that other mechanisms of deformation occur simultaneously but the magnitude of elastic strain is not altered.

With a good estimate of elastic strains during shear it is possible to subtract the elastic strains from those observed in the laboratory and to analyze the residual strains in terms of sliding.

E. Experimental Results

Results of the tests performed on the various materials are shown in plots of stress ratio and volumetric strain versus axial strain in Fig. 19 to 29. Both elastic strains and inelastic strains are present in the data. If the elastic strains are accounted for in the data, the remaining strain can be attributed to grain crushing, sliding, rolling and rotation. Grain crushing was not significant below 1500 psi. (Fig. 30 to 33). This means that for the lower confining pressures sliding caused the major part of the inelastic strain. The shaded area in Fig. 19 to 26 represents the approximate elastic portion of each test.

The modification of these curves was accomplished by subtracting the predicted strains from those observed in the laboratory. 1) For a chosen stress ratio a predicted axial strain was subtracted from the observed axial strain and the stress ratio versus modified axial strain curve was replotted. 2) To obtain the volumetric strain versus axial strain plot, predicted axial and volumetric strains were subtracted from those observed in the laboratory at corresponding stress ratios. The resultant volumetric and axial strains were plotted in Fig. 19 to 29.

The deformation equations become indeterminate and cannot be solved when sliding has occurred. At this point, it was assumed that no additional energy was elastically stored in the sample. In other words from the point

where sliding began until failure of the sample, there was no additional increase in elastic volumetric strain and elastic axial strain. The maximum value of the elastic volumetric and axial strains taken at the point where sliding began was removed from the remainder of the observed axial and volumetric data. This resulted in modified strain curves which are a result of sliding friction.

The modified curves were used to compute points on the plot of $\frac{\sigma_1}{\sigma_3} - (1+\frac{\delta v}{\delta \epsilon_1})$ versus $\frac{\sigma_1}{\sigma_3}+(1+\frac{\delta v}{\delta \epsilon_1})$ (Tinoco and Handy 1967). The plot should be a straight line whose slope is dependent of the sliding friction. There seems to be no major change when elastic strain is removed, but the plots of $\frac{\sigma_1}{\sigma_3} - (1+\frac{\delta v}{\delta \epsilon_1})$ versus $\frac{\sigma_1}{\sigma_3} - (1+\frac{\delta v}{\delta \epsilon_1})$ are slightly improved (Fig. 34 to 44).

Several high pressure tests exhibited sharp increases in the slope of $\frac{\sigma_1}{\sigma_3} - (1+\frac{\delta v}{\delta \epsilon_1})$ versus $\frac{\sigma_1}{\sigma_3} - (1+\frac{\delta v}{\delta \epsilon_1})$ near maximum stress ratio which could be the result of grain crushing which would decrease dilation (Fig. 37 to 40).

F. Effects of Void Ratio

Void ratio affects the shape of the stress-strain curve, and the more dense samples, i.e., lower void ratios, exhibit higher initial tangent modulii and lower axial strains at the peak stress ratio. At higher pressure there was little difference in the void ratio after consolidation regardless of the initial void ratio, thus the stress-strain characteristics did not change greatly with changes in initial density.

The initial void ratio does not affect the interparticle friction, where interparticle friction is a material property dependent upon the mineral and the nature of its surface (Bowden and Tabor 1956).

The angle of friction is dependent on the void ratio, and increases in the void ratio bring marked reductions in the angle of internal friction. This is the

same as the results published by Seed and Lee (1967) (Fig 4.).

Volumetric strains change significantly as the void ratio changes. Loose samples have unstable structures with few points of contact. Shear must then decrease the volume until the structure becomes more dense and able to sustain the loads. The more dense samples, however, have a much more stable structure and often expand in volume when sheared. This property called dilation was first recognized by Reynolds (1885).

The high void ratios shown by even the most dense tailing samples were such that modification of experimental data for elastic strains produced no significant change (Fig. 28 & 29). The highly unstable structure of the tailings thus did not work in this type of analysis. High void ratios in many of the silt samples led to similar results (Fig. 25 & 27).

G. Effects of Confining Pressure

Confining pressures produced marked changes from test to test. At high pressures the stress-strain curve becomes more flattened, and required higher strains to reach peak stress ratios. The angle of interparticle friction increased with increasing cell pressure as shown in Fig. 18. The friction values used in this figure were taken from plots of $\frac{\sigma_1}{\sigma_3} - (1 + \frac{\delta v}{\delta \epsilon_1})$ versus $\frac{\sigma_1}{\sigma_3} - (1 + \frac{\delta v}{\delta \epsilon_1})$ with data modified for elastic strains.

This increased friction between grains may be the result of plowing at the points of contact or the absence of rolling or rotation which require less energy.

The percentage of elastic strains is increased with higher cell pressures as shown by the shifts in the plots of stress ratio versus axial strain and the volumetric strain versus axial strain. Therefore, it appears that elasticity

is more important at the higher pressures (Fig. 21 & 23). Plots of $\frac{\sigma_1}{\sigma_3} - (1 + \frac{\delta v}{\delta \epsilon_1})$ versus $\frac{\sigma_1}{\sigma_3} + (1 + \frac{\delta v}{\delta \epsilon_1})$ indicate that sliding appears to be the only major component left in the strain data once it is modified by removing elastic deformations. Thus the amount of elastic deformation is significant if the sample is dense and the cell pressure high.

The overall angle of internal friction decreased, as shown by Seed and Lee (1967), for increases in cell pressure. This result was caused by the reduced effect of dilation.

H. Effects of Grain Size

There appears to be an increase in calculated interparticle friction with reductions in the grain size. All materials were essentially quartz but the interparticle friction angles of silt were much greater than that of Ottawa sand (Fig. 18). This result appears to confirm the suggestions of Rowe (1962). It should be noted, however, that the materials differ in more ways than grain size. The Ottawa sand was very clean while the silt had a fairly large percentage of colloid size particles. These particles could affect the surface of contact and thus alter the interparticle friction. The Meramec river sand had some of these colloids but not in significant quantities. However, the river sand was composed of some rounded grains and some very angular grains, thus indicating possible differences in the mechanisms of shear from the other materials which were composed primarily of rounded grains.

I. Summary of Material Behavior

Ottawa sand clearly showed the effect of reduced dilation at higher confining pressures (Fig. 19 to 21). The predicted strains also made up a

larger portion of the observed strains as the pressure increased (Fig. 21). At 1500 psi. elastic deformation appeared to be quite significant.

The Meramec river sand showed similar results to those of Ottawa sand. Dilation reduced, elastic strains closely approximated the observed strains and intergranular friction increased with increasing cell pressure (Fig. 23 & 24).

The silt, however, experienced such large strains and volume reductions that the magnitude of predicted elastic strains are negligible by comparison. This material also exhibited an increase in intergranular friction with increased cell pressures (Fig. 18).

Like the silt, the tailings were at such high void ratios that predicted elastic strains were not significant (Fig. 28 & 29). However, the tailings showed a slight decrease in the angle of interparticle friction with increased cell pressures (Fig. 18). When the confining pressure exceeded 200 psi., this reduction of interparticle friction was contrary to what would be expected and deserves further study.

J. Testing and Calculation Errors

No allowance was made for machine deflections. It is doubtful that this omission would seriously affect strain readings, but it could be a factor at the high pressures. The most serious calculation errors resulted from the use of divided differences in calculating $(\frac{\delta v}{\delta \epsilon_1})$. Small scatter in either variable tends to produce larger scatter in the plot of $\frac{\sigma_1}{\sigma_3} - (1 + \frac{\delta v}{\delta \epsilon_1})$ versus $\frac{\sigma_1}{\sigma_3} - (1 + \frac{\delta v}{\delta \epsilon_1})$.

The most serious problem in this type of testing is sample uniformity. Constructing two consecutive tests to duplicate results is quite difficult. Some

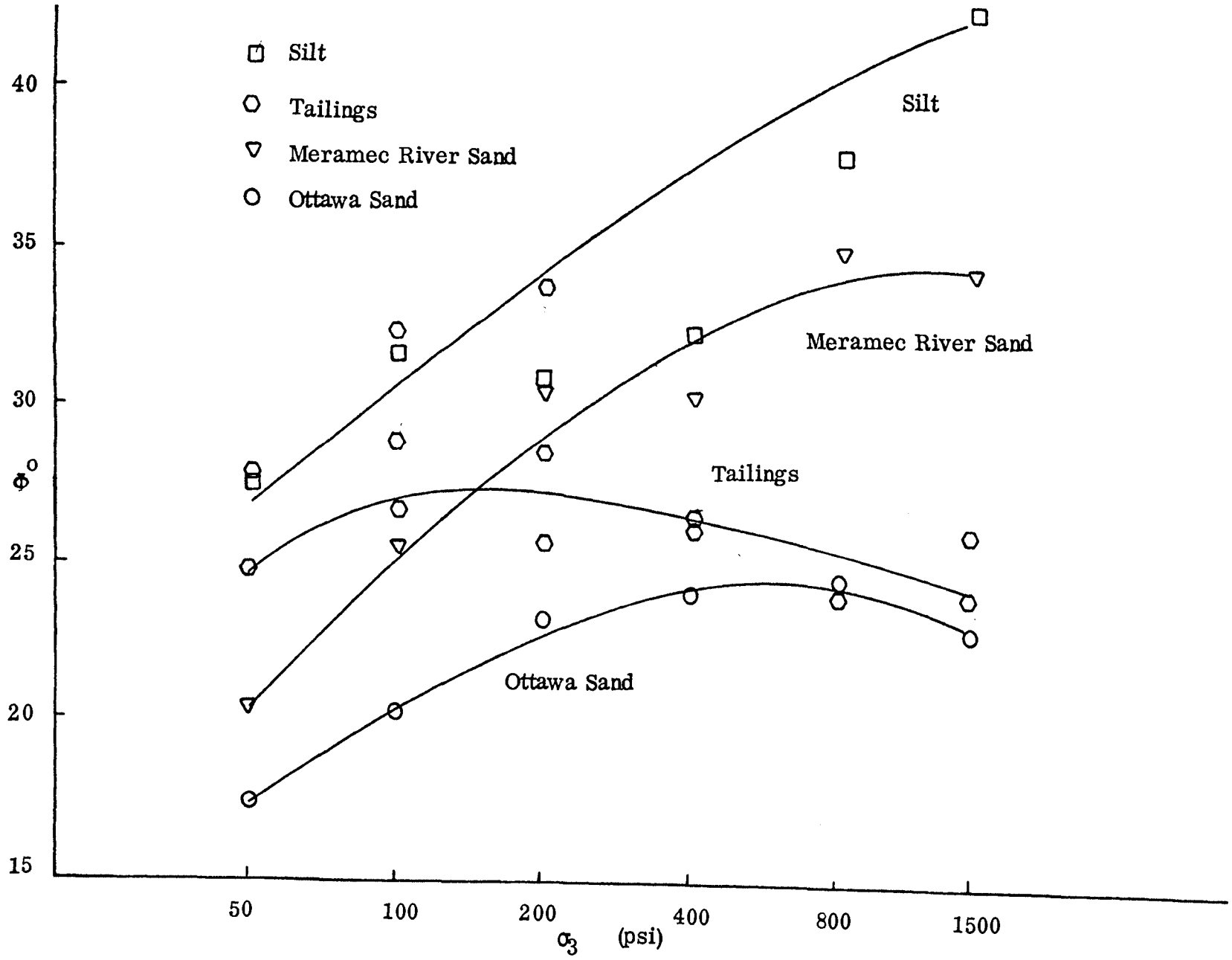

Fig. 18 Effect of Confining Pressure on Intergranular Friction

of the variations in data may be due to problems in controlling void ratio and uniformity within the sample.

VI CONCLUSIONS

Three methods of computing elastic strains based on arrays of equal radii spheres were evaluated. Analysis of the predicted data and the results of integrating this data with observed laboratory data has led to the following conclusions:

1) Duffy and Mindlin' s simultaneous differential equations over predict the initial tangent modulus of a real granular soil and under predicts volume change.

2) The loose three dimensional array used by Armstrong also over predicts the initial tangent modulus and under predicts the volume changes.

3) Elastic strains alone do not adequately describe sample behavior, but if laboratory data is modified for predicted elastic strains the modified data can be adequately analyzed in terms of sliding friction.

4) Sliding friction increased with increased cell pressure for the Ottawa sand, Meramec river sand, and the silt. This increase is a result of the increased plowing at the points of contact.

VII RECOMMENDATIONS

Better techniques in producing uniform samples is desired to improve the reproducibility of test results. Also a computer technique of taking observed data, subtracting predicted elastic strains, and calculating $\frac{\delta v}{\delta \epsilon_1}$ would be of great assistance in speeding up the tedious calculations.

Duffy and Mindlin (1956) measured the velocity of a wave in a packing to calculate a tangent modulus of the packing. It could be possible to shear a soil and simultaneously send waves through the soil and measure the tangent modulus as a function of principal stresses. If the amplitude of the wave is made sufficiently small, the motion will be elastic and contain no sliding. With a plot of E as a function of principal stresses, it would be possible to integrate this curve and calculate the stress ratio versus strain curve on the basis of measured elastic properties of the soil and not with the use of an assumed array.

$$E = f(\sigma_1)$$

$$\therefore \epsilon_1 = \frac{\Delta \sigma_1}{E(\sigma_1)}$$

where:

$E_{(\sigma_1)}$ = Tangent modulus of elasticity evaluated at some σ_1

In other words the change in axial strain for an increment of deviator stress is equal to the change in deviator stress divided by the tangent modulus evaluated at that average principal stress for that increment. This procedure would facilitate a more accurate analysis of elastic and inelastic strains.

VIII APPENDICES

1MAR68 IBM OS/360 BASIC FORTRAN IV (E) COMPILATION

```
      SOLUTION TO DUFFY AND MINDLIN'S EQUATIONS
      DIMENSION A(18,18),B(18),D(18),S(18),C(18),AA(18),Z(18,18)
      DIMENSION BB(18),R(18),Y(18)
      DIMENSION E1(200),E2(200),E3(200),E4(200),E5(200),E6(200),E7(200)
      DIMENSION E8(200),G(18)
      N=18
      R(1)=1.0
      R(2)=1.0
      R(3)=1.0
      R(4)=1.0
      R(5)=1.0
      R(6)=1.0
C     PH=CELL PRESSURE              W=RAIDUS OF SPHERES
C     U=YOUNG'S MODULUS             F=COEFFICENT OF FRICTION
      PH=50.0
      W=0.01
      U=0.30E+07
      V=0.30
      F=0.40
      AP=3.0*W*W
      DNH=PH*AP/(4.0*1.414)
      DO 44 I=1,18
   44 B(I)=0.0
      DO 10 I=7,12
   10 B(I)=DNH
      E1(1)=0.0
      E2(1)=0.0
      E3(1)=0.0
      E4(1)=0.0
      E5(1)=0.0
      E6(1)=0.0
      E7(1)=0.0
      E8(1)=0.0
C     DPXX  DPYY  DPZZ = NORMAL FORCES ON PRINCIPLE PLANES
C     DPXY  DPZX DPYZ = SHEARING FORCES ON PRINPIPLE PLANES
      DPXX=PH*AP
      DPYY=PH*AP
      DPZZ=PH*AP
      DPXY=0.0
      DPZX=0.0
      DPYZ=0.0
      WRITE(3,102)DPXX,DPYY,DPZZ
C     A= COEFFICIENT MATRIX OF SIMULTANEOUS EQUATIONS
      DO 25 I=1,18
      DO 25 J=1,18
   25 A(I,J)=0.0
```

```
      DO 30 I=1,6
   30 A(I,I)=4.0
      DO 35 I=1,3
   35 A(I,I+6)=4.0
      A(7,1)=2.0*(2.0)**(1.0/2.0)
      A(8,1)=A(7,1)
      A(13,1)=-A(7,1)
      A(14,1)=A(7,1)
      A(8,2)=A(7,1)
      A(9,2)=A(7,1)
      A(14,2)=-A(7,1)
      A(15,2)=A(7,1)
      A(7,3)=A(7,1)
      A(9,3)=A(7,1)
      A(13,3)=A(7,1)
      A(15,3)=-A(7,1)
      A(8,4)=A(7,1)
      A(10,4)=A(7,1)
      A(14,4)=A(7,1)
      A(16,4)=-A(7,1)
      A(9,5)=A(7,1)
      A(11,5)=A(7,1)
      A(15,5)=A(7,1)
      A(17,5)=-A(7,1)
      A(7,6)=A(7,1)
      A(12,6)=A(7,1)
      A(13,6)=A(7,1)
      A(18,6)=-A(7,1)
      A(10,7)=-A(7,1)
      A(11,7)=-A(7,1)
      A(16,7)=A(7,1)
      A(17,7)=-A(7,1)
      A(11,8)=-A(7,1)
      A(12,8)=-A(7,1)
      A(17,8)=A(7,1)
      A(18,8)=-A(7,1)
      A(10,9)=-A(7,1)
      A(12,9)=-A(7,1)
      A(16,9)=-A(7,1)
      A(18,9)=A(7,1)
      CP=(1-V)/(2.0*U)
      SP=(2-V)/(4.0*U)
      J=2
C     S=COMPLIANCES FOR SHEAR FORCES
C     C=COMPLIANCES FOR NORMAL FORCES
   13 DO 15 I=7,12
      AA(I)=((3.0*(1-V)*W*D(I))/(8.0*U))**(1.0/3.0)
```

```
   15 C(I)=CP/AA(I)
      WRITE(3,102)(D(I),I=1,18)
      S(1)=SP*R(1)/AA(9)
      S(2)=SP*R(2)/AA(7)
      S(3)=SP*R(3)/AA(8)
      S(4)=SP*R(4)/AA(12)
      S(5)=SP*R(5)/AA(10)
      S(6)=SP*R(6)/AA(11)
      WRITE(3,102)(S(I),I=1,6)
      S(13)=S(2)
      S(14)=S(3)
      S(15)=S(1)
      S(16)=S(5)
      S(17)=S(6)
      S(18)=S(4)

      A(1,13)=-1.414*S(1)
      A(1,14)=A(1,13)
      A(2,16)=-1.414*S(2)
      A(2,17)=A(2,16)
      A(3,10)=-1.414*S(3)
      A(3,11)=A(3,10)
      A(4,15)=-1.414*S(4)
      A(5,18)=-1.414*S(5)
      A(6,12)=-1.414*S(6)
      A(7,10)=C(7)
      A(7,12)=C(7)
      A(7,14)=C(7)
      A(7,15)=-C(7)
      A(8,13)=C(8)
      A(8,15)=C(8)
      A(8,18)=-C(8)
      A(8,17)=C(8)
      A(9,11)=C(9)
      A(9,16)=C(9)
      A(9,18)=C(9)
      A(9,12)=-C(9)
      A(10,11)=-C(10)
      A(10,13)=-C(10)
      A(11,14)=-C(11)
      A(11,16)=-C(11)
      A(12,10)=-C(12)
      A(12,17)=-C(12)
      A(13,10)=S(13)
      A(13,12)=S(13)
      A(13,14)=-S(13)
      A(13,15)=S(13)
      A(14,13)=S(14)
```

```
      A(14,15)=S(14)
      A(14,17)=-S(14)
      A(14,18)=S(14)
      A(15,11)=-S(15)
      A(15,12)=S(15)
      A(15,16)=S(15)
      A(15,18)=S(15)
      A(16,11)=-S(16)
      A(16,13)=S(16)
      A(17,14)=-S(17)
      A(17,16)=S(17)
      A(18,10)=S(18)
      A(18,17)=-S(18)
   16 DO 45 I=1,18
C     Z=THE TRANSPOSE OF A
      DO 45 K=1,18
   45 Z(K,I)=A(I,K)
C     B=PRODUCT MATRIX
      B(1)=DPXX+DPXY+DPZX
      B(2)=DPYY+DPYZ+DPXY
      B(3)=DPZZ+DPZX+DPYZ
      B(4)=DPXY+DPXY-DPZX
      B(5)=DPYY+DPYZ-DPXY
      B(6)=DPZZ+DPZX-DPYZ
      B(7)=-DPXX+DPXY+DPZX
      B(8)=-DPYY+DPYZ+DPXY
      B(9)=-DPZZ+DPZX+DPYZ
      DO 17 I=10,18
   17 B(I)=0.0
      WRITE(3,102)(B(I),I=1,18)
      DO 19 I=1,18
   19 BB(I)=B(I)
C     SIMQ YIELDS SOLUTION TO SIMULTANEOUS EQUATIONS
      CALL SIMQ(Z,B,N,KS)
      IF(KS)99,1,99
    1 WRITE(3,102)(B(I),I=1,18)
   21 DO 130 I=1,18
  130 G(I)=0.0
C     G=CHECK ON SOLUTION BY RECALCUATION OF PRODUCT MATRIX
      DO 125 I=1,18
      DO 125 II=1,18
  125 G(I)=G(I)+A(II,I)*B(II)
      WRITE(3,102)(G(I),I=1,18)
      IF(ABS((B(8)-D(8))/D(8))-0.01)91,14,14
C     D=UPDATED VALUES OF INTERGRANULAR FORCES
   14 DO 12 I=1,18
   12 D(I)=B(I)+D(I)
```

```
      WRITE(3,102)(D(I),I=1,18)
      GO TO 92
   99 WRITE(3,103)KS
      GO TO 2
C     T7=TANGENTAL FORCES AT POINTS OF CONTACT
   92 T7=SQRT(D(2)*D(2)+D(13)*D(13))
C     CHECK FOR SLIDING
      IF(T7-ABS(F*D(7)))89,299,299
   89 T8=SQRT(D(3)*D(3)+D(14)*D(14))
      IF(T8-ABS(F*D(8)))88,299,299
   88 T9=SQRT(D(1)*D(1)+D(15)*D(15))
      IF(T9-ABS(F*D(9)))87,299,299
   87 T10=SQRT(D(5)*D(5)+D(16)*D(16))
      IF(T10-ABS(F*D(10)))86,299,299
   86 T11=SQRT(D(6)*D(6)+D(17)*D(17))
      IF(T11-ABS(F*D(11)))85,299,299
   85 T12=SQRT(D(4)*D(4)+D(18)*D(18))
      IF(T12-ABS(F*D(12)))66,299,299
  299 WRITE(3,105)
      GO TO 2
C     CHECK IF 0<DN/DT<1/F AND USE APPROPRIATE COMPLIENCE
   66 SS=F*ABS(B(7)/SQRT(B(2)*B(2)+B(13)*B(13)))
      IF(SS-1.0)71,72,72
   71 IF(B(7))172,171,171
  172 SS=-SS
  171 B(2)=SS+(1.0-SS)/((1.0-T7/(F*D(7)))**(1.0/3.0))
      GO TO 73
   72 B(2)=1.0
   73 SS=F*ABS(B(8)/SQRT(B(3)*B(3)+B(14)*B(14)))
      IF(SS-1.0)74,75,75
   74 IF(B(8))175,174,174
  175 SS=-SS
  174 B(3)=SS+(1.0-SS)/((1.0-T8/(F*D(8)))**(1.0/3.0))
      GO TO 76
   75 B(3)=1.0
   76 SS=F*ABS(B(9)/SQRT(B(1)*B(1)+B(15)*B(15)))
      IF(SS-1.0)77,78,78
   77 IF(B(9))178,177,177
  178 SS=-SS
  177 B(4)=SS+(1.0-SS)/((1.0-T9/(F*D(9)))**(1.0/3.0))
      GO TO 79
   78 B(1)=1.0
   79 SS=F*ABS(B(10)/SQRT(B(5)*B(5)+B(16)*B(16)))
      IF(SS-1.0)80,81,81
   80 IF(B(10))181,180,180
  181 SS=-SS
  180 B(5)=SS+(1.0-SS)/((1.0-T10/(F*D(10)))**(1.0/3.0))
```

```
      GO TO 82
   81 B(5)=1.0
   82 SS=F*ABS(B(11)/SQRT(B(6)*B(6)+B(17)*B(17)))
      IF(SS-1.0)83,84,84
   83 IF(B(11))184,183,183
  184 SS=-SS
  183 B(6)=SS+(1.0-SS)/((1.0-T11/(F*D(11)))**(1.0/3.0))
      GO TO 69
   84 B(6)=1.0
   69 SS=F*ABS(B(12)/SQRT(B(4)*B(4)+B(18)*B(18)))
      IF(SS-1.0)68,67,67
   68 IF(B(12))168,167,167
  168 SS=-SS
  167 B(4)=SS+(1.0-SS)/((1.0-T12/(F*D(12)))**(1.0/3.0))
      GO TO 91
   67 B(4)=1.0
C     CALCULATE STRAINS
   91 E1(J)=(B(8)*C(8)+B(14)*S(14)+B(11)*C(11)+B(17)*S(17))/(4.0*W)+E1(J
     2-1)
      E2(J)=(B(9)*C(9)+B(15)*S(15)+B(12)*C(12)+B(18)*S(18))/(4.0*W)+E2(J
     2-1)
      E3(J)=(B(7)*C(7)+B(13)*S(13)+B(10)*C(10)+B(16)*S(16))/(4.0*W)+E3(J
     2-1)
      E4(J)=(B(8)*C(8)-B(11)*C(11))/(2.0*W)+E4(J-1)
      E5(J)=(B(9)*C(9)-B(12)*C(12))/(2.0*W)+E5(J-1)
      E6(J)=(B(7)*C(7)-B(10)*C(10))/(2.0*W)+E6(J-1)
      E7(J)=E1(J)+E2(J)+E3(J)
      E8(J)=E8(J-1)+2.0
      WRITE(3,203)E1(J),E2(J),E3(J),E4(J),E5(J),E6(J),E7(J),E8(J)
      J=J+1
C     INCREMENT DEVIATOR STRESS
      DPXX=2.0*AP
      DPYY=0.0
      DPZZ=0.0
      GO TO 13
    2 CONTINUE
      J=J-1
      CALL PPLT(E1,E8,J)
      WRITE(3,200)

      CALL PPLT(E1,E7,J)
      WRITE(3,201)
      CALL PPLT(E1,E2,J)
      WRITE(3,202)
  200 FORMAT(//20X'STRESS  STRAIN')
  201 FORMAT(//20X'VOL. STRAIN  V.S.  AXIAL STRAIN')
  202 FORMAT(//20X'LAT. STRAIN  V.S.  AXIAL STRAIN')
  203 FORMAT(8E14.5)
```

```
  102 FORMAT(6E15.6)
  103 FORMAT(//20X'KS N.C.')
  105 FORMAT(//20X'SLIDDING HAS OCCURED')
      STOP
      END

        SIZE OF COMMON  000000    PROGRAM  015468

                        END OF COMPILATION  MAIN
```

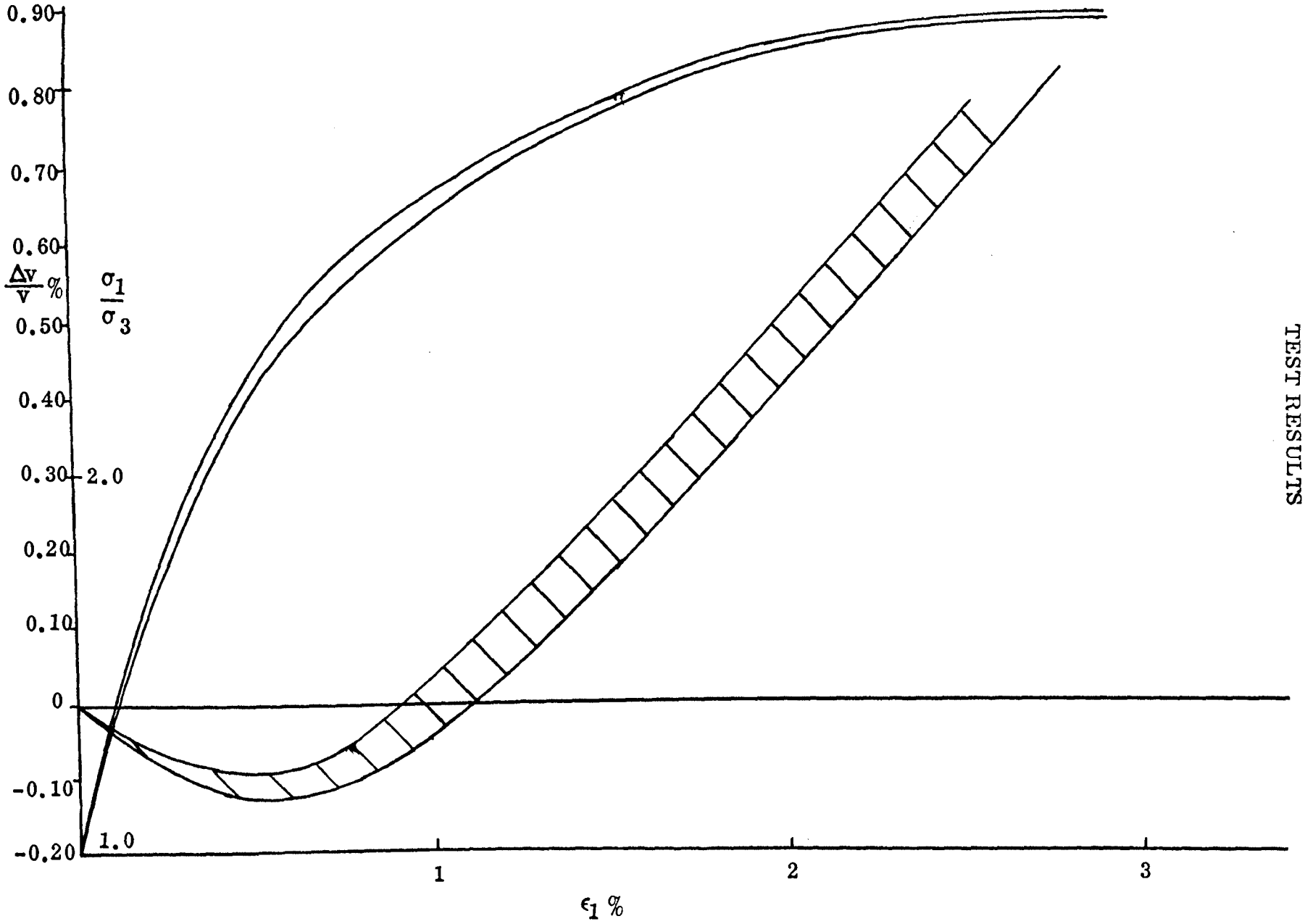

Fig. 19 Results of Test 1 - 2 - 1

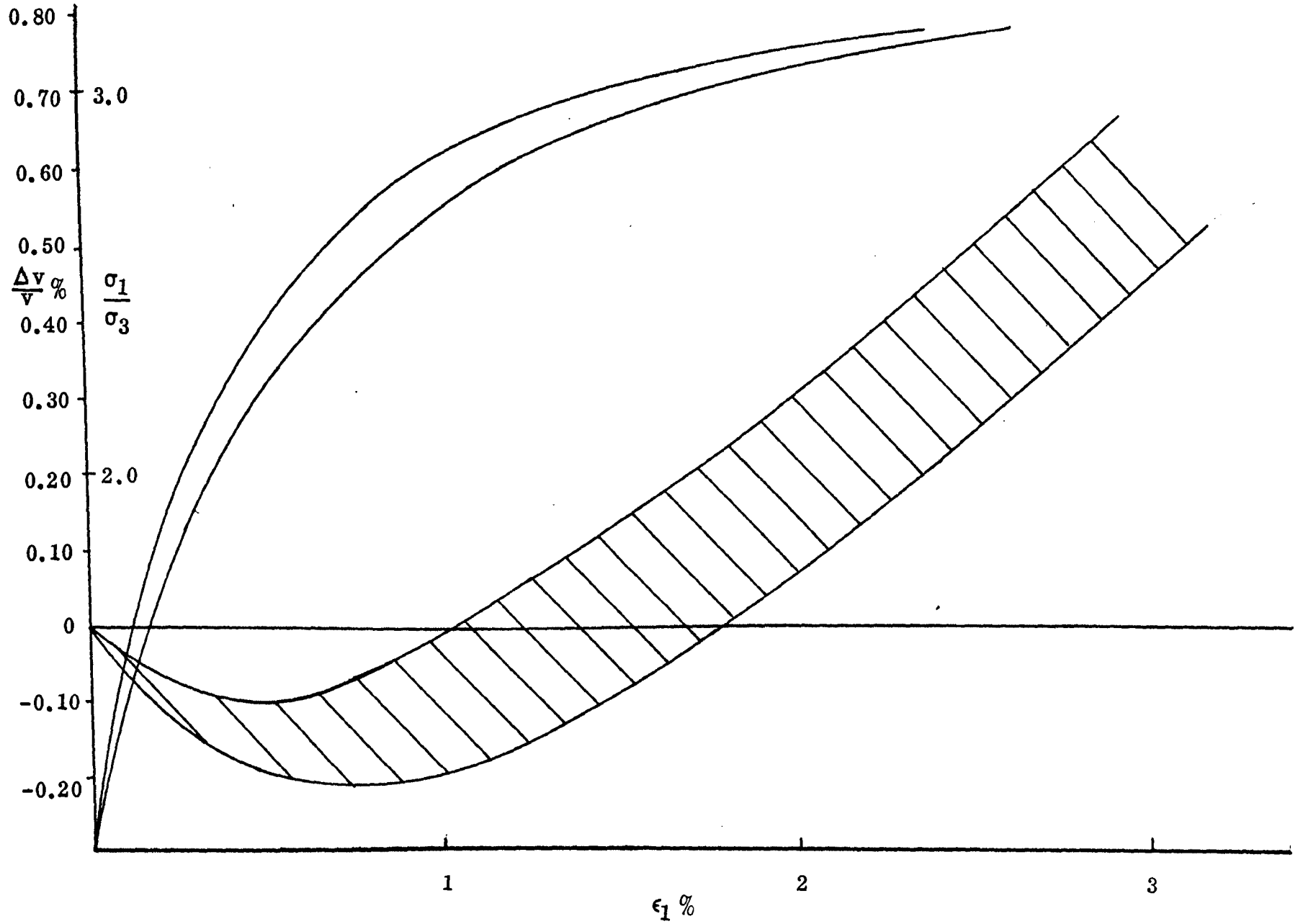

Fig. 20 Results of Test 1 - 4 - 1

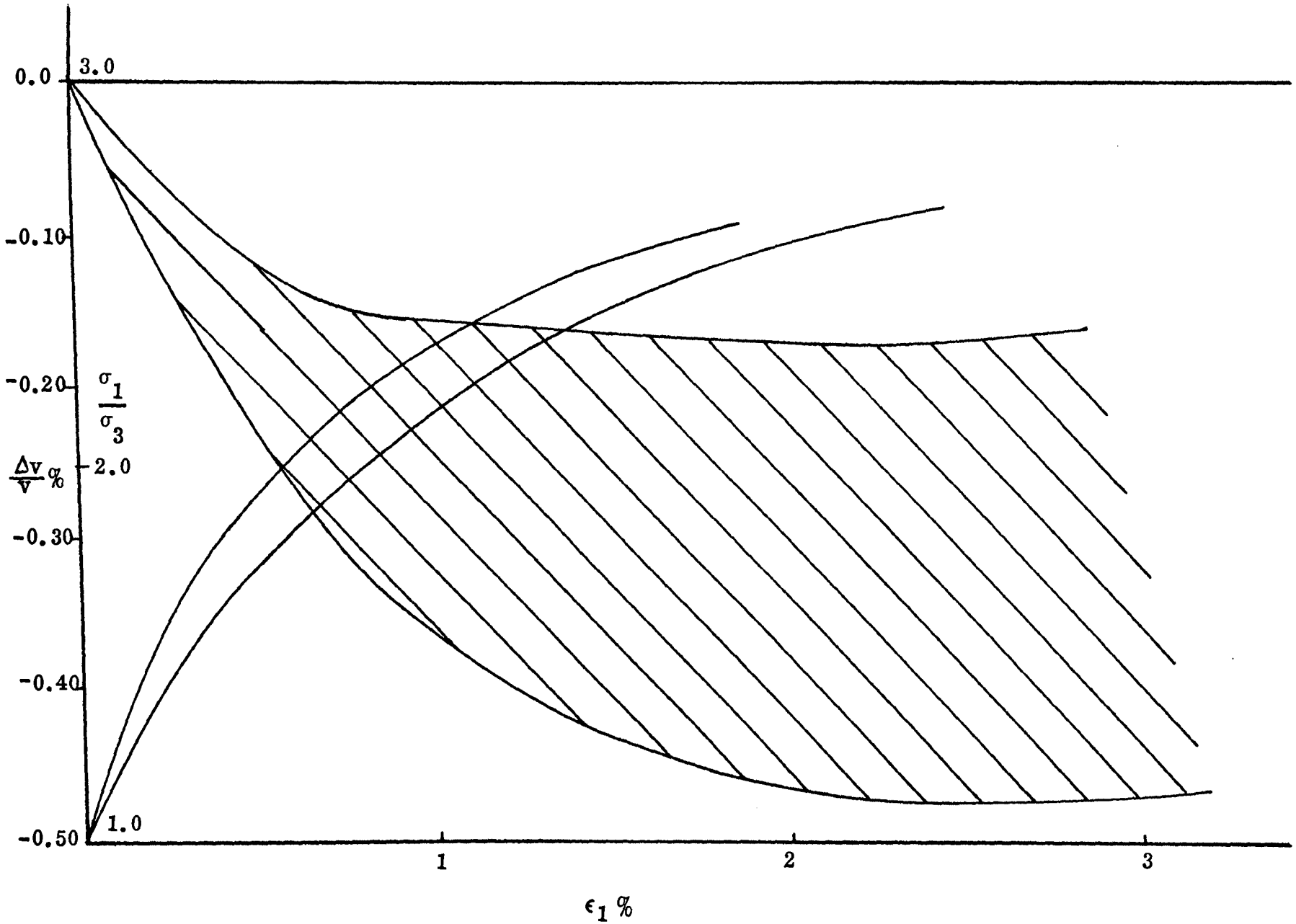

Fig. 21 Results of Test 1 - 6 - 1

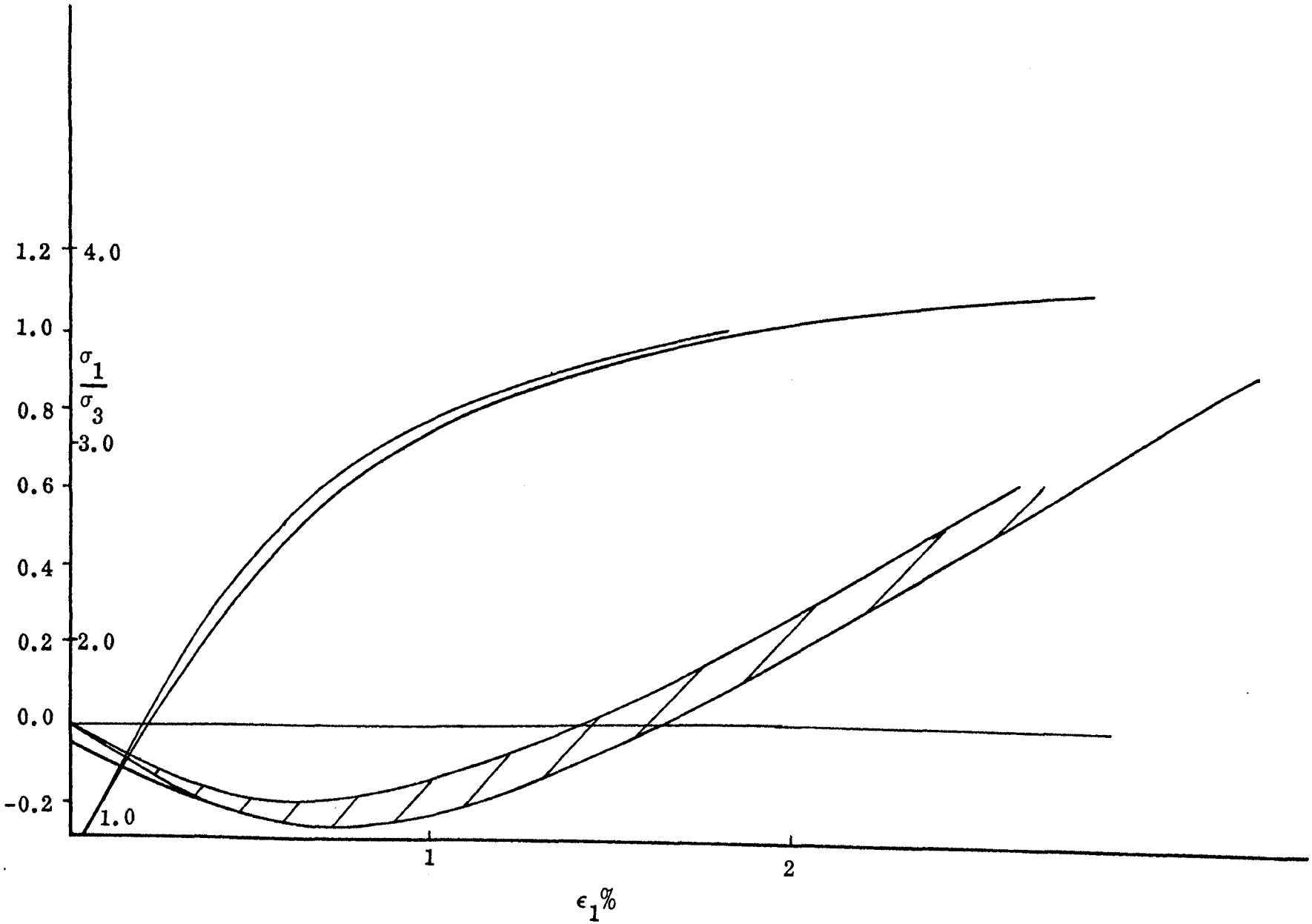

Fig. 22 Results of Test 2 - 2 - 2

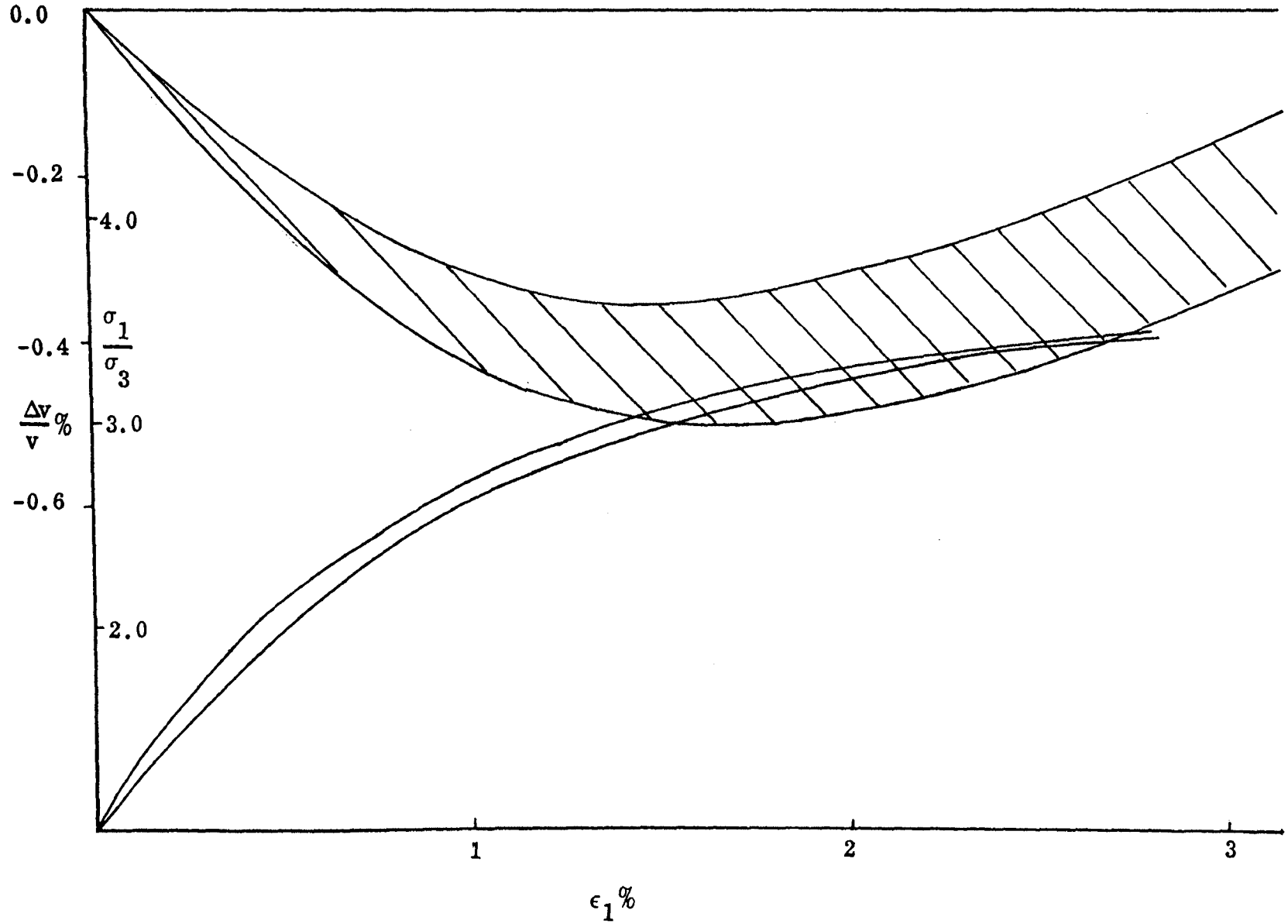

Fig. 23 Results of Test 2 - 4 - 1

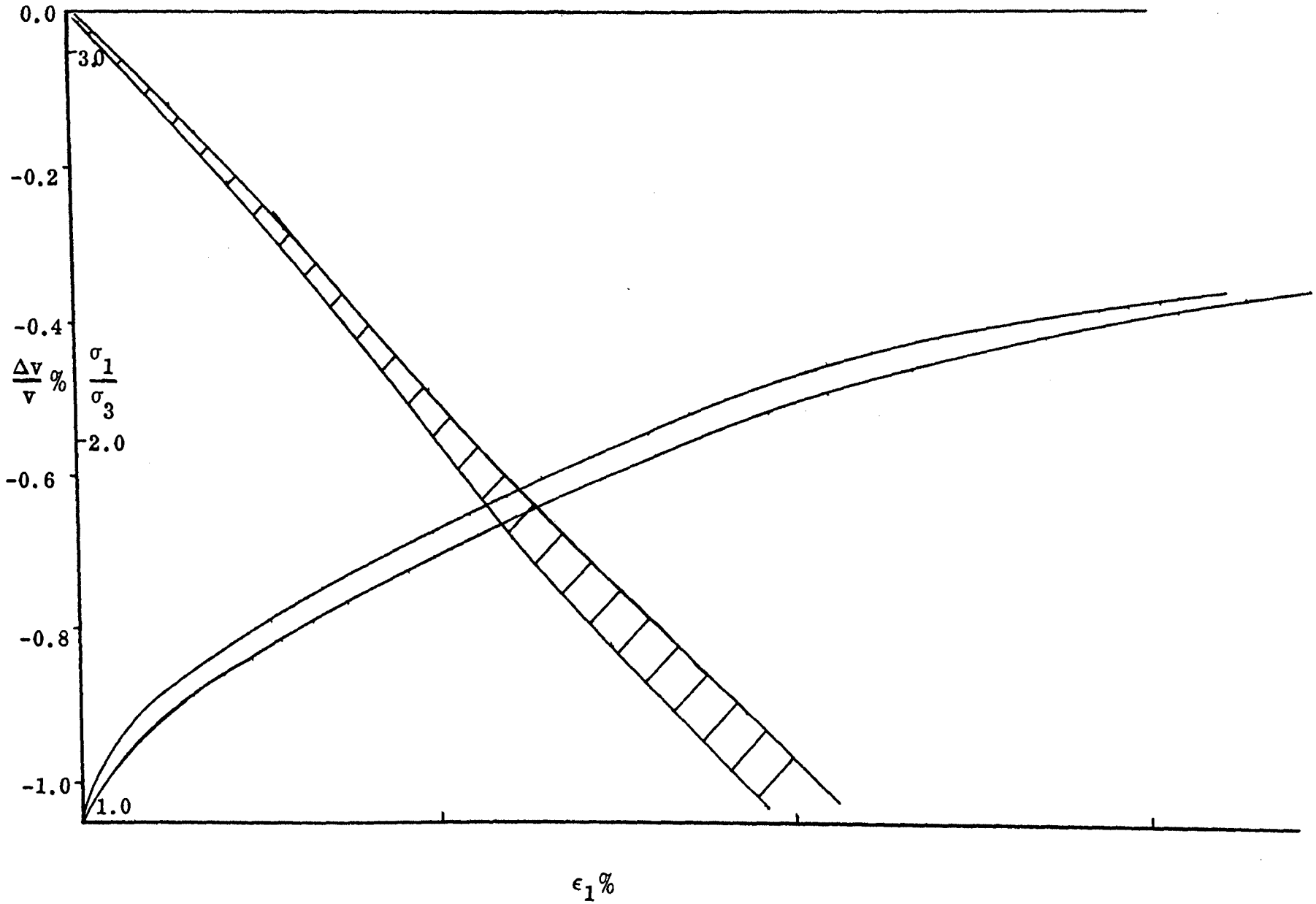

Fig. 24 Results of Test 2 - 6 - 1

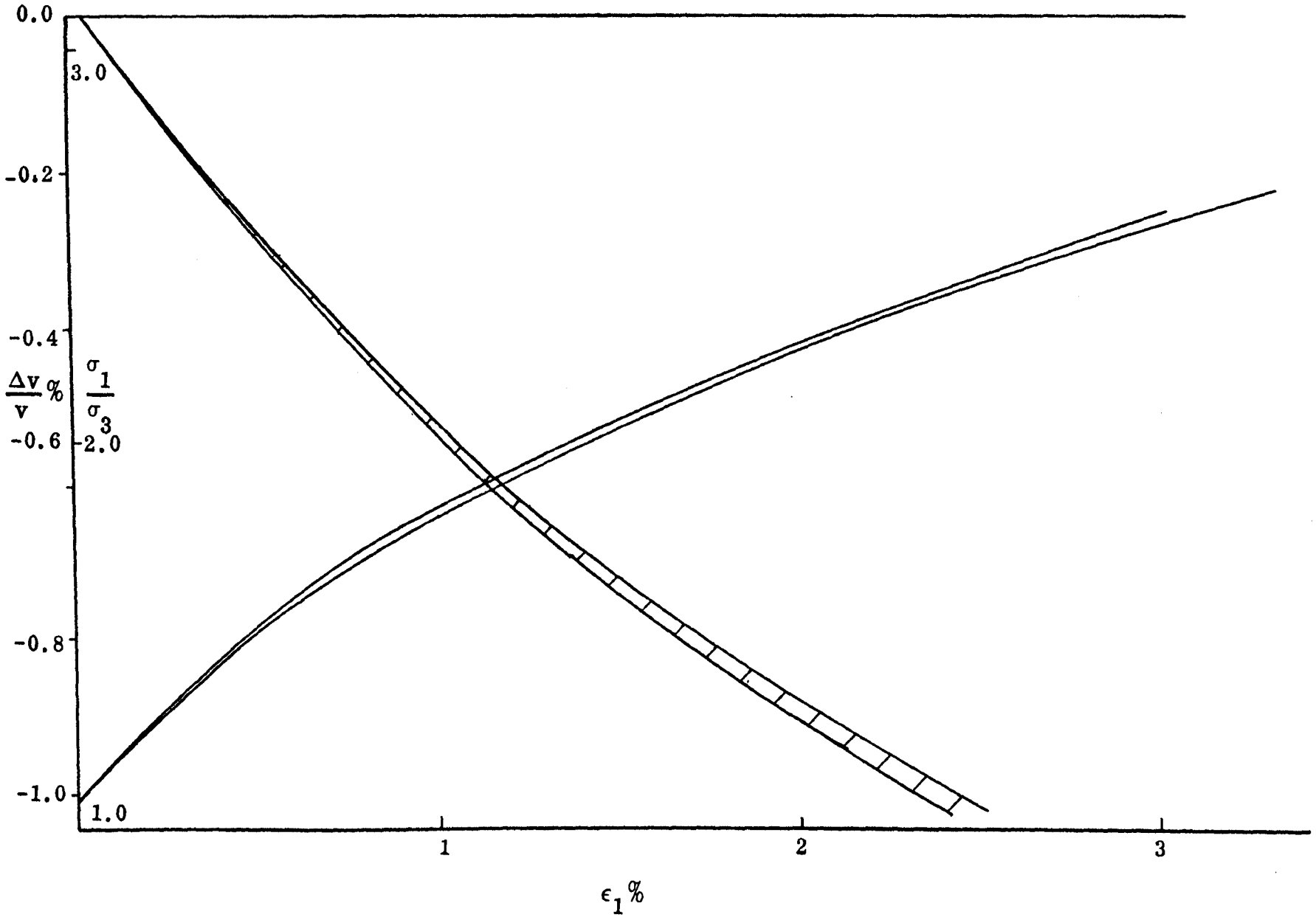

Fig. 25 Results of Test 3 - 2 - 1

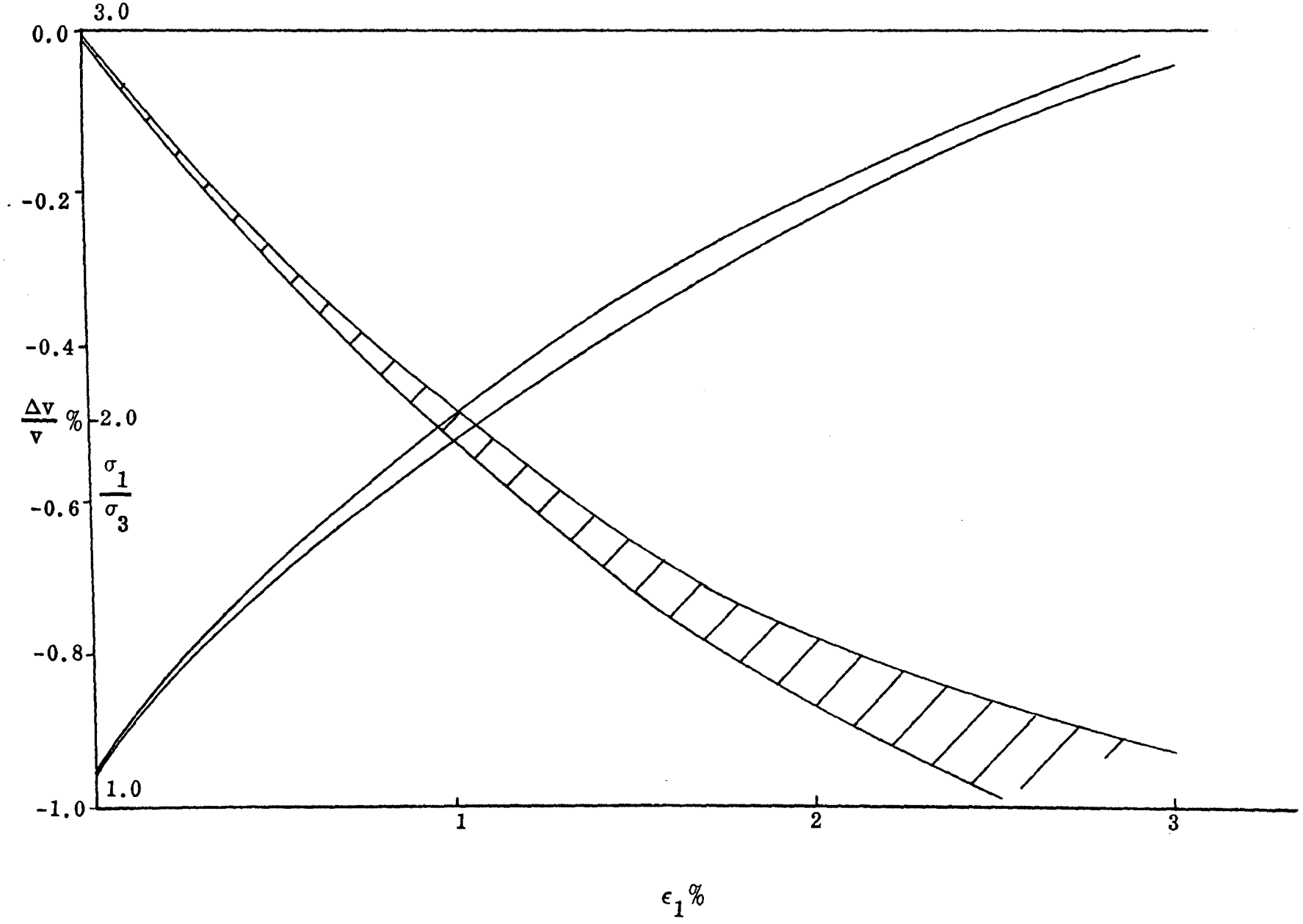

Fig. 26 Results of Test 3 - 4 - 1

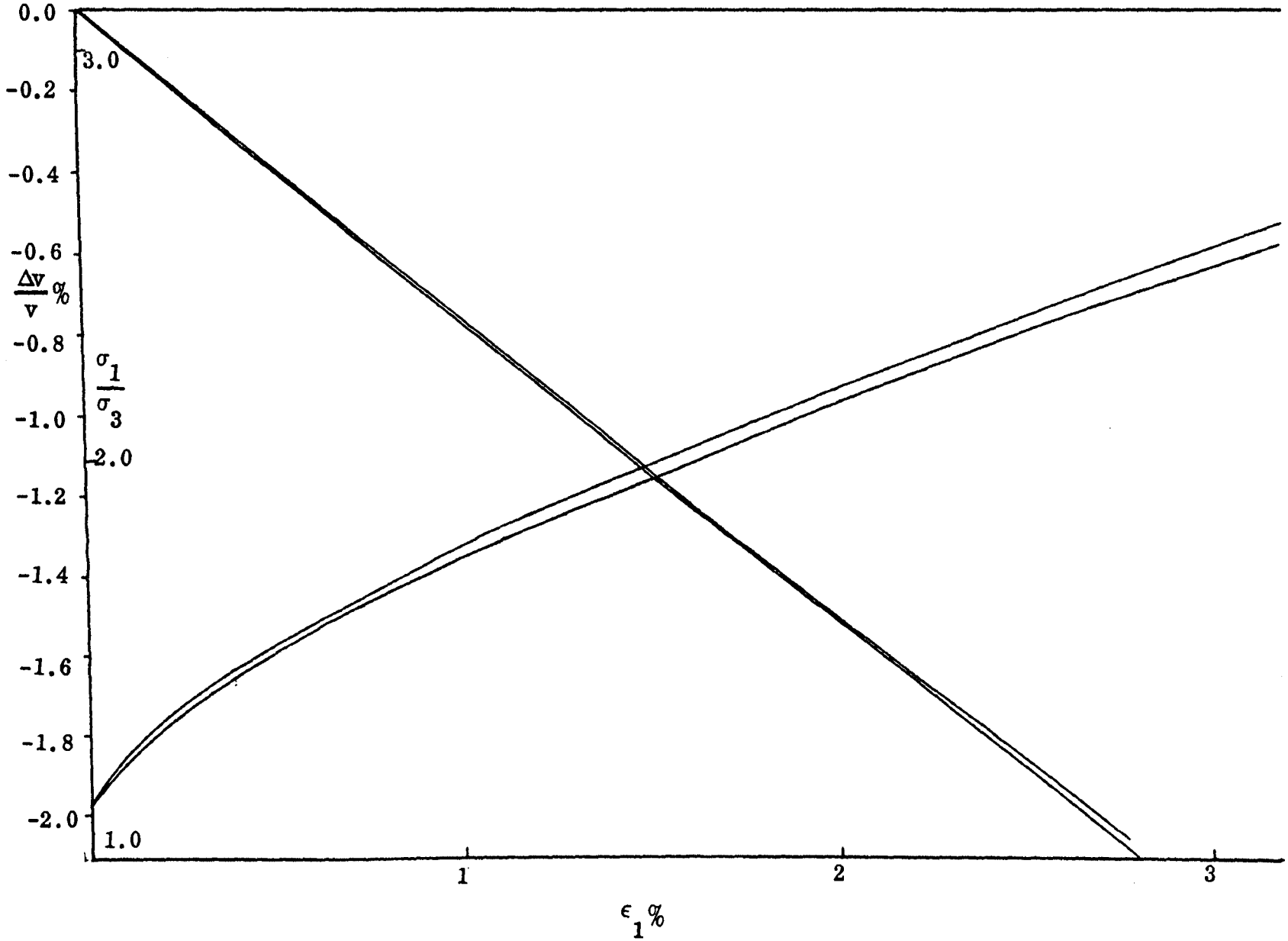

Fig. 27 Results of Test 3 - 6 - 1

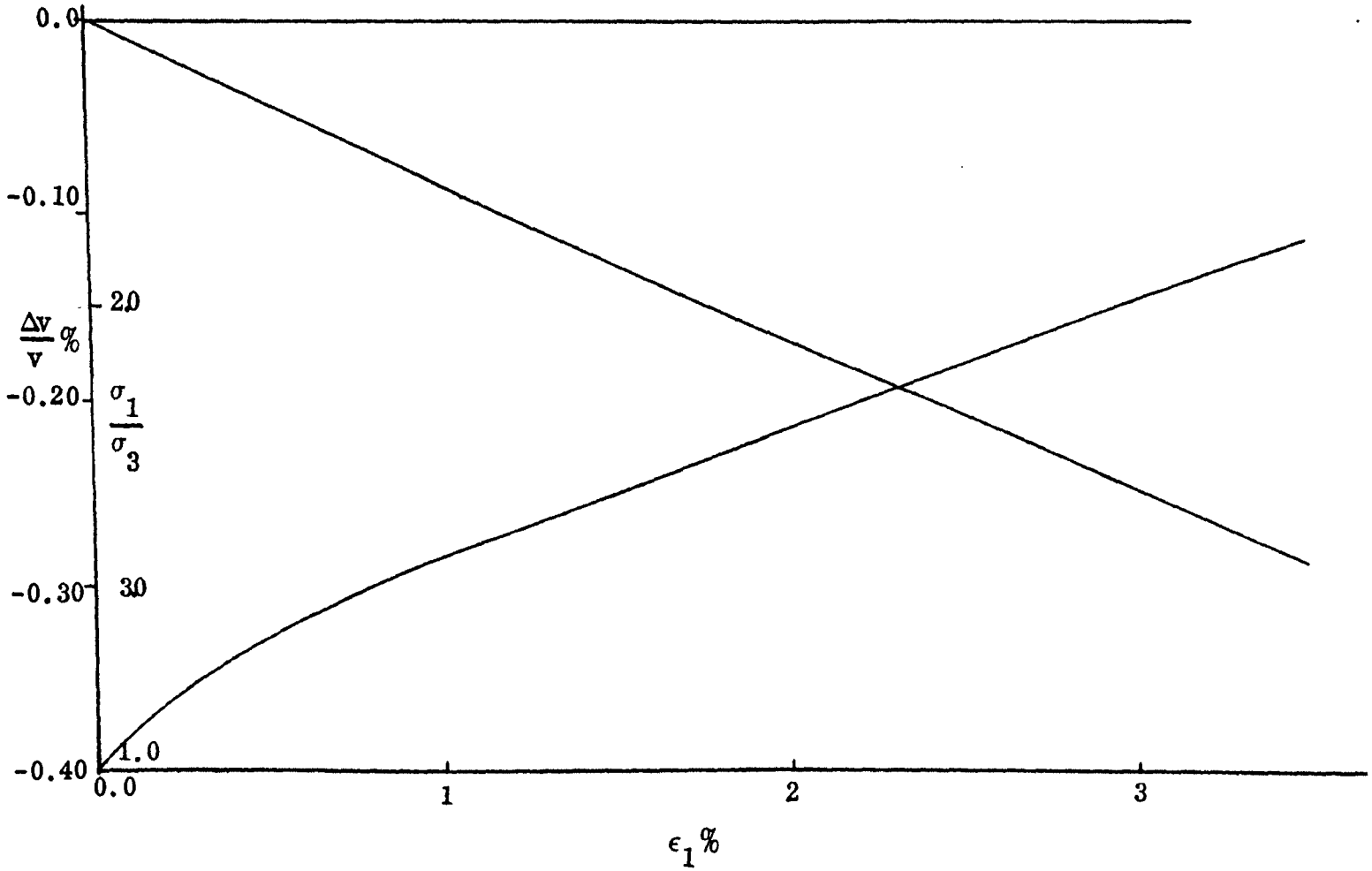

Fig. 28 Results of Test 4 - 3 - 1

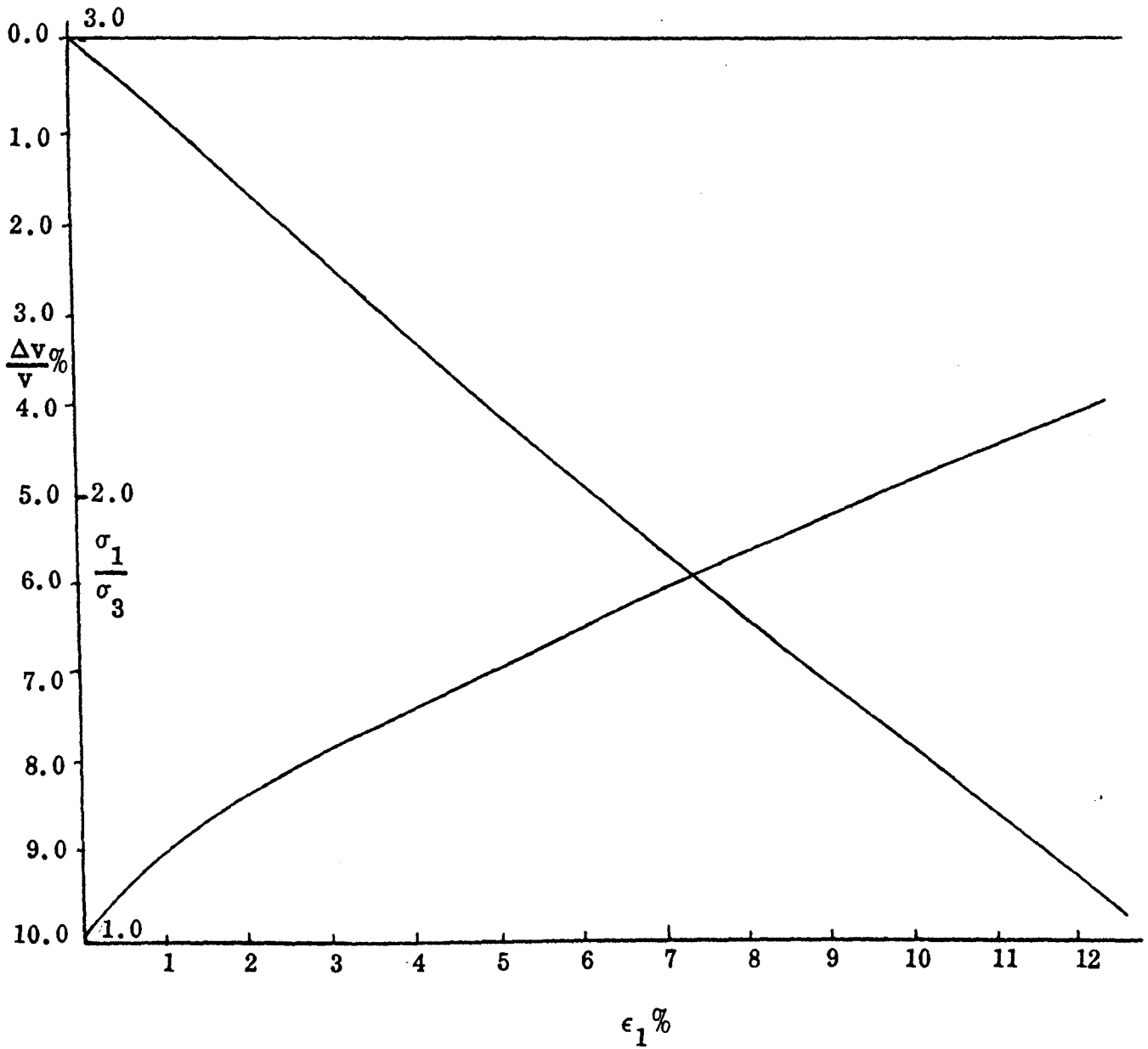

Fig. 29 Results of Test 4 - 6 - 2

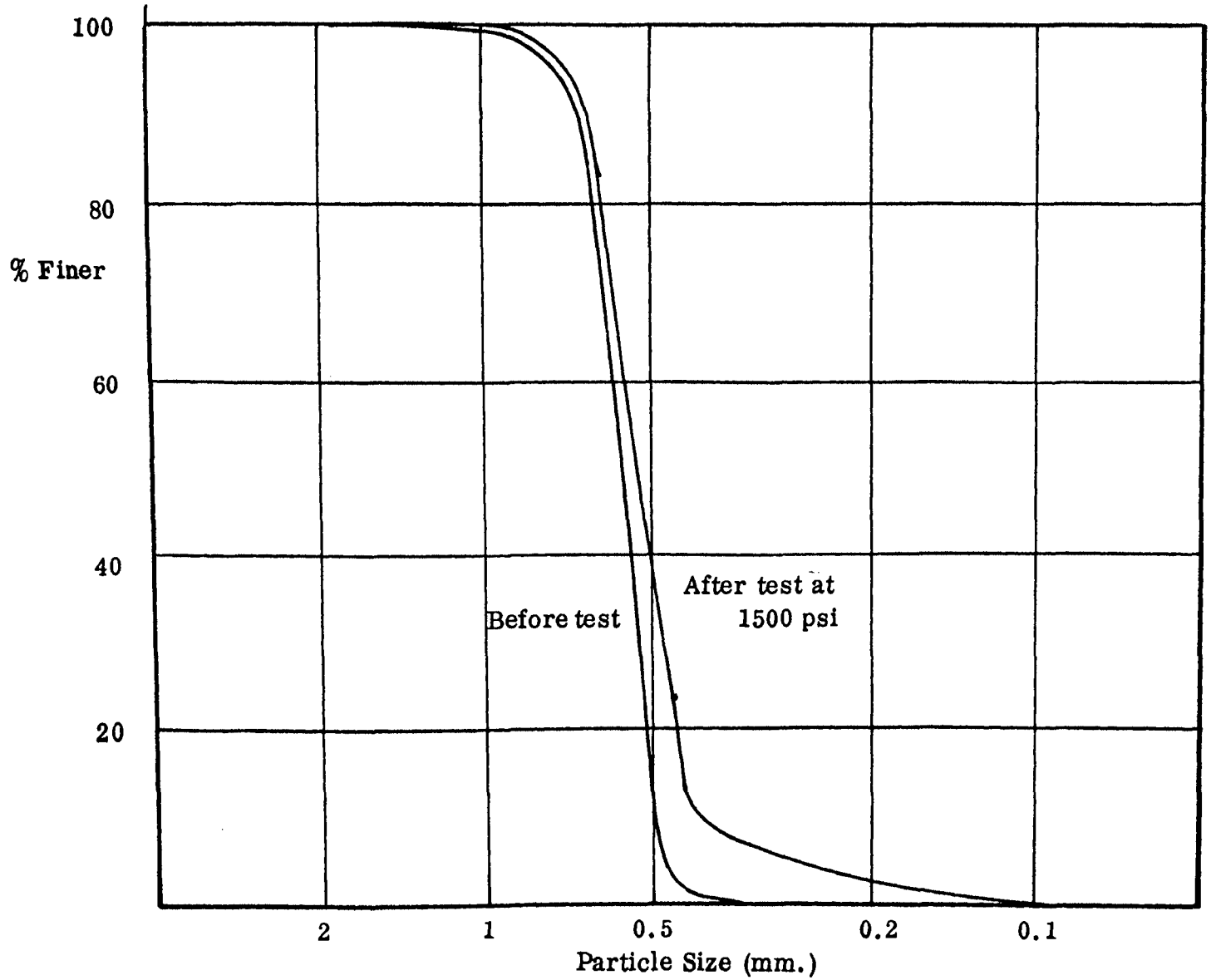

Fig. 30 Effect of High F Pressures on Ottawa Sand

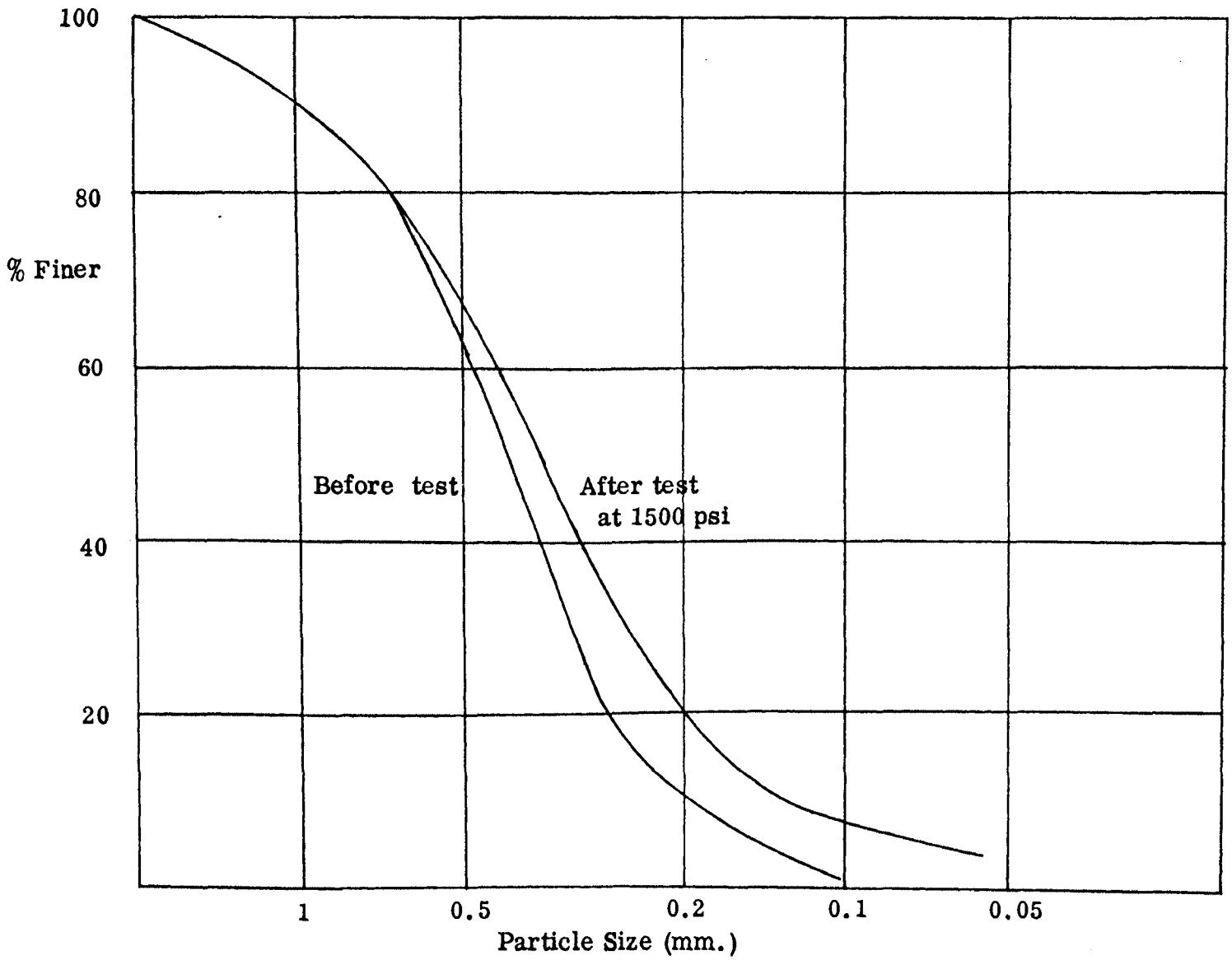

Fig. 31 Effect of High Pressures on Meramec River Sand

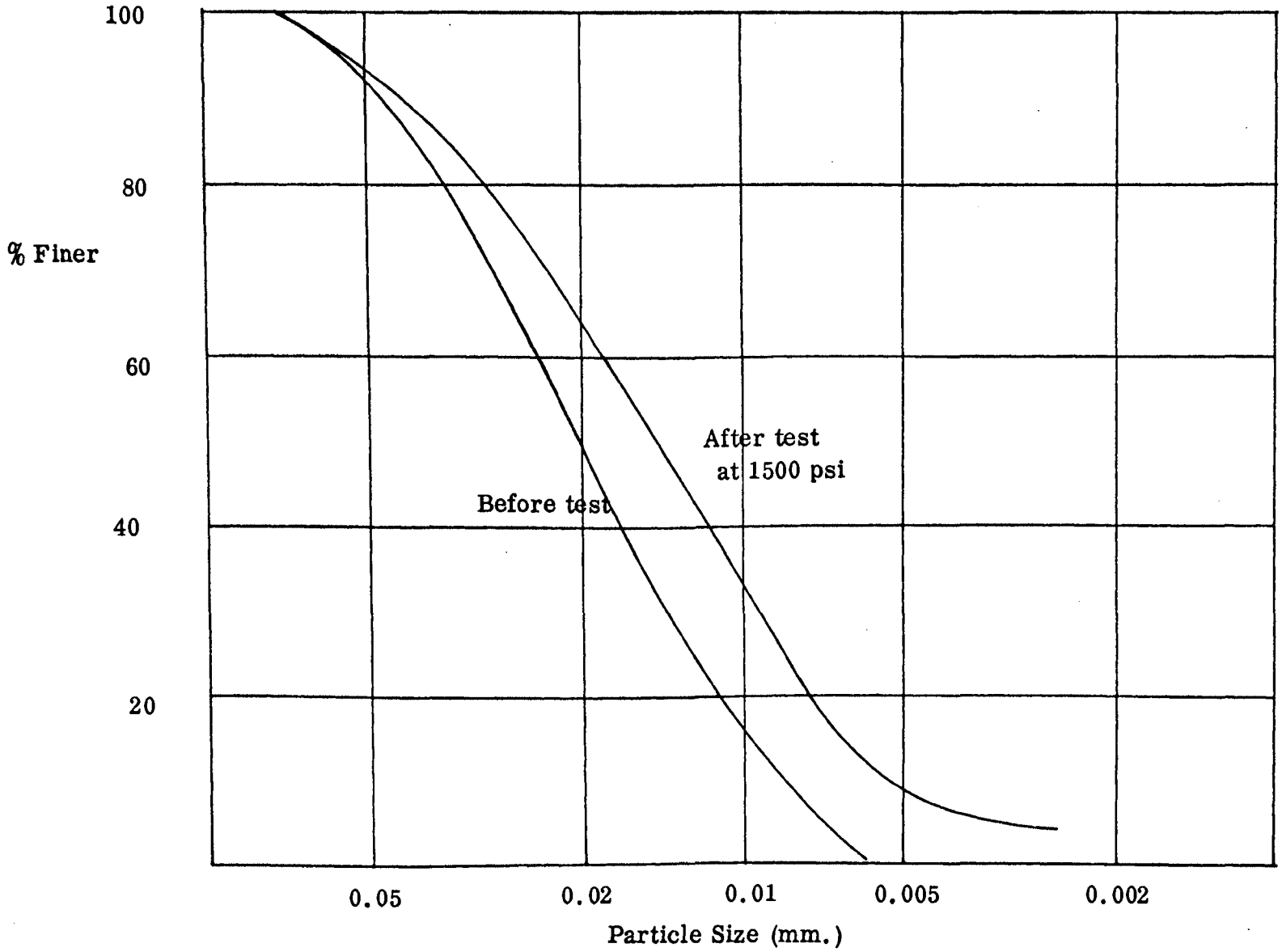

Fig. 32 Effect of High Pressures on Silt

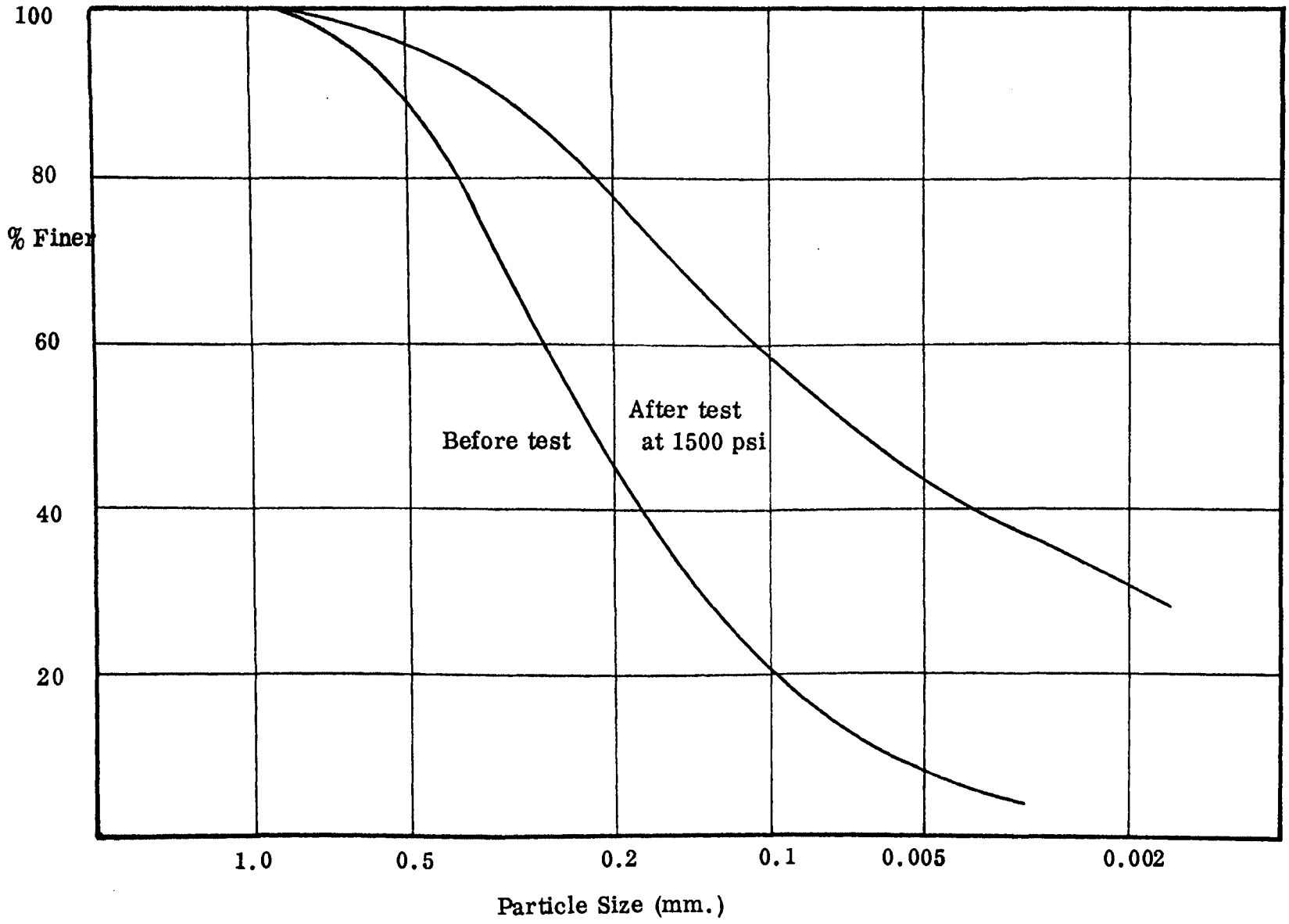

33. Effect of High Pressures on Tailings

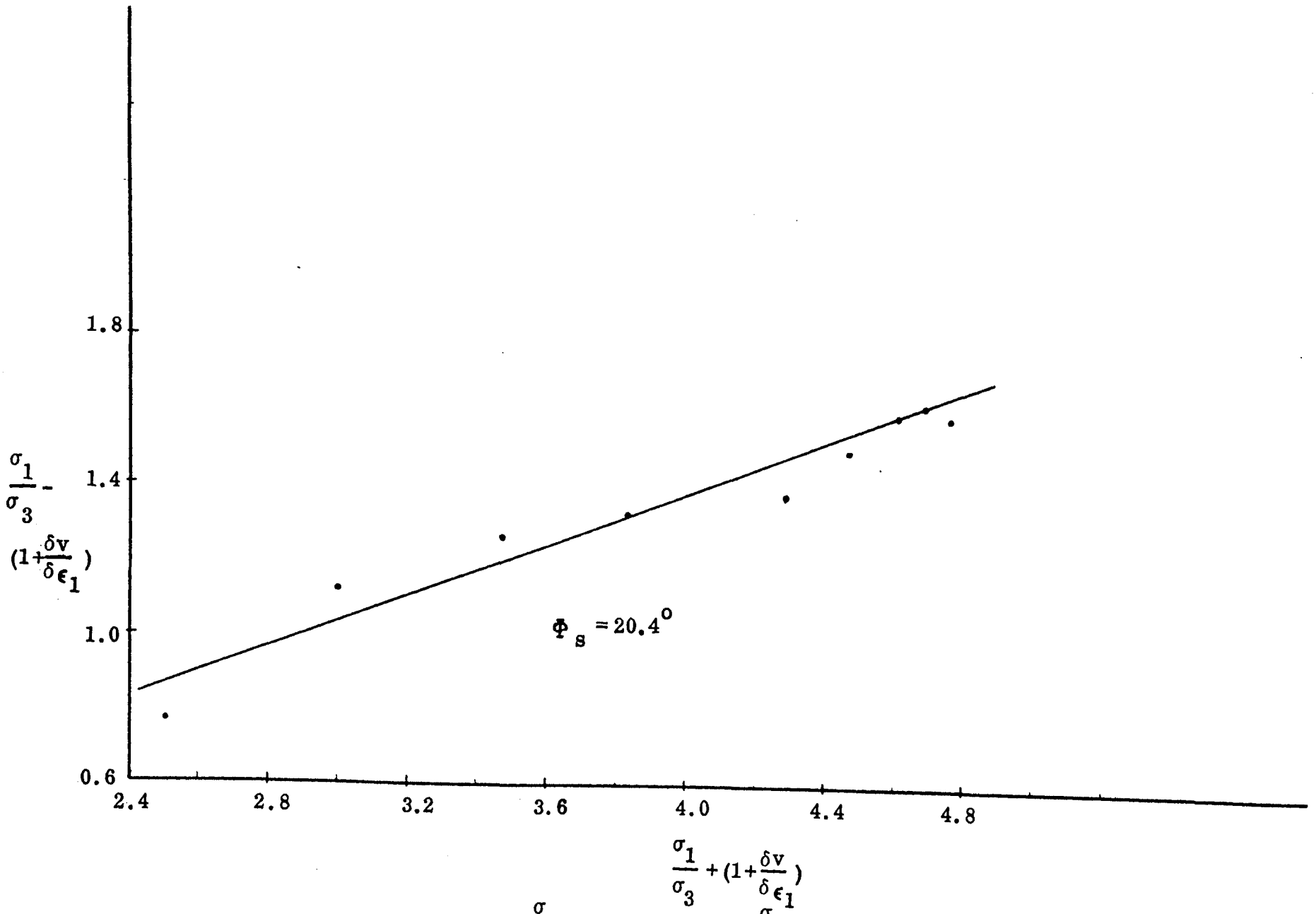

Fig. 34 $\frac{\sigma_1}{\sigma_3} - (1+\frac{\delta v}{\delta \epsilon_1})$ versus $\frac{\sigma_1}{\sigma_3} + (1+\frac{\delta v}{\delta \epsilon_1})$ for Test 1 - 2 - 1

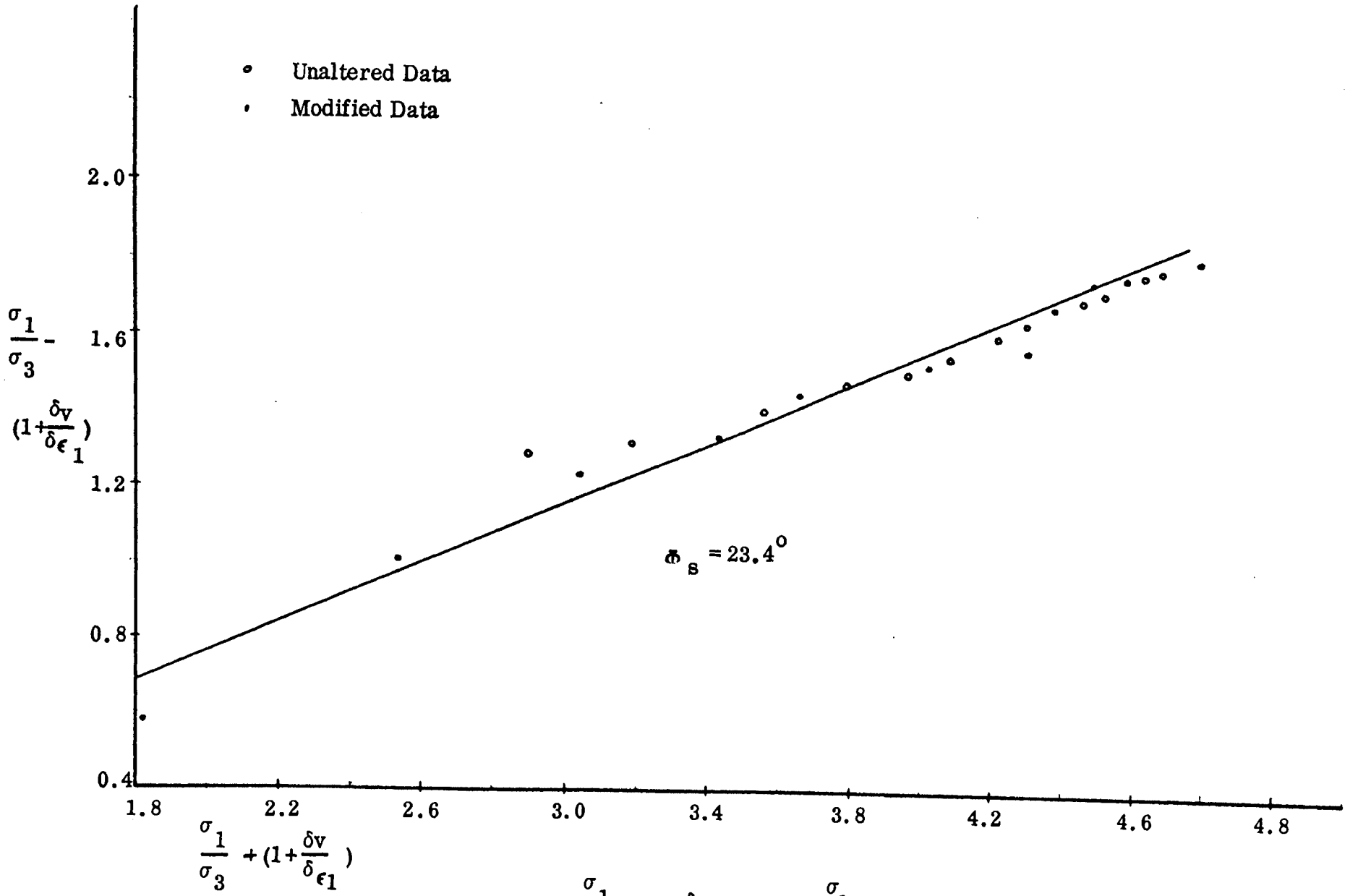

Fig. 35 $\frac{\sigma_1}{\sigma_3} - (1+\frac{\delta v}{\delta \epsilon_1})$ versus $\frac{\sigma_1}{\sigma_3} + (1+\frac{\delta v}{\delta \epsilon_1})$ for Test 1 - 3 - 1

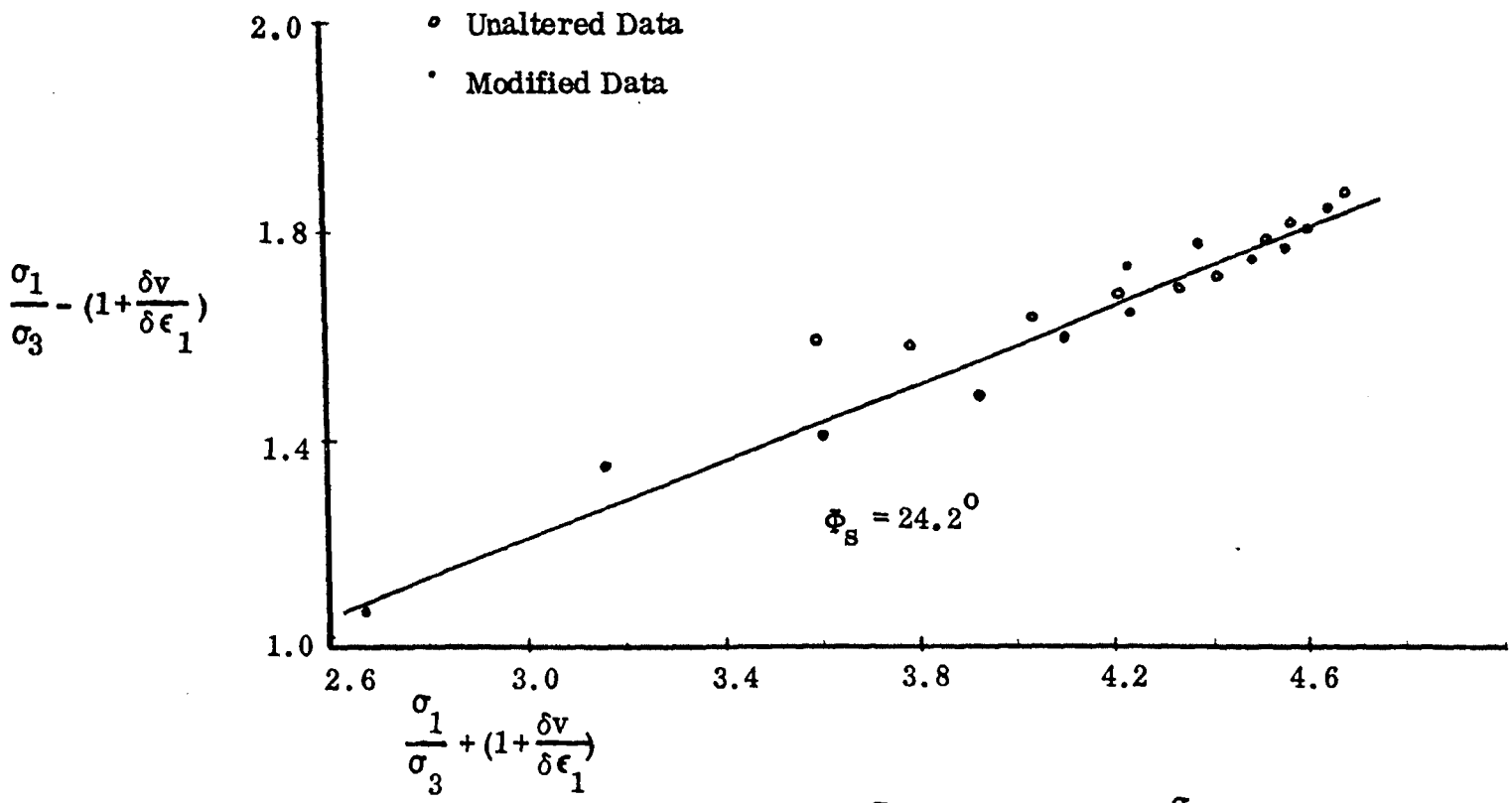

Fig. 36 $\frac{\sigma_1}{\sigma_3} - (1+\frac{\delta v}{\delta \epsilon_1})$ versus $\frac{\sigma_1}{\sigma_3} + (1+\frac{\delta v}{\delta \epsilon_1})$ for Test 1 - 4 - 1

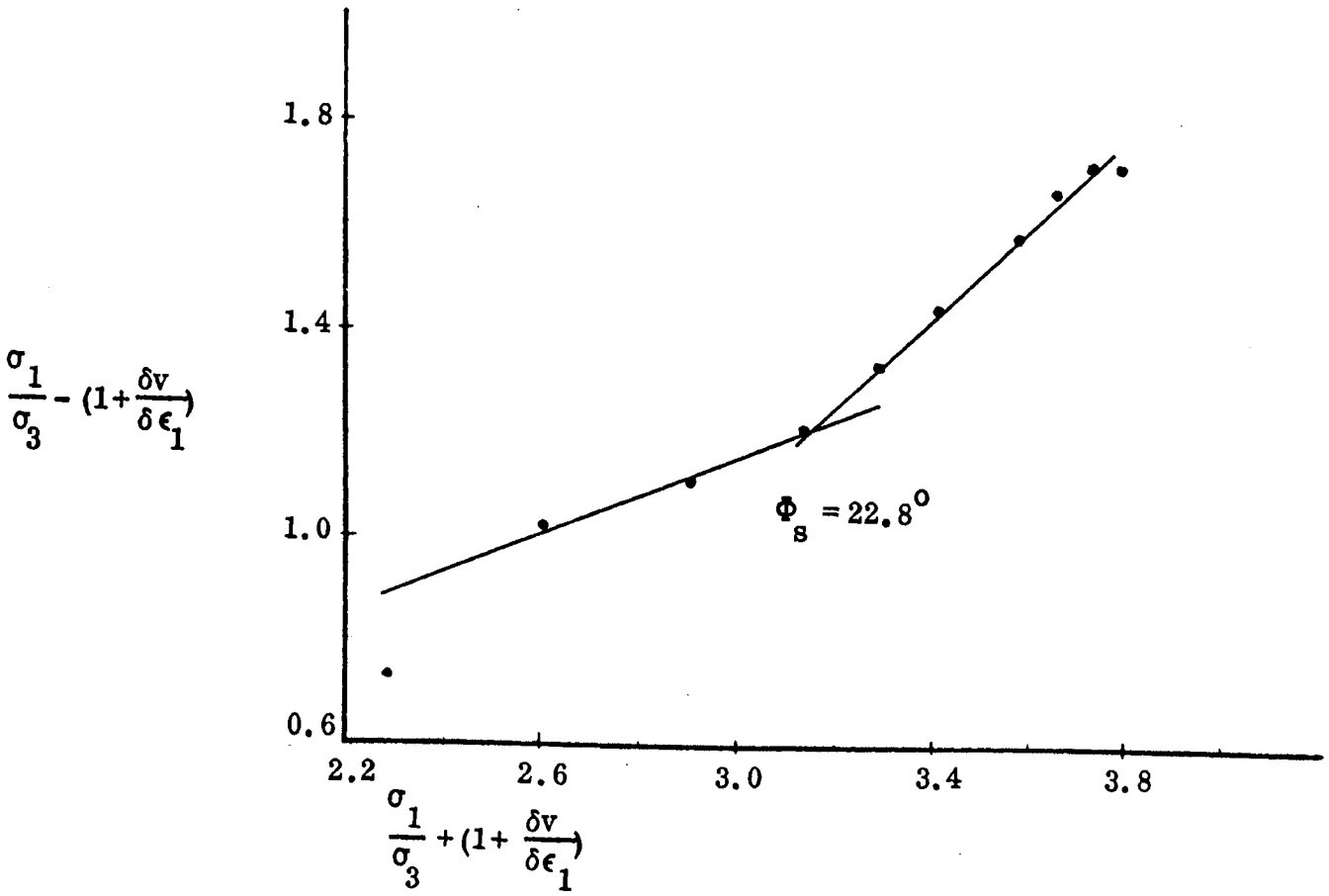

Fig. 37 $\frac{\sigma_1}{\sigma_3} - (1+\frac{\delta v}{\delta \epsilon_1})$ versus $\frac{\sigma_1}{\sigma_3} + (1+\frac{\delta v}{\delta \epsilon_1})$ for Test 1 - 6 - 1

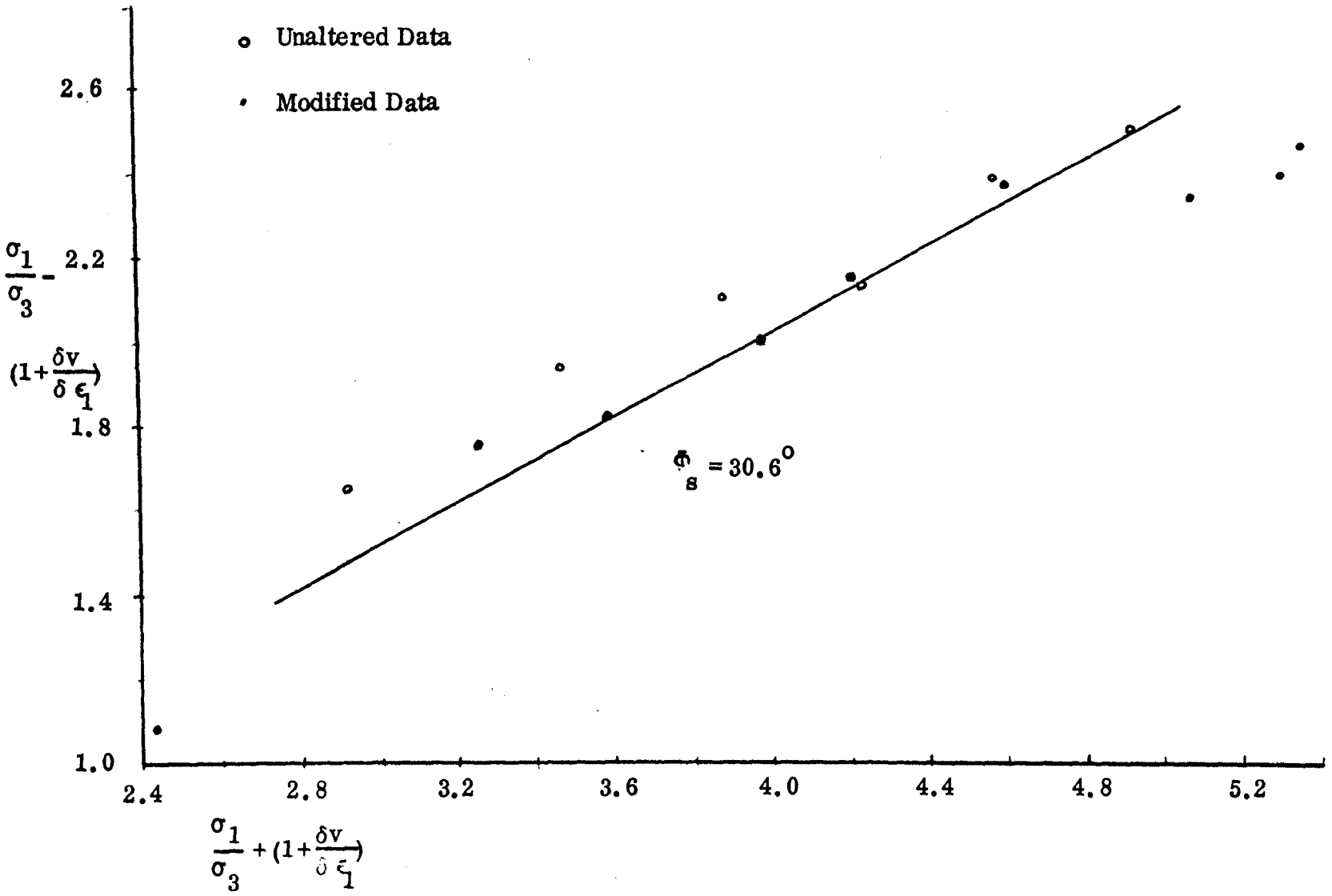

Fig. 38 $\frac{\sigma_1}{\sigma_3} - (1+\frac{\delta v}{\delta \epsilon_1})$ versus $\frac{\sigma_1}{\sigma_3} + (1+\frac{\delta v}{\delta \epsilon_1})$ for Test 2 - 3 - 1

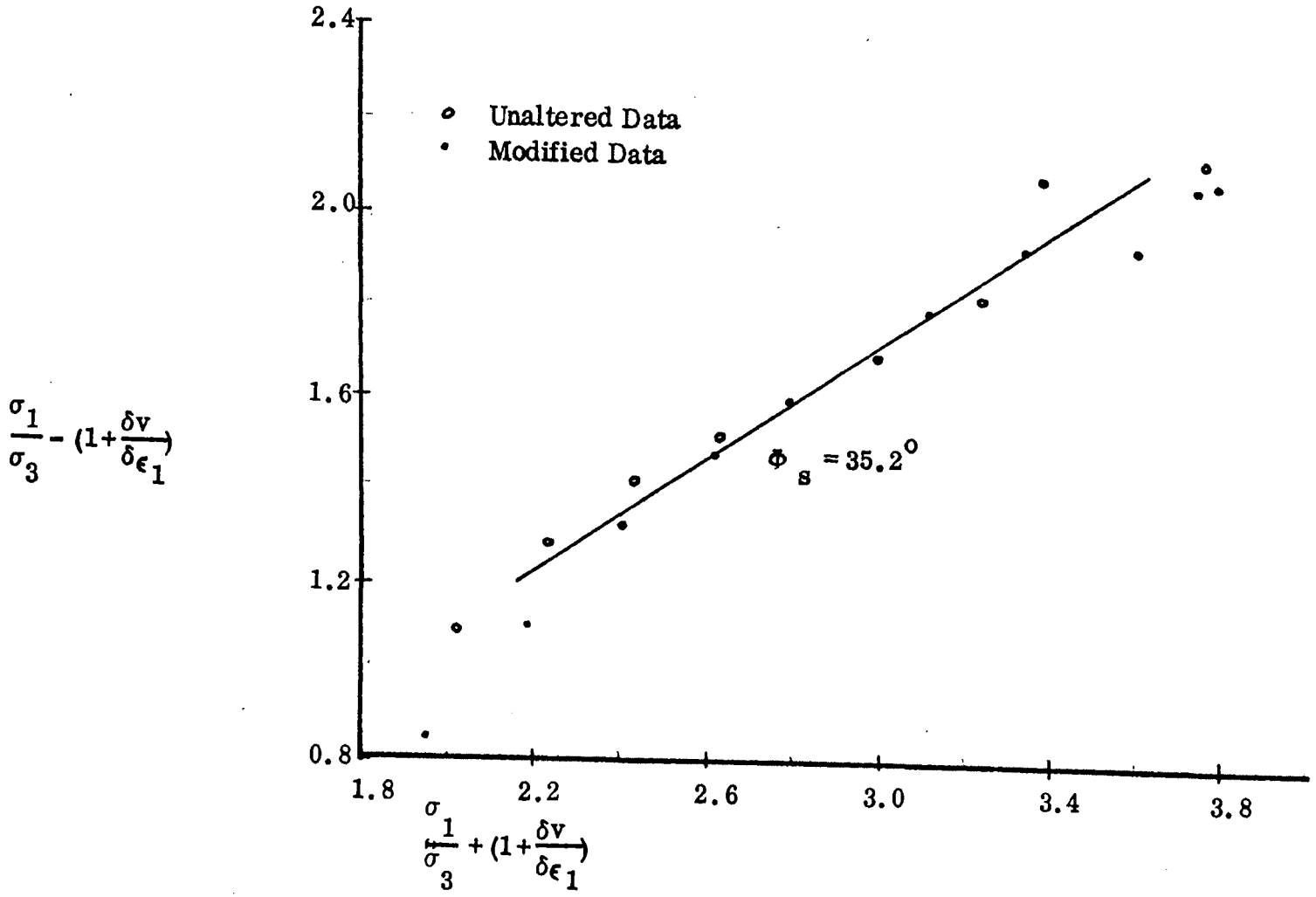

Fig. 39 $\frac{\sigma_1}{\sigma_3} - (1+\frac{\delta v}{\delta \epsilon_1})$ versus $\frac{\sigma_1}{\sigma_3} + (1+\frac{\delta v}{\delta \epsilon_1})$ for Test 2 - 5 - 1

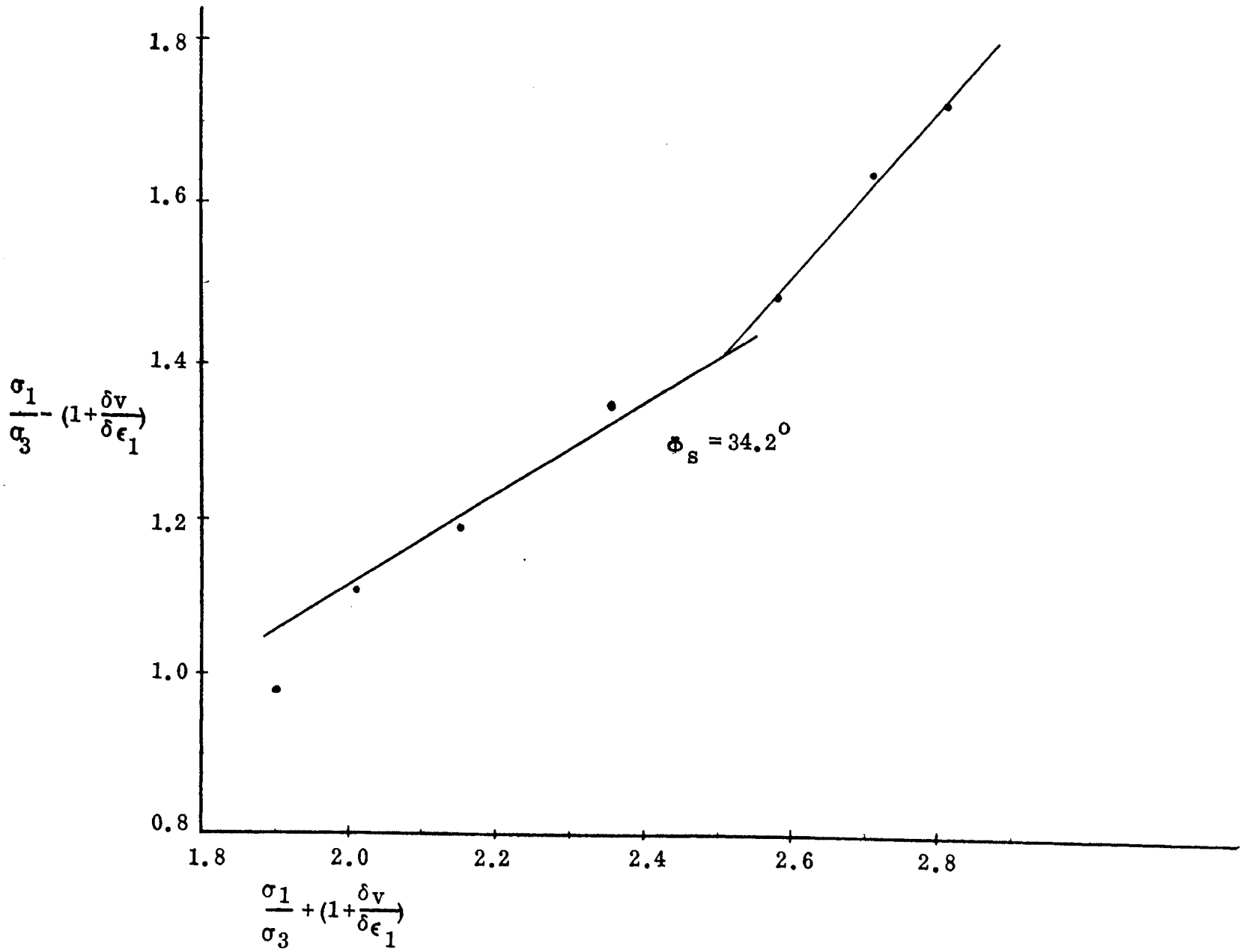

Fig. 40 $\frac{\sigma_1}{\sigma_3} - (1+\frac{\delta v}{\delta \epsilon_1})$ versus $\frac{\sigma_1}{\sigma_3} + (1+\frac{\delta v}{\delta \epsilon_1})$ for Test 2 - 6 - 1

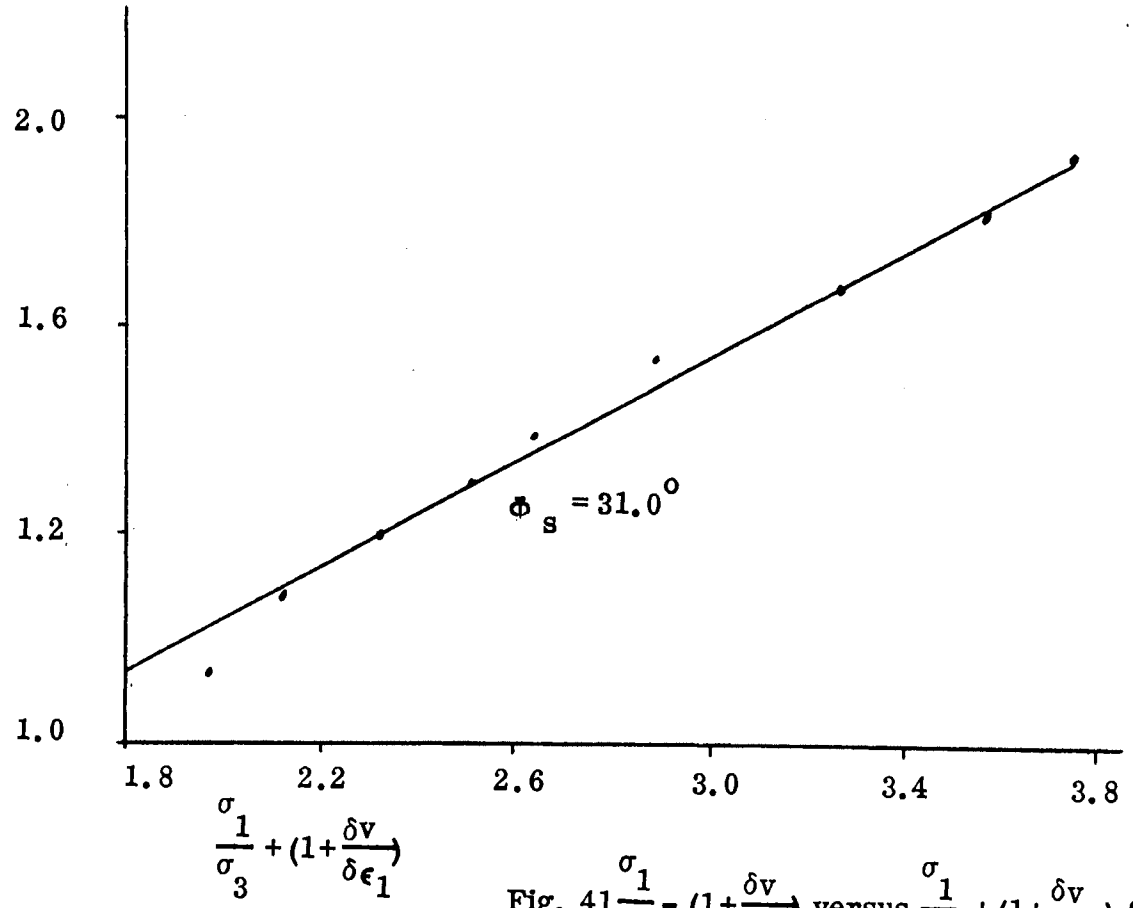

Fig. 41 $\frac{\sigma_1}{\sigma_3} - (1+\frac{\delta v}{\delta \epsilon_1})$ versus $\frac{\sigma_1}{\sigma_3} + (1+\frac{\delta v}{\delta \epsilon_1})$ for Test 3 - 3 - 1

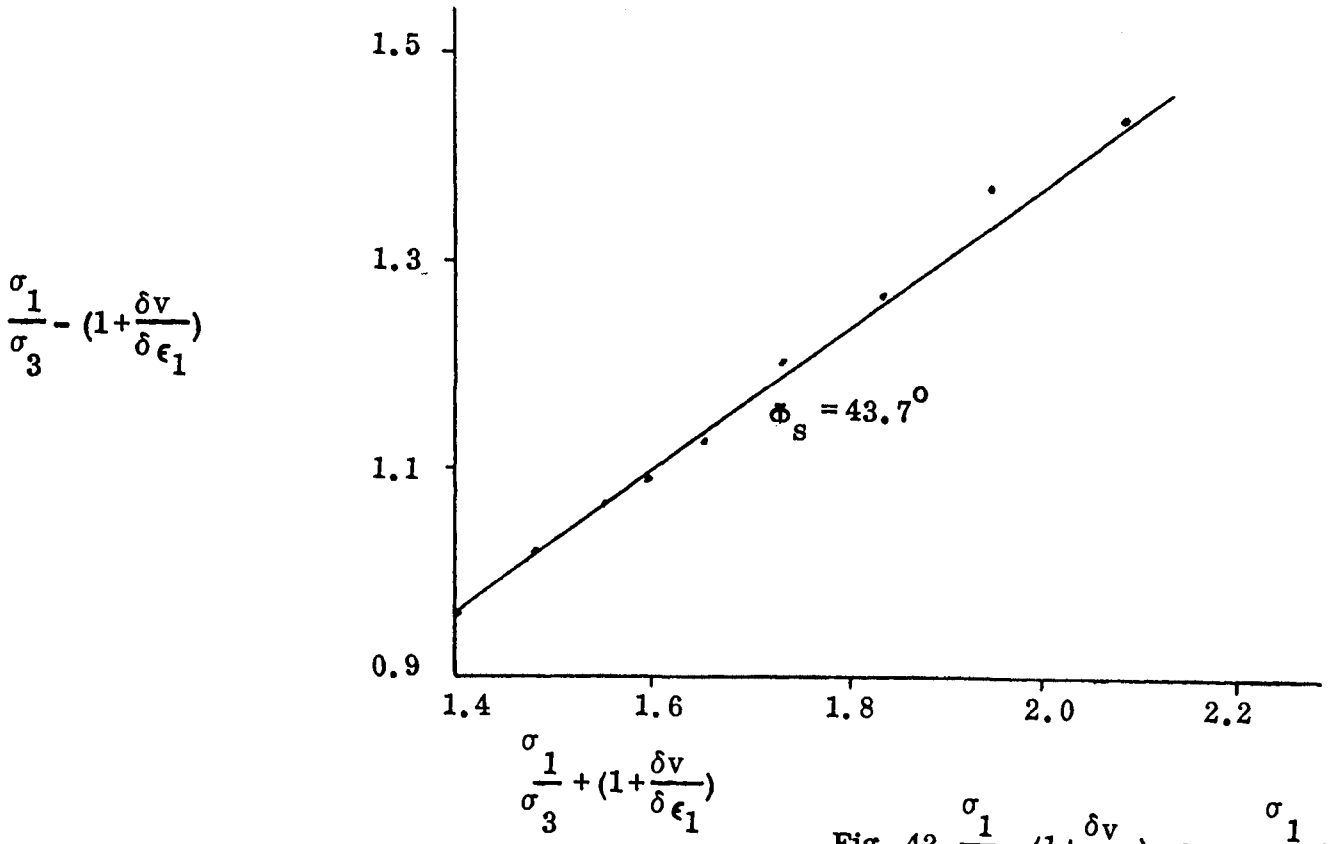

Fig. 42 $\frac{\sigma_1}{\sigma_3} - (1+\frac{\delta v}{\delta \epsilon_1})$ versus $\frac{\sigma_1}{\sigma_3} + (1+\frac{\delta v}{\delta \epsilon_1})$ for Test 3 - 6 - 1

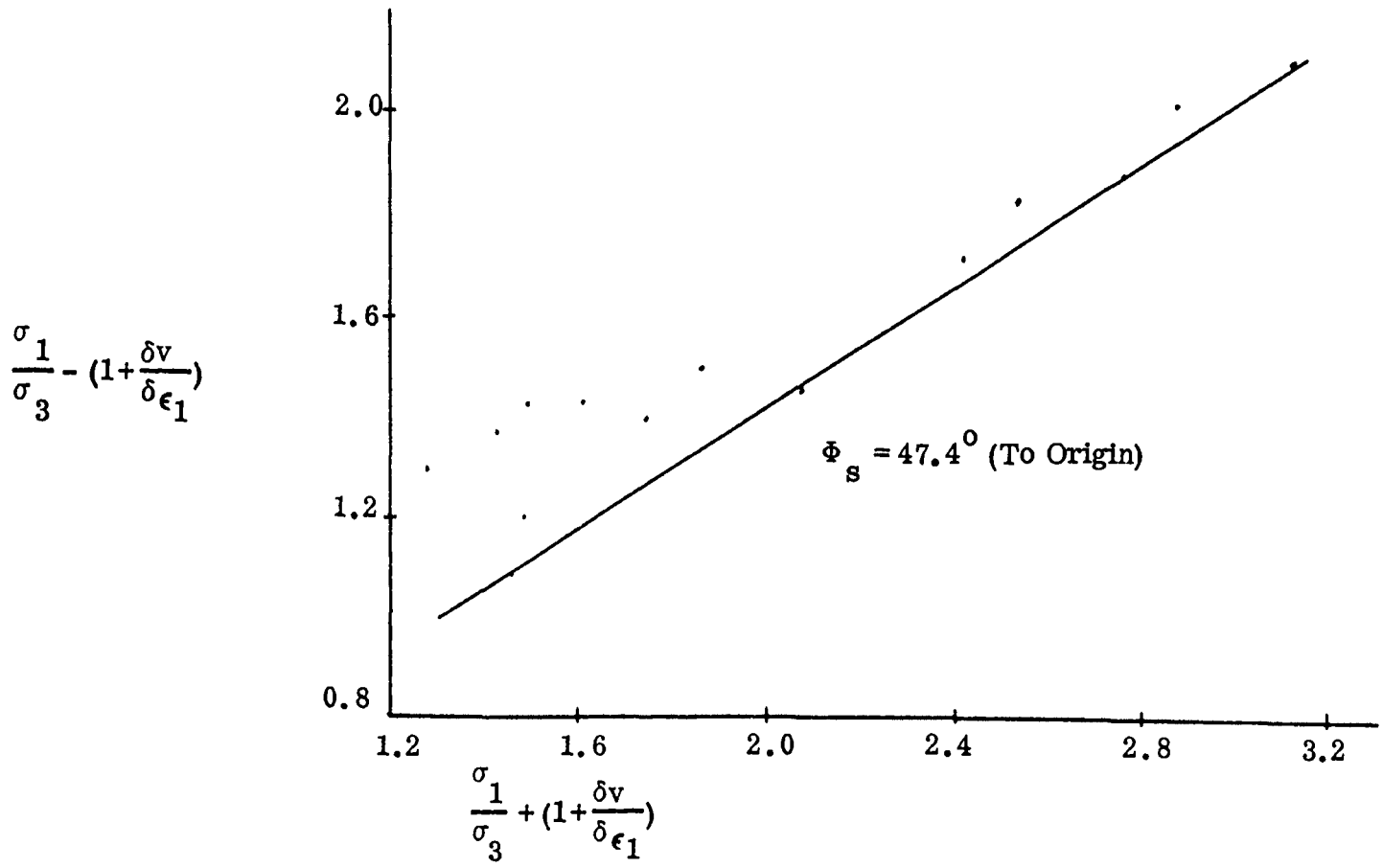

Fig. 43 $\frac{\sigma_1}{\sigma_3} - (1+\frac{\delta v}{\delta \epsilon_1})$ versus $\frac{\sigma_1}{\sigma_3} + (1+\frac{\delta v}{\delta \epsilon_1})$ for Test 4 - 3 - 1

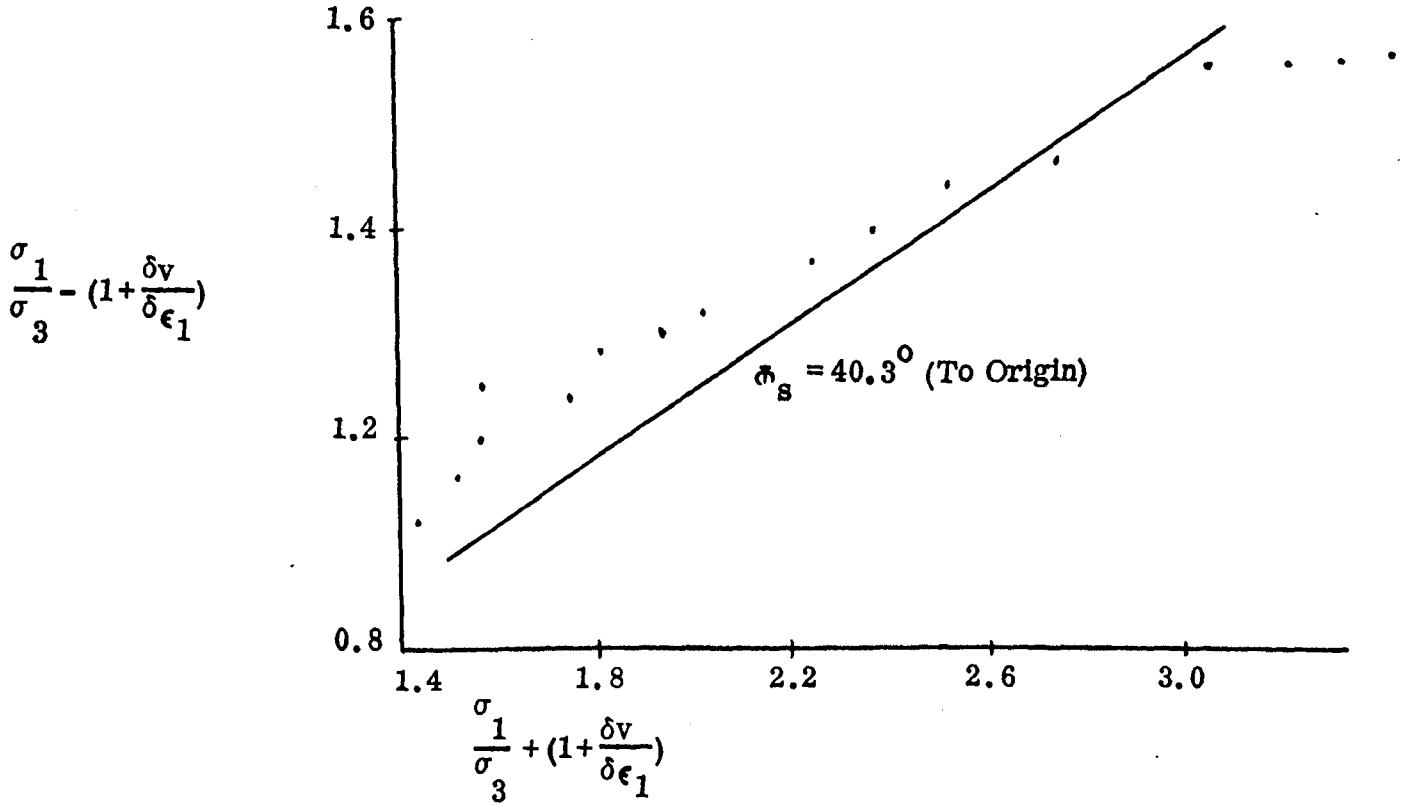

Fig. 44 $\frac{\sigma_1}{\sigma_3} - (1+\frac{\delta v}{\delta \epsilon_1})$ versus $\frac{\sigma_1}{\sigma_3} + (1+\frac{\delta v}{\delta \epsilon_1})$ for Test 4 - 6 - 2

IX BIBLIOGRAPHY

1. AMONTONS, (1699), De la resistance cquse' e dans les machines. Academie Royale des Sciences, Paris France, Histoire avec les Mémoire de Mathématique et de Physique 1699: 206-227 in Tinoco, F. H. and Handy, R. L., "Shear Strength of Granular Materials", Engineering Research Institute Iowa State University, Contribution No. 67-9; pp. 1-100.

2. ARMSTRONG, JAMES C., and DUNLAP, WAYNE A., (1966), "The Use of Particulate Mechanics in the Simulation of Stress-Strain Characteristics of Granular Materials", Research Report Number 99-1, Texas Transportation Institute, College Station, Texas, pp. 1-106.

3. BISHOP, A.W., (1954), Correspondence to Secretary, The Institute of Civil Engineers, Géotechnique, vol. IV, 1954, pp. 43-45.

4. BISHOP, A.W., (1966), "The Strength of Soils as Engineering Materials", Sixth Rankine Lecture, Geotechnique, vol. XVI, No. 2, June 1960, pp. 91-126.

5. BOWDEN, F. P. and TABOR, D., (1956), Friction and Lubrication, Methuen' s Monographs on Physical Subjects, Aberdeen University Press, Chapter III, pp. 20-22.

6. CATTANEO, C., (1938) "Sui contatto di due Corpi Elastici", Accademia dei Lincei, Rendieonti, Series 6, vol. 27, 1938, pp. 342-348, 434-436, and 474-478, in Mindlin, R. D. and Deresiewicz, H., 1952, "Elastic Spheres in Contact Under Varying Oblique Forces", The American Society of Mechanical Engineers, Applied Mechanics Division, November 5, 1952. Paper No. 53-APM-14, pp. 327-344.

7. COULOMB, C.A. (1781), Theorie des machines simples, ev ayant égard au frottement de leurs partied, et a la roideur des cordages. Academie Royale des Sciences, Paris, France, Mémoires de Mathématique et de Physique 10, No. 2:161-332. 1785. in Tinoco, F. H. and Handy, R. L., "Shear Strength of Granular Materials", Engineering Research Institute Iowa State University, Contribution No. 67-9: 1-100.

8. DERESIEWICS, H. (1957), "Stress-Strain Relations For A Simple Model of Granular Medium", Office of Naval Research Project Nr-064-388, Technical Report No. 18, April, 1957, pp. 1-19.

9. DUFFY, J. and MINDLIN, R. D., (1956) "Stress-Strain Relations and Vibrations of a Granular Medium", Applied Mechanics Division of the American Society of Mechanical Engineers. No. 57-Apm-39, Dec. 3, 1956, pp. 585-593.

10. HENDRON, A.J. JR., FULTON, R.E., and MOHRAZ, BIJAN, (1963) "The Energy Absorption Capacity of Granular Materials in One-Dimensional Compression," Technical Documentary Report No. AFSWC-TDR-62-91, Department of Civil Engineering, University of Illinois, Jan., 1963, pp. 1-186.

11. HERTZ, H. (1881), J. Math (Crelle' s J.), vol. 92, 1881, in Timoshenko, S. and Goodier, J.N., Theory of Elasticity, McGraw-Hill Book Company, Inc., 1951, pp. 372-377.

12. HIRSCHFELD, R.C., and POULOS, S.J. (1963), "High-Pressure Triaxial Tests on a Compacted Sand and an Undistrubed Silt", Symposium on Laboratory Shear Testing of Soils, American Society for Testing and Materials and The National Research Council of Canada, Advance Copy, June 1963, pp. 1-13.

13. MINDLIN, R.D. (1949), "Compliance of Elastic Bodies in Contact", Journal of Applied Mechanics, Trans. ASME, vol. 71, 1949, pp. A-259-268 in Mindlin, R. D. and Deresiewicz, H., 1952, "Elastic Spheres in Contact Under Varying Oblique Forces", The American Society of Mechanical Engineers, Applied Mechanics Division, November 5, 1952. Paper No. 53-APM-14, pp. 327-344.

14. PECK, R.B., HANSON, W. E., and THORNBURN, T. H., (1953), Foundation Engineering, John Wiley and Sons, 1953, pp. 219-246.

15. REYNOLDS, O. (1885). "On the Dilatancy of Media Composed of Rigid Particles in Contact" With Experimental Illustrations. Phil. Mag. 20, pp. 469-481 in Rowe, P.W. (1969) "Osborne Reynolds and Dilatancy", Géothecnique vol. 19, No. 1, pp. 1-5.

16. ROSCOE, K.H., SCHOFIELD, A.N. and THURZIRAJAH, A. (1963), "Yielding of Clays in States Wetter Than the Critical", Geotechnique vol. 13, No. 3, pp. 211-240.

17. ROWE, P.W. (1962) "The Stress-Dilatancy Relation For Static Equilibrium of An Assembly of Particles in Contact", Royal Society of London, London, England, Proceedings Series A, 269, pp. 500-529.

18. ROWE, P.W., BARDEN, L., and LEE, I.K. (1964) "Energy Components During The Triaxial Cell and Direct Shear Tests", Géothecnique vol. XIV, No. 3, Sept. 1964, pp. 247-261.

19. SEARS, F.W., and ZEMANSKEY, M.W. (1949) University Physics, Addison-Wesley Publishing Company, Inc. pp. 28.

20. SEED, H.B., and LEE, K. L. (1967) "Drained Strength Characteristics of Sands", Journal of the Soil Mechanics and Foundations Division, Proceedings of the American Society of Civil Engineers, vol. 93, No. Sm6 No. 1967 pp. 117-141.

21. TAYLOR, D.W. (1948) Fundamentals of Soil Mechanics, John Wiley and Sons Inc., New York, 1948 Chap. 14, pp. 329-361.

22. TINOCO, F. H., and HANDY, R.L. (1967), "Shear Strength of Granular Materials," Engineering Research Institute, Iowa State University, Contribution No. 67-9:1-100.

23. WHITMAN, R.V. (1957), "The Behavior of Soils Under Transent Loadings", Proceedings 4th Int. Conf. Soil Mech. and Found. Engr. vol. 1, 1957, pp. 207 as described by Scott, R. F., Principles of Soil Mechanics, Addison-Wesley Publishing Company, Inc. 1963, pp. 331-333.

24. VESIC, A. S. and CLOUGH, G.W., "Behavior of Granular Material Under High Stresses", Journal of The Soils Mechanics and Foundations Division, Proceedings of the American Society of Civil Engineers, vol. 94, No. Sm3, May 1968, pp. 661-688.

X VITA

Christopher Byron Groves was born August 13, 1946 at Chicago, Illinois. He received his primary and secondary education in Rolla, Missouri. In August of 1967 he was registered as an "Engineer-in-training" in Missouri. In January of 1968 he received a Bachelor of Science Degree in Civil Engineering from the University of Missouri - Rolla. From January 1968 to May 1968 he held a teaching assistantship at the University of Missouri - Rolla. In the summer of 1968 he worked on a research project directed by Dr. F. Tinoco. From September 1968 to May 1969 he worked on a National Science Foundation Assistantship while attending Graduate School at the University of Missouri - Rolla. During 1968 and 1969 he assisted in numerous consulting jobs which Dr. T. S. Fry, Dr. J. C. Armstrong, Dr. F. Tinoco and Dr. N. O. Schmidt were engaged in.